



Inflammasome Regulates Hematopoiesis through Cleavage of the Master Erythroid Transcription Factor GATA1

Sylwia D Tyrkalska, Ana B Pérez-Oliva, Lola Rodríguez-Ruiz, Francisco J Martínez-Morcillo, Francisca Alcaraz-Pérez, Francisco J Martínez-Navarro, Christophe Lachaud, Nouraiz Ahmed, Timm Schroeder, Irene Pardo-Sánchez, et al.

► To cite this version:

Sylwia D Tyrkalska, Ana B Pérez-Oliva, Lola Rodríguez-Ruiz, Francisco J Martínez-Morcillo, Francisca Alcaraz-Pérez, et al.. Inflammasome Regulates Hematopoiesis through Cleavage of the Master Erythroid Transcription Factor GATA1. Immunity, 2019, Epub ahead of print. 10.1016/j.immuni.2019.05.005 . hal-02148333

HAL Id: hal-02148333

<https://hal.science/hal-02148333>

Submitted on 5 Jun 2019

HAL is a multi-disciplinary open access archive for the deposit and dissemination of scientific research documents, whether they are published or not. The documents may come from teaching and research institutions in France or abroad, or from public or private research centers.

L'archive ouverte pluridisciplinaire **HAL**, est destinée au dépôt et à la diffusion de documents scientifiques de niveau recherche, publiés ou non, émanant des établissements d'enseignement et de recherche français ou étrangers, des laboratoires publics ou privés.

INFLAMMASOME REGULATES HEMATOPOIESIS THROUGH CLEAVAGE OF THE MASTER ERYTHROID TRANSCRIPTION FACTOR GATA1

Sylwia D. Tyrkalska^{1,&#}, Ana B. Pérez-Oliva^{1,#,*}, Lola Rodríguez-Ruiz¹, Francisco J. Martínez-Morcillo¹, Francisca Alcaraz-Pérez², Francisco J. Martínez-Navarro¹, Christophe Lachaud³, Nouraz Ahmed⁴, Timm Schroeder⁴, Irene Pardo-Sánchez¹, Sergio Candel^{1,\$}, Azucena López-Muñoz¹, Avik Choudhuri⁵, Marlies P. Rossmann⁵, Leonard I. Zon^{5,6}, María L. Cayuela², Diana García-Moreno^{1,*}, Victoriano Mulero^{1,*,#}

¹Universidad de Murcia, IMIB-Arrixaca, Murcia, Spain.

²Hospital Clínico Universitario Virgen de la Arrixaca, IMIB-Arrixaca, Murcia, Spain.

³Aix-Marseille University, Inserm, CNRS, Institut Paoli-Calmettes, CRCM, Marseille, France.

⁴Department of Biosystems Science and Engineering, ETH Zurich, Basel, Switzerland.

⁵Harvard University, Cambridge, MA 02138, USA; Stem Cell Program and Division of Hematology/Oncology, Children's Hospital Boston, Howard Hughes Medical Institute, Boston, MA 02115, USA.

⁶Dana-Farber Cancer Institute, Boston, MA 02215, USA; Harvard Stem Cell Institute, Boston, MA 02115, USA; Harvard Medical School, Boston, MA 02115, USA.

[&]Current address: Cambridge Institute for Medical Research, University of Cambridge, Cambridge CB2 0XY, UK.

^{\$}Current address: Department of Medicine, University of Cambridge, MRC Laboratory of Molecular Biology, Cambridge CB2 0QH, UK.

[#]These authors contributed equally

^{*}Corresponding authors: ABPO (anabpo@um.es), DGM (dianagm@um.es) and VM (vmulero@um.es)

[¶]Lead contact: VM (vmulero@um.es)

Summary (word count 149)

Chronic inflammatory diseases are associated with altered hematopoiesis that could result in neutrophilia and anemia. Here we report that genetic or chemical manipulation of different inflammasome components altered the differentiation of hematopoietic stem and progenitor cells (HSPC) in zebrafish. Although the inflammasome was dispensable for the emergence of HSPC, it was intrinsically required for their myeloid differentiation. In addition, Gata1 transcript and protein amounts increased in inflammasome-deficient larvae, enforcing erythropoiesis and inhibiting myelopoiesis. This mechanism is evolutionarily conserved, since pharmacological inhibition of the inflammasome altered erythroid differentiation of human erythroleukemic K562 cells. In addition, caspase-1 inhibition rapidly upregulated GATA1 protein in mouse HSPC promoting their erythroid differentiation. Importantly, pharmacological inhibition of the inflammasome rescued zebrafish disease models of neutrophilic inflammation and anemia. These results indicate that the inflammasome plays a major role in the pathogenesis of neutrophilia and anemia of chronic diseases and reveal druggable targets for therapeutic interventions.

Keywords: Hematopoiesis, GATA1, Caspase-1, inflammasome, anemia, neutrophilic inflammation, zebrafish, mouse.

Introduction

Hematopoiesis is the process of blood cell formation that occurs during embryonic development and across adulthood to produce the blood system (Jagannathan-Bogdan and Zon, 2013). In vertebrates, blood development involves two main waves of hematopoiesis: the primitive one during early embryonic development, and the definitive one, which occurs in later stages (Gore et al., 2018). Definitive hematopoiesis engages multipotent hematopoietic stem cells (HSC), which migrate eventually to the bone marrow, or kidney marrow in zebrafish, and give rise to all blood lineages (Birbrair and Frenette, 2016; Cumano and Godin, 2007). HSC maturation involves the diversification of the lymphoid (T, B and NK cells) and myeloid and erythroid cell lineages (megakaryocytes, erythrocytes, granulocytes and macrophages) (Kondo, 2010; Kondo et al., 2003; Weissman, 2000). The decision for erythroid and myeloid fates depends mainly on two transcription factors GATA1 and SPI1 (also known as PU.1) that show a cross-inhibitory relationship resulting in physical interaction and direct competition between them for target genes (Nerlov et al., 2000; Rekhtman et al., 1999). However, there are many controversies about the factors responsible for terminal erythroid and myeloid differentiation and many unknown pathways being probably involved in its regulation (Cantor and Orkin, 2002; Hoppe et al., 2016). These unidentified pathways might have important clinical implications, since hematopoietic lineage bias is associated with increased incidence of diseases with prominent inflammatory components including atherosclerosis, autoimmunity, neurodegenerative disease, and carcinogenesis (Elias et al., 2017).

The inflammasomes are part of innate immune system and as intracellular receptors and sensors, they regulate the activation of inflammatory caspases, namely caspase-1 and caspase-11, which induce inflammation in response to infectious microbes and endogenous danger signals (Latz et al., 2013; Martinon et al., 2009). Typically inflammasome multiprotein complexes contain sensor proteins (nucleotide binding domain and leucine rich repeat gene family, NLRs), adaptor proteins (Apoptosis-associated speck-like protein containing a CARD, ASC), and effector caspases in a zymogen form, all being able to interact among themselves by homotypic interactions (Broz and Monack, 2011; Sharma and Kanneganti, 2016). Recently, it has been shown that also guanylate binding protein (GBP) protein family forms part of these multiprotein complexes (Pilla et al., 2014; Santos et al., 2018; Tyrkalska et al., 2016; Wallet et al., 2017; Zwack et al., 2017). Oligomerization of pro-caspases and

their autoproteolytic maturation lead to the processing and secretion of the pro-inflammatory cytokines interleukin-1 β (IL-1 β) and IL-18, and the induction of a form of programmed cell death called pyroptosis (Lamkanfi and Dixit, 2014). Lately, it has been reported that inflammasomes play crucial roles not only in infection and sterile inflammation but also in maintaining the basic cellular functions and controlling cellular homeostasis (Rathinam and Fitzgerald, 2016). Hence, additional uncovered regulatory functions for the inflammasomes have been shown in cell metabolism, proliferation, gene transcription and tumorigenesis (Rathinam and Fitzgerald, 2016; Sharma and Kanneganti, 2016). Although up to date little is known about the impact of the inflammasomes on hematopoiesis in general, it has been shown that the master erythroid transcription factor GATA1 can be cleaved *in vitro* by many caspases and *in vivo* by caspase-3 (De Maria et al., 1999).

Zebrafish has recently arisen as a powerful and useful model to study hematopoiesis (Berman et al., 2012; Ellett and Lieschke, 2010). Moreover, the genetic programs controlling hematopoiesis in the zebrafish are conserved with mammals, including humans, making them clinically relevant model systems (Jagannathan-Bogdan and Zon, 2013). Here we show the critical role played by the inflammasome in the regulation of erythroid and myeloid cell fate decision, and terminal erythroid differentiation. Furthermore, the results also have important clinical implications, since pharmacological inhibition of the inflammasome rescued zebrafish disease models of neutrophilic inflammation and anemia.

Results

Inflammasome inhibition decreases the number of neutrophils and macrophages in zebrafish larvae

Using zebrafish transgenic lines with green fluorescent neutrophils *Tg(mpx:eGFP)ⁱ¹¹⁴* or macrophages *Tg(mpeg1:eGFP)^{gl22}*, we quantitated the total number of both cell populations in whole larvae at 72 hpf. Genetic inhibition of several inflammasome components, namely Gbp4 and Asc resulted in significant decreased numbers of both neutrophils (Figure 1A, 1B) and macrophages (Figure S1A, S1B). Similarly, pharmacological inhibition of caspase-1 with the irreversible inhibitor Ac-YVAD-CMK (Tyrkalska et al., 2016) also resulted in decreased numbers of myeloid

cells (Figure 1C, 1D, S1C, S1D). These results were confirmed using an independent transgenic line *Tg(lyz:dsRED)^{nz50}* with labeled neutrophils (Figure S2A-S2D). Similarly, forced expression of the GTPase-deficient mutant of Gbp4 (KS/AA) as well as its double mutant (DM: KS/AA; Δ CARD), both of which behave as dominant negatives (DN) and inhibit inflammasome-dependent caspase-1 activation (Tyrkalska et al., 2016), resulted in decreased neutrophil number (Figure 1E, 1F). In addition, although activation of the inflammasome by forced expression of either Gbp4 or Asc failed to increase neutrophil (Figure 1E-1H) or macrophage (Figure S1E-S1F) numbers, it was able to rescue myeloid cell number and caspase-1 activity Asc-deficient fish (Figure 1G, 1H). Notably, however, simultaneous expression of Asc and Caspa, the functional homolog of mammalian CASP1 (Kuri et al., 2017; Masumoto et al., 2003; Tyrkalska et al., 2016), significantly increased the number of neutrophils (Figure 1I, 1J) and macrophages (Figure S1E, S1F).

The inflammasome regulates HSPC differentiation but is dispensable for their emergence

The differentiation of hematopoietic stem and progenitor cells (HSPC) into various blood cell types is controlled by multiple extrinsic and intrinsic factors and the deregulation in hematopoiesis can result in a number of hematological abnormalities (Morrison et al., 1997; Yang et al., 2007). Chronic inflammatory disorders are usually associated to neutrophilia and anemia, the so-called anemia of chronic diseases (ACD). Therefore, we next examined if the inflammasome also regulated erythropoiesis using a zebrafish transgenic line *Tg(lcr:eGFP)*, which has specific erythroid GFP expression (Ganis et al., 2012). The results showed that inflammasome activity had the inverse effect on erythrocytes than on myeloid cells; that is, erythrocyte abundance increased following genetic and pharmacological inflammasome inhibition, as assayed by flow cytometry (Figures 1K, 1L and S3). However, the expression of *cmyb* and *runx1*, which begins by 36 hpf and marks emerging definitive HSPC (Burns et al., 2005), was unaffected in guanylate binding protein-4 (Gbp4)- and Asc-deficient larvae at 48 hpf, as assayed by whole-mount in situ hybridization (WISH) (Figure S4). Similarly, the expression of *rag1*, which is expressed in differentiated thymic T cells was apparently unaffected by 5 dpf in inflammasome-deficient larvae (Figure S4). Collectively, these

results suggest a specific role of the inflammasome in the regulation of the balance between myelopoiesis and erythropoiesis.

To further confirm the role of the inflammasome in HSPC differentiation, we quantitated the number of HSPC in the transgenic line *Tg(runx1:GAL4; UAS:nfsB-mCherry)* which has fluorescently labeled HSPC (Tamplin et al., 2015), upon genetic or pharmacological inhibition of the inflammasome at different developmental stages (24 and 48 hpf). Inhibition of caspase-1 resulted in no changes in HSPC number at any point of the treatment, the result being confirmed in *Asc*-deficient larvae (Figure 2A-H). Furthermore, genetic inhibition of the inflammasome in neutrophils and HSPC by forced expression of DN forms of *Asc* (*Asc*ΔCARD) or *Gbp4* (*Gbp4*KS/AA) (Tyrkalska et al., 2016) using the specific promoters *mpx* and *runx1*, respectively, showed that the number of neutrophils declined in HSPC, but not in neutrophil, inflammasome-deficient larvae (Figure 2I-2L). Collectively these results confirm the dispensability of the inflammasome for HSPC emergence and renewal, but that is intrinsically required for HSPC differentiation.

Zebrafish is an elegant model for cell ablation by use of the specific transgenic lines that expresses the bacterial nitroreductase, encoded by the *nfsB* gene, under the control of specific promoters (Davison et al., 2007). The nitroreductase enzyme converts the drug metronidazole (Mtz) to a cytotoxic product, which induces cell death in expressing cells to achieve tissue-specific ablation having no effect on other cell populations (Curado et al., 2007; Curado et al., 2008; Prajsnar et al., 2012). Using this approach, we ablated neutrophils in *Tg(mpx:Gal4; UAS:nfsB-mCherry)* zebrafish by applying Mtz for 24h and then analyzed neutrophil recovery in the presence or absence of the caspase-1 inhibitor for 6 days (Figure 3). Mtz robustly reduced neutrophil number, which began to recover by 4 days post-ablation in control larvae (Figure 3). However, pharmacological inhibition of the inflammasome impaired neutrophil recovery upon ablation and strongly decreased neutrophil abundance in non-ablated larvae (Figure 3). As expected, continuous Mtz treatment resulted in drastic neutrophil decline but did not show any toxic effect on control larvae that did not express the nitroreductase (Figure 3). These results indicate that the inflammasome is indispensable for myeloid differentiation of HSPC.

Inflammasome inhibition impairs demand-driven myelopoiesis

In response to infection, the hematopoietic tissue enhances production and mobilization of neutrophils, which have short lifespan and are needed in large numbers to fight infections. This process is called demand-driven or emergency hematopoiesis (Hall et al., 2012). To check whether only steady-state or also demand-driven hematopoiesis were regulated by the inflammasome, we infected with *Salmonella enterica* serovar Typhimurium in the otic vesicle of 48 hpf larvae and counted total neutrophil numbers at 24 hpi in the presence or absence of the irreversible caspase-1 inhibitor Ac-YVAD-CMK. It was observed that pharmacological inhibition of the inflammasome was able to abrogate infection-driven myelopoiesis, which resulted in increased number of neutrophils in infected larvae (Figure 4A, 4B). Notably, forced expression of granulocyte colony-stimulating factor (Gcsf), which stimulates both steady-state and demand-driven granulopoiesis in zebrafish (Hall et al., 2012; Stachura et al., 2013), increased neutrophil number to similar amounts in wild type and Asc-deficient larvae, as well as in larvae treated with the caspase-1 inhibitor, without affecting caspase-1 activity (Figure 4C-4F). Nevertheless, Gcsf was unable to rescue the higher susceptibility to *S. Typhimurium* infection of Asc-deficient and caspase-1 inhibitor-treated larvae (Figure 4G, 4H), confirming previous results in Gbp4-deficient larvae (Tyrkalska et al., 2016). All these results also suggest that the inflammasome regulates the myeloid and erythroid fate decision besides the function of mature myeloid cells.

*The inflammasome shifts the *spi1/gata1* balance favoring myeloid differentiation*

The regulation of Spi1 and Gata1 has been shown to be critical for the differentiation of myeloid and erythroid cells, respectively, in all vertebrates. As inhibition of the inflammasome resulted in a hematopoietic lineage bias, that is, reduced myeloid and increased erythroid blood cells, we next analyzed *spi1* and *gata1* transcript amounts by RT-qPCR and whole-mount *in situ* hybridization (WISH). We observed decreased *spi1/gata1* transcript ratio at 24 hpf in Gbp4- and Asc-deficient larvae, while the transcript amounts of the genes encoding Spi1-downstream pivotal macrophage and neutrophil growth factors, namely macrophage- and granulocyte colony stimulating factors (*mcsf* and *gcsf* genes), were unaffected (*mcsf* and *gcsf*) (Figures 4I, S4). Importantly, Gata1 protein amounts were also fine-tuned by the inflammasome, since

genetic inhibition of either Asc or Gbp4 was able to increase Gata1, while forced expression of Asc and Caspa, which resulted in increased number of neutrophils and macrophages (Figure 1I, 1J, S1E, S1F), robustly decreased Gata1 (Figure 4J). Therefore, the inflammasome regulates HSPC fate decision through fine-tuning Gata1 amounts.

The regulation of HSPC differentiation by the inflammasome is evolutionarily conserved

We next sought to determine if the inflammasome also regulates mouse hematopoiesis. We quantified the impact of CASP1 inhibition on GATA1 and SPI1 protein amounts in single mouse hematopoietic stem cells (HSC) using time-lapse microscopy immediately following their isolation. Time-lapse movies were acquired for 24 h to quantify early dynamics in GATA1 amounts before the first cell division using a homozygous and extensively validated GATA1 and SPI1 reporter mouse line expressing a fusion of GATA1 and monomeric Cherry (mCherry) and SPI1 and enhanced yellow fluorescent protein (eYFP) from the endogenous *Gata1* and *Spil* genomic loci, respectively (Hoppe et al., 2016). Inhibition of CASP1 up-regulated Gata1-mCherry protein in differentiating HSC within 18 h, while SPI1-eYFP protein amounts were unaffected (Figures 5A-5C). In line with these results, CASP1 inhibition increased megakaryocyte-erythrocyte (MegE) colony output of mouse HSCs at expense of granulocyte-monocyte (GM) colonies (Figure 5D). These data demonstrate that at the time of normal lineage decision making in HSC, the manipulation of GATA1 protein amounts through the inflammasome can alter lineage choice, further confirming our *in vivo* studies in zebrafish.

To further explore the relevance of the inflammasome in erythroid differentiation, we then used the human erythroleukemic K562 cell line, which can be differentiated to erythrocytes in the presence of hemin (Andersson et al., 1979; Koeffler and Golde, 1980). GATA1 amounts and activity were found to increase in the early stages of erythropoiesis, while they decreased in the late phase to allow terminal erythroid differentiation (Ferreira et al., 2005; Whyatt et al., 2000). As expected, we observed that hemin promoted gradual hemoglobin accumulation and decreased GATA1 protein amounts from 0 to 48 h (Figure 6A, 6D). Notably, the transcript

amounts of *NLRC4*, *NLRP3* and *CASP1* gradually increased, while those of *PYCARD* peaked at 12 h and then declined to basal amounts (Figure S5). Furthermore, *CASP1* activity (Figure 6B) and protein amounts (Figure 6C) progressively increased during erythroid differentiation, and *CASP1* was uniformly distributed in both the cytosol and the nucleus (Figure 6C). In addition, pharmacological inhibition of *CASP1* in K562 cells impaired hemin-induced erythroid differentiation, assessed as hemoglobin accumulation, and inhibited GATA1 decline at both 24 (Figure 6E) and 48 h (Figure 6F, 6G). As the Ac-YVAD-CMK inhibitor may also inhibit *CASP4*, we used the *CASP4* and *CASP5* inhibitor Ac-LEVD-CHO and found that it failed to affect the erythroid differentiation of K562 cells and their GATA1 amounts (Figure S6A).

CASP1 may target several proteins to regulate HSPC differentiation. One possibility is that *CASP1* directly cleaves GATA1, as it has been reported for *CASP3*, which negatively regulates erythropoiesis through GATA1 cleavage (De Maria et al., 1999). Therefore, we studied whether recombinant human *CASP1* was able to cleave human GATA1 *in vitro*. The results showed that recombinant *CASP1* cleaved GATA1 generating N- and C-terminal proteolytic fragments of about 30 and 15 kDa, respectively (Figure S7A-S7C). *CASP1* cleavage of GATA1 at residues D276 and/or D300 may generate the obtained fragments, so we generated single and double *CASP1* mutants (D276E and D300E) and found that *CASP1* was only able to cleave GATA1 at residue D300 (Figure S7D). Collectively, all these results uncover an evolutionarily conserved role of the inflammasome in the regulation of erythroid vs. myeloid fate decision and terminal erythroid differentiation via cleavage of GATA1.

Pharmacological inhibition of the inflammasome rescues zebrafish models of neutrophilic inflammation and anemia

Hematopoietic lineage bias is associated with chronic inflammatory diseases, cancer and aging (Elias et al., 2017; Marzano et al., 2018; Wu et al., 2014). Neutrophilic dermatosis are a group of diseases characterized by the accumulation of neutrophils in the skin (Marzano et al., 2018). We used a zebrafish *Spint1a*-deficient line as model of neutrophilic dermatosis, since it is characterized by strong neutrophil infiltration into the skin (Carney et al., 2007; Mathias et al., 2007). It was found that *Spint1a*-deficient larvae had increased caspase-1 activity (Figure 7A) and an altered *spil/gata1* ratio (Figure 7B). Notably, although pharmacological inhibition of caspase-1 failed to rescue

neutrophil skin infiltration of *Spint1a*-deficient animals (Figure 7C, 7E), it was able to rescue their robust neutrophilia (Figure 7D, 7E). Similarly, genetic inactivation of *caspa* with CRISPR-Cas9 also rescued neutrophilia, but not neutrophil infiltration, of *Spint1a*-deficient animals (Figure 7F, 7G). However, CASP4 and CASP5 inhibition failed to rescue both neutrophilia and neutrophil infiltration in this animal model (Figure S6B).

We next model Diamond-Blackfan anemia, a ribosomopathy caused by inefficient translation of GATA1 (Danilova and Gazda, 2015), in zebrafish larvae by reducing Gata1 amounts using a specific morpholino. We firstly titrated the morpholino and found that 1.7 ng/egg resulted in larvae with mild, moderate and severe anemia (Figure 7H), while 0.85 ng/egg and 3.4 ng/egg had little or drastic effects, respectively (data not shown). We thus examined whether pharmacological inhibition of caspase-1 could rescue hemoglobin alterations of Gata1-deficient larvae. For these experiments, we treated larvae with the reversible inhibitor of caspase-1 Ac-YVAD-CHO for 24 to 48 hpf and analyzed hemoglobin at 72 hpf to allow terminal erythroid differentiation in the absence of caspase-1 inhibition. The results show that treatment of larvae for 24 h with this reversible inhibitor of caspase-1 partially rescued hemoglobin defects in Gata1-deficient larvae and *Spi1*/Gata1 protein ratio (Figure 7I, 7J). These results taken together demonstrate that pharmacological inhibition of caspase-1 rescues hematopoietic lineage bias *in vivo*.

Discussion

We report here an evolutionarily conserved signaling pathway which links the inflammasome with HSPC differentiation. Although previous reports have shown that proinflammatory signals are indispensable for HSPC emergence (Espin-Palazon et al., 2018), the roles of these signals, and in particular the inflammasome, in HSPC formation, maintenance and differentiation are largely unknown. During periods of hematopoietic stress induced by chemotherapy or viral infection, activation of NLRP1a prolongs cytopenia, bone marrow hypoplasia, and immunosuppression (Masters et al., 2012). This effect is mediated by the CASP1-dependent, but ASC-independent, pyroptosis of hematopoietic progenitor cells (Masters et al., 2012). In addition, the NLRP3 inflammasome has been found to drive clonal expansion and pyroptotic cell death in myelodysplastic syndromes (Basiorka et al., 2016). Our results demonstrate that although the inflammasome is dispensable for HSPC emergence in zebrafish, it cell-intrinsically regulates HSPC differentiation in homeostasis conditions at two

different levels: erythroid vs. myeloid cell fate decision and terminal erythroid differentiation. Although CASP1 may target several proteins to regulate both processes, one plausible scenario is the cleavage of GATA1 at residue D300 by CASP1, which would result in the quick degradation of GATA1, since we were unable to detect processed GATA1 in zebrafish larvae or K562 cells. The rapid induction of GATA1 protein amounts in mouse HSC upon pharmacological inhibition of CASP1 supports this hypothesis. Although SPI1 protein amounts were unaffected by CASP1 inhibition in HSC, SPI1 expression will be reduced at later stages of differentiation, but as a consequence of reduced GM differentiation, not as a reason for it (Strasser et al., 2018). Our model is compatible with our recent report showing that the expression of SPI1 is not relevant for the erythroid vs. myeloid switch, since sometimes is already downregulated or off when GATA1 expression starts but sometimes is still expressed (Hoppe et al., 2016; Strasser et al., 2018). However, once GATA1 starts to be expressed, the HSPC always differentiate into MegE with GATA1 high and SPI1 low or off (Hoppe et al., 2016). Therefore, reduced GATA1 amounts upon inflammasome activation lead to reduced erythropoiesis and thus increased myelopoiesis. At the same time, inflammatory signaling through TNF and IL1b has recently been shown to directly upregulate SPI1 protein directly in HSCs in vitro and *in vivo* (Etzrodt et al., 2018; Pietras et al., 2016).

Similarly, terminal erythroid differentiation also requires GATA1 cleavage by CASP1. Thus, we observed that pharmacological inhibition of CASP1 leads to GATA1 accumulation and altered erythroid differentiation of K562 cells. This is not unexpected, since GATA1 inhibits terminal erythroid differentiation *in vitro* (Whyatt et al., 1997) and *in vivo* (Whyatt et al., 2000). Although it remains to be elucidated the signals responsible for the activation of the inflammasome in erythroid vs. myeloid cell fate decision and terminal erythroid differentiation as well as the inflammasome components involved, our genetic studies in zebrafish show that Gbp4 and Asc are both intrinsically required *in vivo* by HSPC to regulate their differentiation. A mild activation of CASP1 is anticipated to avoid the pyroptotic cell death of hematopoietic cells. This may be achieved by the assembly of small ASC specks and/or the low abundance of caspase-1 in hematopoietic progenitor cells and erythroid precursors, as occurs in neutrophils that exhibit sustained interleukin-1 β (IL-1 β) release without pyroptosis compared to macrophages (Boucher et al., 2018; Chen et al., 2014).

Hematopoietic lineage bias is associated to increased incidence of diseases with prominent inflammatory components, including atherosclerosis, autoimmunity, neurodegenerative disease and carcinogenesis (Elias et al., 2017). In particular, neutrophilic dermatosis is characterized by the accumulation of neutrophils in the skin and cutaneous lesions (Marzano et al., 2018). We observed that the robust neutrophilia of a zebrafish model of skin inflammation is reversed by pharmacological inhibition of Caspa, despite skin lesions and neutrophil infiltration are largely unaffected. Therefore, inflammasome activation alters granulopoiesis through altered Gata1 expression and, more importantly, its pharmacological inhibition restores the Gata1 regulation and neutrophil counts. Furthermore, the critical role of the inflammasome in the regulation of Gata1 has also been pointed out by the ability of pharmacological inhibition of Caspa to restore erythroid hemoglobin and Gata1 amounts, and to decline Spi1 amounts, in a zebrafish model of reduced Gata1, as occurs in Diamond-Blackfan anemia (Danilova and Gazda, 2015). Collectively, all these results point out to the ability of inflammasome inhibition as a therapeutic approach to treat human diseases with associated hematopoietic lineage bias, such as neutrophilic inflammation (Marzano et al., 2018; Ray and Kolls, 2017), ACD(Weiss, 2015) and chemotherapy-induced anemia (Testa et al., 2015). The availability of an orally active CASP1 inhibitor, VX-765, with high specificity, excellent pharmacokinetic properties and efficacy in rheumatoid arthritis and skin inflammation mouse models (Wannamaker et al., 2007), further supports the clinical testing of CASP1 inhibitors in hematopoietic lineage bias disorders.

Acknowledgments

We strongly acknowledge I. Fuentes and P. Martínez for their excellent technical assistance with the zebrafish experiments. We also thank Profs. S.A. Renshaw, P. Crosier, G. Lieschke, M. Hammerschmidt, and M. Halpern for the zebrafish lines, N. Inohara for the zebrafish Asc-Myc and Caspa constructs, C. Hall for the zebrafish Gcsfa construct, D. Holden for the ST strain, and P. Pelegrín and A. Baroja-Mazo for critical reading of the manuscript.

Funding

This work was supported by the Spanish Ministry of Science, Innovation and Universities (grants BIO2014-52655-R and BIO2017-84702-R to VM and PI13/0234 to

MLC, PhD fellowship to FJMM and Juan de la Cierva postdoctoral contract to FAP), all co-funded with Fondos Europeos de Desarrollo Regional/European Regional Development Funds), Fundación Séneca-Murcia (grant 19400/PI/14 to MLC), the University of Murcia (postdoctoral contracts to ABPO and DGM, and PhD fellowship to FJMM), SNF grant 179490 to TS, and the European 7th Framework Initial Training Network FishForPharma (PhD fellowship to SDT, PITG-GA-2011-289209). The funders had no role in study design, data collection and analysis, decision to publish, or preparation of the manuscript.

Author contributions

VM conceived the study; SDT, ABPO, CL, TS, LIZ, MLC, DGM and VM designed research; SDT, ABPO, LRR, FJMM, FAP, FJMN, CL, NA, IPS, SC, ALM, AC, MPR and DGM performed research; SDT, ABPO, LRR, FJMM, FAP, FJMN, CL, NA, TS, IPS, SC, ALM, AC, MPR, LIZ, MLC, DGM and VM analyzed data; and SDT and VM wrote the manuscript with minor contribution from other authors.

Conflict of interest

L.I.Z. is a founder and stockholder of Fate Therapeutics, Inc., Scholar Rock and Camp4 Therapeutics. A patent for the use of caspase-1 inhibitors to treat anemia has been registered by Universidad de Murcia, Boston Children's Hospital and Instituto Murciano de Investigación Biosanitaria (#P201831288).

References

- Andersson, L.C., Nilsson, K., and Gahmberg, C.G. (1979). K562--a human erythroleukemic cell line. *Int J Cancer* 23, 143-147.
- Angosto, D., Lopez-Castejon, G., Lopez-Munoz, A., Sepulcre, M.P., Arizcun, M., Meseguer, J., and Mulero, V. (2012). Evolution of inflammasome functions in vertebrates: Inflammasome and caspase-1 trigger fish macrophage cell death but are dispensable for the processing of IL-1beta. *Innate Immun* 18, 815-824.
- Basiorka, A.A., McGraw, K.L., Eksioglu, E.A., Chen, X., Johnson, J., Zhang, L., Zhang, Q., Irvine, B.A., Cluzeau, T., Sallman, D.A., *et al.* (2016). The NLRP3 inflammasome functions as a driver of the myelodysplastic syndrome phenotype. *Blood* 128, 2960-2975.
- Berman, J., Payne, E., and Hall, C. (2012). The zebrafish as a tool to study hematopoiesis, human blood diseases, and immune function. *Adv Hematol* 2012, 425345.
- Birbrair, A., and Frenette, P.S. (2016). Niche heterogeneity in the bone marrow. *Ann N Y Acad Sci* 1370, 82-96.

- Boucher, D., Monteleone, M., Coll, R.C., Chen, K.W., Ross, C.M., Teo, J.L., Gomez, G.A., Holley, C.L., Bierschenk, D., Stacey, K.J., *et al.* (2018). Caspase-1 self-cleavage is an intrinsic mechanism to terminate inflammasome activity. *J Exp Med* *215*, 827-840.
- Broz, P., and Monack, D.M. (2011). Molecular mechanisms of inflammasome activation during microbial infections. *Immunol Rev* *243*, 174-190.
- Burger, A., Lindsay, H., Felker, A., Hess, C., Anders, C., Chiavacci, E., Zaugg, J., Weber, L.M., Catena, R., Jinek, M., *et al.* (2016). Maximizing mutagenesis with solubilized CRISPR-Cas9 ribonucleoprotein complexes. *Development* *143*, 2025-2037.
- Burns, C.E., Traver, D., Mayhall, E., Shepard, J.L., and Zon, L.I. (2005). Hematopoietic stem cell fate is established by the Notch-Runx pathway. *Genes Dev* *19*, 2331-2342.
- Cabezas-Wallscheid, N., Klimmeck, D., Hansson, J., Lipka, D.B., Reyes, A., Wang, Q., Weichenhan, D., Lier, A., von Paleske, L., Renders, S., *et al.* (2014). Identification of regulatory networks in HSCs and their immediate progeny via integrated proteome, transcriptome, and DNA methylome analysis. *Cell Stem Cell* *15*, 507-522.
- Cantor, A.B., and Orkin, S.H. (2002). Transcriptional regulation of erythropoiesis: an affair involving multiple partners. *Oncogene* *21*, 3368-3376.
- Carney, T.J., von der Hardt, S., Sonntag, C., Amsterdam, A., Topczewski, J., Hopkins, N., and Hammerschmidt, M. (2007). Inactivation of serine protease Matrilysin1 by its inhibitor Hail1 is required for epithelial integrity of the zebrafish epidermis. *Development* *134*, 3461-3471.
- Chen, K.W., Gross, C.J., Sotomayor, F.V., Stacey, K.J., Tschopp, J., Sweet, M.J., and Schroder, K. (2014). The neutrophil NLRC4 inflammasome selectively promotes IL-1 β maturation without pyroptosis during acute Salmonella challenge. *Cell Rep* *8*, 570-582.
- Cumano, A., and Godin, I. (2007). Ontogeny of the hematopoietic system. *Annu Rev Immunol* *25*, 745-785.
- Curado, S., Anderson, R.M., Jungblut, B., Mumm, J., Schroeter, E., and Stainier, D.Y. (2007). Conditional targeted cell ablation in zebrafish: a new tool for regeneration studies. *Dev Dyn* *236*, 1025-1035.
- Curado, S., Stainier, D.Y., and Anderson, R.M. (2008). Nitroreductase-mediated cell/tissue ablation in zebrafish: a spatially and temporally controlled ablation method with applications in developmental and regeneration studies. *Nat Protoc* *3*, 948-954.
- Danilova, N., and Gazda, H.T. (2015). Ribosomopathies: how a common root can cause a tree of pathologies. *Dis Model Mech* *8*, 1013-1026.
- Davison, J.M., Akitake, C.M., Goll, M.G., Rhee, J.M., Gosse, N., Baier, H., Halpern, M.E., Leach, S.D., and Parsons, M.J. (2007). Transactivation from Gal4-VP16 transgenic insertions for tissue-specific cell labeling and ablation in zebrafish. *Dev Biol* *304*, 811-824.
- De Maria, R., Zeuner, A., Eramo, A., Domenichelli, C., Bonci, D., Grignani, F., Srinivasula, S.M., Alnemri, E.S., Testa, U., and Peschle, C. (1999). Negative regulation of erythropoiesis by caspase-mediated cleavage of GATA-1. *Nature* *401*, 489-493.
- de Oliveira, S., Reyes-Aldasoro, C.C., Candel, S., Renshaw, S.A., Mulero, V., and Calado, A. (2013). Cxcl8 (IL-8) mediates neutrophil recruitment and behavior in the zebrafish inflammatory response. *J Immunol* *190*, 4349-4359.

- Elias, H.K., Bryder, D., and Park, C.Y. (2017). Molecular mechanisms underlying lineage bias in aging hematopoiesis. *Semin Hematol* 54, 4-11.
- Ellett, F., and Lieschke, G.J. (2010). Zebrafish as a model for vertebrate hematopoiesis. *Curr Opin Pharmacol* 10, 563-570.
- Ellett, F., Pase, L., Hayman, J.W., Andrianopoulos, A., and Lieschke, G.J. (2011). mpeg1 promoter transgenes direct macrophage-lineage expression in zebrafish. *Blood* 117, e49-56.
- Espin-Palazon, R., Weijts, B., Mulero, V., and Traver, D. (2018). Proinflammatory Signals as Fuel for the Fire of Hematopoietic Stem Cell Emergence. *Trends Cell Biol* 28, 58-66.
- Etzrodt, M., Ahmed, N., Hoppe, P.S., Loeffler, D., Skylaki, S., Hilsenbeck, O., Kokkaliaris, K.D., Kaltenbach, H.M., Stelling, J., Nerlov, C., and Schroeder, T. (2018). Inflammatory signals directly instruct PU.1 in HSCs via TNF. *Blood*.
- Ferreira, R., Ohneda, K., Yamamoto, M., and Philipsen, S. (2005). GATA1 function, a paradigm for transcription factors in hematopoiesis. *Mol Cell Biol* 25, 1215-1227.
- Ganis, J.J., Hsia, N., Trompouki, E., de Jong, J.L., DiBiase, A., Lambert, J.S., Jia, Z., Sabo, P.J., Weaver, M., Sandstrom, R., *et al.* (2012). Zebrafish globin switching occurs in two developmental stages and is controlled by the LCR. *Dev Biol* 366, 185-194.
- Gore, A.V., Pillay, L.M., Venero Galanternik, M., and Weinstein, B.M. (2018). The zebrafish: A fantastic model for hematopoietic development and disease. *Wiley Interdiscip Rev Dev Biol* 7, e312.
- Hall, C., Flores, M.V., Storm, T., Crosier, K., and Crosier, P. (2007). The zebrafish lysozyme C promoter drives myeloid-specific expression in transgenic fish. *BMC Dev Biol* 7, 42.
- Hall, C.J., Flores, M.V., Oehlers, S.H., Sanderson, L.E., Lam, E.Y., Crosier, K.E., and Crosier, P.S. (2012). Infection-responsive expansion of the hematopoietic stem and progenitor cell compartment in zebrafish is dependent upon inducible nitric oxide. *Cell Stem Cell* 10, 198-209.
- Halpern, M.E., Rhee, J., Goll, M.G., Akitake, C.M., Parsons, M., and Leach, S.D. (2008). Gal4/UAS transgenic tools and their application to zebrafish. *Zebrafish* 5, 97-110.
- Hilsenbeck, O., Schwarzfischer, M., Loeffler, D., Dimopoulos, S., Hastreiter, S., Marr, C., Theis, F.J., and Schroeder, T. (2017). fastER: a user-friendly tool for ultrafast and robust cell segmentation in large-scale microscopy. *Bioinformatics* 33, 2020-2028.
- Hilsenbeck, O., Schwarzfischer, M., Skylaki, S., Schauburger, B., Hoppe, P.S., Loeffler, D., Kokkaliaris, K.D., Hastreiter, S., Skylaki, E., Filipczyk, A., *et al.* (2016). Software tools for single-cell tracking and quantification of cellular and molecular properties. *Nat Biotechnol* 34, 703-706.
- Hoppe, P.S., Schwarzfischer, M., Loeffler, D., Kokkaliaris, K.D., Hilsenbeck, O., Moritz, N., Ende, M., Filipczyk, A., Gambardella, A., Ahmed, N., *et al.* (2016). Early myeloid lineage choice is not initiated by random PU.1 to GATA1 protein ratios. *Nature* 535, 299-302.
- Jagannathan-Bogdan, M., and Zon, L.I. (2013). Hematopoiesis. *Development* 140, 2463-2467.
- Kiel, M.J., Yilmaz, O.H., Iwashita, T., Yilmaz, O.H., Terhorst, C., and Morrison, S.J. (2005). SLAM family receptors distinguish hematopoietic stem and progenitor cells and reveal endothelial niches for stem cells. *Cell* 121, 1109-1121.

Koeffler, H.P., and Golde, D.W. (1980). Human myeloid leukemia cell lines: a review. *Blood* 56, 344-350.

Kondo, M. (2010). Lymphoid and myeloid lineage commitment in multipotent hematopoietic progenitors. *Immunol Rev* 238, 37-46.

Kondo, M., Wagers, A.J., Manz, M.G., Prohaska, S.S., Scherer, D.C., Beilhack, G.F., Shizuru, J.A., and Weissman, I.L. (2003). Biology of hematopoietic stem cells and progenitors: implications for clinical application. *Annu Rev Immunol* 21, 759-806.

Kuri, P., Schieber, N.L., Thumberger, T., Wittbrodt, J., Schwab, Y., and Leptin, M. (2017). Dynamics of in vivo ASC speck formation. *J Cell Biol* 216, 2891-2909.

Kwan, K.M., Fujimoto, E., Grabher, C., Mangum, B.D., Hardy, M.E., Campbell, D.S., Parant, J.M., Yost, H.J., Kanki, J.P., and Chien, C.B. (2007). The Tol2kit: a multisite gateway-based construction kit for Tol2 transposon transgenesis constructs. *Dev Dyn* 236, 3088-3099.

Lamkanfi, M., and Dixit, V.M. (2014). Mechanisms and functions of inflammasomes. *Cell* 157, 1013-1022.

Latz, E., Xiao, T.S., and Stutz, A. (2013). Activation and regulation of the inflammasomes. *Nat Rev Immunol* 13, 397-411.

Le Guyader, D., Redd, M.J., Colucci-Guyon, E., Murayama, E., Kissa, K., Briolat, V., Mordelet, E., Zapata, A., Shinomiya, H., and Herbomel, P. (2008). Origins and unconventional behavior of neutrophils in developing zebrafish. *Blood* 111, 132-141.

Liongue, C., Hall, C.J., O'Connell, B.A., Crosier, P., and Ward, A.C. (2009). Zebrafish granulocyte colony-stimulating factor receptor signaling promotes myelopoiesis and myeloid cell migration. *Blood* 113, 2535-2546.

Lopez-Castejon, G., Sepulcre, M.P., Mulero, I., Pelegrin, P., Meseguer, J., and Mulero, V. (2008). Molecular and functional characterization of gilthead seabream *Sparus aurata* caspase-1: the first identification of an inflammatory caspase in fish. *Mol Immunol* 45, 49-57.

Martinon, F., Mayor, A., and Tschopp, J. (2009). The inflammasomes: guardians of the body. *Annu Rev Immunol* 27, 229-265.

Marzano, A.V., Borghi, A., Wallach, D., and Cugno, M. (2018). A Comprehensive Review of Neutrophilic Diseases. *Clin Rev Allergy Immunol* 54, 114-130.

Masters, S.L., Gerlic, M., Metcalf, D., Preston, S., Pellegrini, M., O'Donnell, J.A., McArthur, K., Baldwin, T.M., Chevrier, S., Nowell, C.J., *et al.* (2012). NLRP1 inflammasome activation induces pyroptosis of hematopoietic progenitor cells. *Immunity* 37, 1009-1023.

Masumoto, J., Zhou, W., Chen, F.F., Su, F., Kuwada, J.Y., Hidaka, E., Katsuyama, T., Sagara, J., Taniguchi, S., Ngo-Hazelett, P., *et al.* (2003). Caspy, a zebrafish caspase, activated by ASC oligomerization is required for pharyngeal arch development. *J Biol Chem* 278, 4268-4276.

Mathias, J.R., Dodd, M.E., Walters, K.B., Rhodes, J., Kanki, J.P., Look, A.T., and Huttenlocher, A. (2007). Live imaging of chronic inflammation caused by mutation of zebrafish *Hai1*. *J Cell Sci* 120, 3372-3383.

Morrison, S.J., Shah, N.M., and Anderson, D.J. (1997). Regulatory mechanisms in stem cell biology. *Cell* 88, 287-298.

Nerlov, C., Querfurth, E., Kulesa, H., and Graf, T. (2000). GATA-1 interacts with the myeloid PU.1 transcription factor and represses PU.1-dependent transcription. *Blood* 95, 2543-2551.

Pfaffl, M.W. (2001). A new mathematical model for relative quantification in real-time RT-PCR. *Nucleic Acids Res* 29, e45.

- Pietras, E.M., Mirantes-Barbeito, C., Fong, S., Loeffler, D., Kovtonyuk, L.V., Zhang, S., Lakshminarasimhan, R., Chin, C.P., Techner, J.M., Will, B., *et al.* (2016). Chronic interleukin-1 exposure drives haematopoietic stem cells towards precocious myeloid differentiation at the expense of self-renewal. *Nat Cell Biol* 18, 607-618.
- Pilla, D.M., Hagar, J.A., Haldar, A.K., Mason, A.K., Degrandi, D., Pfeffer, K., Ernst, R.K., Yamamoto, M., Miao, E.A., and Coers, J. (2014). Guanylate binding proteins promote caspase-11-dependent pyroptosis in response to cytoplasmic LPS. *Proc Natl Acad Sci U S A* 111, 6046-6051.
- Prajsnar, T.K., Hamilton, R., Garcia-Lara, J., McVicker, G., Williams, A., Boots, M., Foster, S.J., and Renshaw, S.A. (2012). A privileged intraphagocyte niche is responsible for disseminated infection of *Staphylococcus aureus* in a zebrafish model. *Cell Microbiol* 14, 1600-1619.
- Rathinam, V.A., and Fitzgerald, K.A. (2016). Inflammasome Complexes: Emerging Mechanisms and Effector Functions. *Cell* 165, 792-800.
- Ray, A., and Kolls, J.K. (2017). Neutrophilic Inflammation in Asthma and Association with Disease Severity. *Trends Immunol* 38, 942-954.
- Rekhtman, N., Radparvar, F., Evans, T., and Skoultschi, A.I. (1999). Direct interaction of hematopoietic transcription factors PU.1 and GATA-1: functional antagonism in erythroid cells. *Genes Dev* 13, 1398-1411.
- Renshaw, S.A., Loynes, C.A., Trushell, D.M., Elworthy, S., Ingham, P.W., and Whyte, M.K. (2006). A transgenic zebrafish model of neutrophilic inflammation. *Blood* 108, 3976-3978.
- Santos, J.C., Dick, M.S., Lagrange, B., Degrandi, D., Pfeffer, K., Yamamoto, M., Meunier, E., Pelczar, P., Henry, T., and Broz, P. (2018). LPS targets host guanylate-binding proteins to the bacterial outer membrane for non-canonical inflammasome activation. *EMBO J* 37.
- Schindelin, J., Arganda-Carreras, I., Frise, E., Kaynig, V., Longair, M., Pietzsch, T., Preibisch, S., Rueden, C., Saalfeld, S., Schmid, B., *et al.* (2012). Fiji: an open-source platform for biological-image analysis. *Nat Methods* 9, 676-682.
- Sharma, D., and Kanneganti, T.D. (2016). The cell biology of inflammasomes: Mechanisms of inflammasome activation and regulation. *J Cell Biol* 213, 617-629.
- Smith, R.D., Malley, J.D., and Schechter, A.N. (2000). Quantitative analysis of globin gene induction in single human erythroleukemic cells. *Nucleic Acids Res* 28, 4998-5004.
- Stachura, D.L., Svoboda, O., Campbell, C.A., Espin-Palazon, R., Lau, R.P., Zon, L.I., Bartunek, P., and Traver, D. (2013). The zebrafish granulocyte colony-stimulating factors (Gcsfs): 2 paralogous cytokines and their roles in hematopoietic development and maintenance. *Blood* 122, 3918-3928.
- Strasser, M.K., Hoppe, P.S., Loeffler, D., Kokkaliaris, K.D., Schroeder, T., Theis, F.J., and Marr, C. (2018). Lineage marker synchrony in hematopoietic genealogies refutes the PU.1/GATA1 toggle switch paradigm. *Nat Commun* 9, 2697.
- Tamplin, O.J., Durand, E.M., Carr, L.A., Childs, S.J., Hagedorn, E.J., Li, P., Yzaguirre, A.D., Speck, N.A., and Zon, L.I. (2015). Hematopoietic stem cell arrival triggers dynamic remodeling of the perivascular niche. *Cell* 160, 241-252.
- Testa, U., Castelli, G., and Elvira, P. (2015). Experimental and investigational therapies for chemotherapy-induced anemia. *Expert Opin Investig Drugs* 24, 1433-1445.
- Thisse, C., Thisse, B., Schilling, T.F., and Postlethwait, J.H. (1993). Structure of the zebrafish *snail1* gene and its expression in wild-type, spadetail and no tail mutant embryos. *Development* 119, 1203-1215.

- Tyrkalska, S.D., Candel, S., Angosto, D., Gomez-Abellan, V., Martin-Sanchez, F., Garcia-Moreno, D., Zapata-Perez, R., Sanchez-Ferrer, A., Sepulcre, M.P., Pelegrin, P., and Mulero, V. (2016). Neutrophils mediate Salmonella Typhimurium clearance through the GBP4 inflammasome-dependent production of prostaglandins. *Nat Commun* 7, 12077.
- Tyrkalska, S.D., Candel, S., Perez-Oliva, A.B., Valera, A., Alcaraz-Perez, F., Garcia-Moreno, D., Cayuela, M.L., and Mulero, V. (2017). Identification of an Evolutionarily Conserved Ankyrin Domain-Containing Protein, Caiap, Which Regulates Inflammasome-Dependent Resistance to Bacterial Infection. *Front Immunol* 8, 1375.
- Wallet, P., Benaoudia, S., Mosnier, A., Lagrange, B., Martin, A., Lindgren, H., Golovliov, I., Michal, F., Basso, P., Djebali, S., *et al.* (2017). IFN-gamma extends the immune functions of Guanylate Binding Proteins to inflammasome-independent antibacterial activities during Francisella novicida infection. *PLoS Pathog* 13, e1006630.
- Wannamaker, W., Davies, R., Namchuk, M., Pollard, J., Ford, P., Ku, G., Decker, C., Charifson, P., Weber, P., Germann, U.A., *et al.* (2007). (S)-1-((S)-2-([1-(4-amino-3-chloro-phenyl)-methanoyl]-amino)-3,3-dimethyl-butanoyl)-pyrrolidine-2-carboxylic acid ((2R,3S)-2-ethoxy-5-oxo-tetrahydro-furan-3-yl)-amide (VX-765), an orally available selective interleukin (IL)-converting enzyme/caspase-1 inhibitor, exhibits potent anti-inflammatory activities by inhibiting the release of IL-1beta and IL-18. *J Pharmacol Exp Ther* 321, 509-516.
- Weiss, G. (2015). Anemia of Chronic Disorders: New Diagnostic Tools and New Treatment Strategies. *Semin Hematol* 52, 313-320.
- Weissman, I.L. (2000). Translating stem and progenitor cell biology to the clinic: barriers and opportunities. *Science* 287, 1442-1446.
- Westerfield, M. (2000). The Zebrafish Book. A Guide for the Laboratory Use of Zebrafish Danio* (Brachydanio) rerio. (Eugene, OR.: University of Oregon Press.).
- White, R.M., Sessa, A., Burke, C., Bowman, T., LeBlanc, J., Ceol, C., Bourque, C., Dovey, M., Goessling, W., Burns, C.E., and Zon, L.I. (2008). Transparent adult zebrafish as a tool for in vivo transplantation analysis. *Cell Stem Cell* 2, 183-189.
- Whyatt, D., Lindeboom, F., Karis, A., Ferreira, R., Milot, E., Hendriks, R., de Bruijn, M., Langeveld, A., Gribnau, J., Grosveld, F., and Philipsen, S. (2000). An intrinsic but cell-nonautonomous defect in GATA-1-overexpressing mouse erythroid cells. *Nature* 406, 519-524.
- Whyatt, D.J., Karis, A., Harkes, I.C., Verkerk, A., Gillemans, N., Elefanty, A.G., Vairo, G., Ploemacher, R., Grosveld, F., and Philipsen, S. (1997). The level of the tissue-specific factor GATA-1 affects the cell-cycle machinery. *Genes Funct* 1, 11-24.
- Wu, W.C., Sun, H.W., Chen, H.T., Liang, J., Yu, X.J., Wu, C., Wang, Z., and Zheng, L. (2014). Circulating hematopoietic stem and progenitor cells are myeloid-biased in cancer patients. *Proc Natl Acad Sci U S A* 111, 4221-4226.
- Yang, L., Wang, L., Kalfa, T.A., Cancelas, J.A., Shang, X., Pushkaran, S., Mo, J., Williams, D.A., and Zheng, Y. (2007). Cdc42 critically regulates the balance between myelopoiesis and erythropoiesis. *Blood* 110, 3853-3861.
- Zwack, E.E., Feeley, E.M., Burton, A.R., Hu, B., Yamamoto, M., Kanneganti, T.D., Bliska, J.B., Coers, J., and Brodsky, I.E. (2017). Guanylate Binding Proteins Regulate Inflammasome Activation in Response to Hyperinjected Yersinia Translocon Components. *Infect Immun* 85.

Figure Legends

Figure 1. Inflammasome inhibition results in decreased neutrophil but increased erythrocyte numbers in zebrafish. *Tg(mpx:eGFP)* (A-J) and *Tg(lcr:eGFP)* (L) zebrafish one-cell embryos were injected with standard control (Std), Asc or Gbp4 MOs (A, B, G, H, K), and/or with antisense (As), Gbp4^{WT}, Gbp4^{KS/AA}, Gbp4^{ΔCARD}, Gbp4^{DM}, Asc or Caspa mRNAs (e-h). Alternatively, *Tg(mpx:eGFP)* (C, D, I, J) and *Tg(lcr:eGFP)* (K) embryos left uninjected were manually dechorionated at 24 or 48 hpf and treated by immersion with DMSO or the irreversible caspase-1 inhibitor Ac-YVAD-CMK (C1INH). Each dot represents the number of neutrophils (A, C, E, G, I) from a single larva or the percentage of erythrocytes from each pool of 50 larvae (K, L), while the mean ± SEM for each group is also shown. The sample size (n) is indicated for each treatment. Representative images of green channels of whole larvae for the different treatments are also shown. Scale bars, 500 μm. Caspase-1 activity in whole larvae was determined for each treatment at 72 hpf (one representative caspase-1 activity assay out of the three carried out is shown) (B, D, F, H, J). *p<0.05; **p<0.01; ***p<0.001 according to ANOVA followed by Tukey multiple range test. See also Figures S1-S4.

Figure 2. The inflammasome is intrinsically required for HSC differentiation but is dispensable for their emergence in zebrafish. (A-H) *Tg(runx1:GAL4; UAS:nfsb-mCherry)* zebrafish embryos were manually dechorionated at 24 or 48 hpf and treated by immersion with DMSO or the irreversible caspase-1 inhibitor Ac-YVAD-CMK (C1INH) for 24 or 48 h (A-F). Alternatively, *Tg(runx1:GAL4; UAS:nfsb-mCherry)* one-cell embryos were injected with standard control (Std) or Asc MOs (G-H). Each dot represents the number of HSCs from a single larva, while the mean ± SEM for each group is also shown. The sample size (n) is indicated for each treatment. Representative images of red channels of whole larvae for the different treatments are also shown (A, C, E, G). Scale bars, 500 μm. Caspase-1 activity was determined for each treatment from 48 or 72 hpf larvae (one representative caspase-1 activity assay out of the three carried out is shown) (B, D, F, H). (I-L) *Tg(runx1:gal4; UAS:Gbp4KS/AA)* (I), *Tg(mpx:gal4; UAS:Gbp4KS/AA)* (J), *Tg(runx1:gal4; UAS:AscΔCARD)* (K), *Tg(mpx:gal4; UAS:AscΔCARD)* (L) larvae were fixed at 72 hpf and stained with Sudan black for the detection of neutrophils. Each dot represents the number of neutrophils

from a single larva, while the mean \pm SEM for each group is also shown. The sample size (n) is indicated for each treatment. ns, not significant; * $p < 0.05$; ** $p < 0.01$; *** $p < 0.001$ according to Student *t* test. See also Figure S4.

Figure 3. Inflammasome activity is indispensable for myelopoiesis in zebrafish.

Tg(mpx:GAL4; UAS:nsfb-mCherry) zebrafish larvae were manually dechorionated at 48 hpf and treated by immersion with metronidazole (Mtz) for 24 h and then with DMSO or the irreversible caspase-1 inhibitor Ac-YVAD-CMK (C1INH) for the next 4 days. Control groups were treated for 5 days with Mtz (all time). (A) Each dot represents the number of neutrophils from a single larva, while the mean \pm SEM for each group is also shown. (B) Representative images of red channels of whole larvae for the different treatments and time points are also shown. Scale bars, 500 μ m. *** $p < 0.001$ according to ANOVA followed by Tukey multiple range test.

Figure 4. Infection is unable to bypass the inflammasome requirement for neutrophil production in zebrafish. (A-H). *Tg(mpx:eGFP)* zebrafish one-cell embryos

were injected with standard control (Std), Gbp4 or Asc MOs in combination with antisense (As), Gcsfa, Asc, Caspa mRNAs (C, D, G, H-J) or left uninjected, manually dechorionated at 48 hpf and treated by immersion with DMSO or the irreversible caspase-1 inhibitor Ac-YVAD-CMK (C1INH) (A, B, E, F). Larvae were then infected at 48 hpf with *S. Typhimurium* (S.I.) in the otic vesicle (A, B) or the yolk sac (G, H) and the number of neutrophils was counted in the whole body at 24 hpi (A, B) or 72 hpf (C-F) and the survival was determined during 5 days after the infection (G, H). Each dot represents the number of neutrophils from a single larva, while the mean \pm SEM for each group is also shown. The sample size (n) is indicated for each treatment. Note that the 4 non-infected group showed no mortality and the 4 lines are overlapping. Representative images of green channels of whole larvae for the different treatments are shown (A-F). Scale bars, 500 μ m. Caspase-1 activity was determined in whole larvae for each treatment at 72 hpf (one representative caspase-1 activity assay out of the three carried out is shown) (B, D, F). (I-J) The mRNA amounts of *spilb*, *gatala*, *mcsf* and *gcsf* in larval tails were measured by RT-qPCR at 24 hpf (I), while the protein amounts of Gatala and histone H3 were determined using western blot in larval tails at 24 hpf (J). A densitometry analysis was performed to check the differences between treatments. ns, not significant; * $p < 0.05$; ** $p < 0.01$; *** $p < 0.001$ according to ANOVA

followed by Tukey multiple range test (A-F, I, J) or log rank test with Bonferroni correction (G, H).

Figure 5. Inflammasome inhibition increases GATA1 protein amounts and megakaryocyte-erythrocyte colony output in mouse HSCs. (A) Flow cytometry gating scheme used for isolation of mouse HSCs. HSCs are sorted as Lin⁻cKit⁺Sca1⁺CD48⁻CD34⁻CD135⁻CD150⁺. Numbers in the plots indicate % of lineage depleted BM cells. (B, C) Caspase1-inhibitor (C1INH) treatment increases Gata1 protein amounts (B) without affecting Spi1 protein amounts (C) in mouse HSCs. Data were acquired by time-lapse imaging of freshly-sorted HSCs (DMSO=605, C1INH=749 HSCs) from 12-week old Spi1-eYFP and Gata1-mCherry fluorescent protein fusion reporter mice in IMDM + BIT + SCF + Epo + Tpo + IL3 + IL6 supplemented with or without 100 μ M of the irreversible caspase-1 inhibitor Ac-YVAD-CMK (2 biological replicates). (D) Caspase1-inhibitor treatment increased MegE colony output at the expense of GM colonies. HSCs from Spi1-eYFP and Gata1-mCherry reporter mice were single-cell sorted into 384 well plates in IMDM + BIT + SCF + Epo + Tpo + IL3 + IL6 supplemented with or without 100 μ M Ac-YVAD-CMK. At day 8, color conjugated CD41-APC and CD16/32-BV421 antibodies were added to the colonies and colonies were imaged and manually scored using morphology, Spi1-eYFP and CD16/32 signal to indicate GM colonies and Gata1-mCherry and CD41 signal to indicate MegE colonies. Data represent mean percentage of types of colonies formed from HSCs from 4 independent experiments (244 total colonies scored, Error bars = SEM). ns, not significant; * p <0.05; ** p <0.01; *** p <0.001 according to two tailed Student's T-test (A, B) and Chi-square test (C).

Figure 6. Pharmacological inhibition of caspase-1 impairs erythroid differentiation of K562 cells. K562 cells were incubated with 50 μ M hemin for the indicated times in the presence or absence of the irreversible caspase-1 inhibitor Ac-YVAD-CMK (C1INH, 100 μ M) and the cell pellets imaged (A, E, F), lysed and resolved by SDS-PAGE and immunoblotted with anti-GATA1 and anti-ACTB antibodies (A, E, F), processed for the quantification of caspase-1 activity using the fluorogenic substrate YVAD-AFC (B, G) and for immunofluorescence using anti-CASP1 (C) and anti-GATA1 (D) antibodies. Cell extracts from HEK293T transfected with GATA1-FLAG and empty FLAG were included as mobility controls in a. Nuclei were stained with

DAPI. One representative caspase-1 activity (B, G), western blot (A, E, F) and hemoglobin accumulation (A, E, F) assay out of the three carried out is shown, while one representative immunofluorescence staining (C, D) assay out of the two carried out is shown. Scale bars, 5 μ m. *** p <0.001 according to ANOVA followed by Tukey multiple range test. See also Figures S5-S7.

Figure 7. Pharmacological inhibition of caspase-1 rescues zebrafish models of neutrophilic inflammation and anemia. (A-G) Wild type and *spint1a* mutant larvae were manually dechorionated and treated from 1-3 dpf with the irreversible caspase-1 inhibitor Ac-YVAD-CMK (C1INH, 100 μ M) (A-E) or one-cell embryos injected with control (std) or *caspa* sgRNA and recombinant Cas9 (F, G). Caspase-1 activity (A), the *spi1b/gata1a* gene expression ratio (B), neutrophil dispersion (C) and the number of neutrophils (D-G) were then determined. Each dot represents the number of neutrophils from a single larva, while the mean \pm SEM for each group is also shown. The sample size (n) is indicated for each treatment. Representative overlay images of green and bright field channels of whole larvae for the different treatments are shown (e, g). Scale bar, 500 μ m. (H-J) Zebrafish one-cell embryos were injected with standard control (Std) or Gata1a MOs, manually dechorionated at 24 hpf and treated by immersion with DMSO or the reversible caspase-1 inhibitor Ac-YVAD-CHO (C1INH) for 24-48 hpf. The inhibitor was then washed off and the larvae incubated until 72 hpf. Representative pictures of Gata1a-deficient larvae with mild, moderate and severe anemia (H), quantification of the phenotype of larval treated with DMSO or C1INH (I) and immunoblot of larval extracts with anti-Gata1a, anti-Spi1b and anti-Actb antibodies (J). One representative caspase-1 activity (A) and western blot (J) assay out of the three and two, respectively, carried out is shown. ns, not significant; * p <0.05; ** p <0.01; *** p <0.001 according to Student *t* test (A, B), ANOVA followed by Tukey multiple range test (C, D, F) and Fisher's exact test (I).

STAR Methods

Contact for Reagent and Resource Sharing

Further information and requests for resources and reagents should be directed to and will be fulfilled by the Lead Contact, Victoriano Mulero (vmulero@um.es).

Experimental Model and Subject Details

Zebrafish (*Danio rerio* H.) were obtained from the Zebrafish International Resource Center and mated, staged, raised and processed as described (Westerfield, 2000). The lines *roy^{a9/a9}*; *nacre^{w2/w2}* (*casper*) (White et al., 2008), *Tg(mpx:eGFP)ⁱ¹¹⁴* (Renshaw et al., 2006), *Tg(mpeg1:eGFP)^{sl22}*, *Tg(mpeg1:GAL4)^{sl25}* (Ellett et al., 2011), *Tg(lyz:dsRED)^{nz50}* (Hall et al., 2007), *Tg(mpx:Gal4.VP16)ⁱ²²²* (Davison et al., 2007), *Tg(lcr:eGFP)^{cz3325}* (Ganis et al., 2012), *Tg(runx1:GAL4)^{utn6}* (Tamplin et al., 2015), *Tg(UAS:nfsB-mCherry)^{c264}* (Davison et al., 2007) and *Tg(spint1a)^{hi2217}* (Carney et al., 2007; Mathias et al., 2007) have been previously described. The experiments performed comply with the Guidelines of the European Union Council (Directive 2010/63/EU) and the Spanish RD 53/2013. Experiments and procedures were performed as approved by the Bioethical Committees of the University of Murcia (approval numbers #75/2014, #216/2014 and 395/2017).

Mouse experiments were performed with 12-16 week old, male, Spi1-eYFP and Gata-mCherry1 reporter mice (C57BL/6J background). Animal experiments were approved according to Institutional guidelines of ETH Zurich and Swiss Federal Law by veterinary office of Canton Basel-Stadt, Switzerland (approval number #2655).

Method Details

DNA Construct and generation of transgenics

The *uas:AscΔCARD-GFP* construct was generated by MultiSite Gateway assemblies using LR Clonase II Plus (Life Technologies) according to standard protocols and using Tol2kit vectors described previously (Kwan et al., 2007). The expression constructs *Gbp4*, *Gbp4KS→AA*, *Gbp4ΔCARD*, *Gbp4KS→AA* and *ΔCARD* (double mutant, DM) and *uas:gbp4KS/AA* (Tyrkalska et al., 2016); *Asc-Myc* and *Caspa* (Masumoto et al., 2003); and *Gcsfa* (Liongue et al., 2009) were previously described.

The line *Tg(UAS:gbp4KS/AA)^{ums3}* was previously described (Tyrkalska et al., 2016). *Tg(UAS:ascΔCARD-GFP)^{ums4}* was generated by microinjecting 0.5-1 nl into the yolk sac of one-cell-stage embryos a solution containing 100 ng/μl *uas:ascΔCARD-GFP* and *uas:gbp4KS→AA* constructs, respectively, and 50 ng/μl Tol2 RNA in microinjection buffer (×0.5 Tango buffer and 0.05% phenol red solution) using a microinjector (Narishige).

Morpholino, RNA and protein injection and chemical treatments of zebrafish larvae

Specific morpholinos (Gene Tools) were resuspended in nuclease-free water at 1 mM (Table S1). *In vitro*-transcribed RNA was obtained following the manufacturer's instructions (mMESSAGE mMACHINE kit, Ambion). Morpholinos and RNA were mixed in microinjection buffer and microinjected into the yolk sac of one-cell-stage embryos using a microinjector (Narishige) (0.5-1 nl per embryo). The same amount of MOs and/or RNA was used in all experimental groups.

For genetic inactivation of *caspa*, injection mixes were prepared with 500 ng/μl EnGen® Cas9 NLS from *Streptococcus pyogenes* (New England Biolabs) and 100 ng/μl control (5'-3') or *caspa* (5'-GAACCAATTCCGAAGGATCC-3') sgRNA in 300 mM KCl buffer, incubated for 5 min at 37°C and used directly without further storage (Burger et al., 2016).

In some experiments, 1-2 dpf embryos were manually dechorionated and treated for 1 to 3 dpf at 28°C by bath immersion with the caspase-1 inhibitors Ac-YVAD-CMK (irreversible) or Ac-YVAD-CHO (reversible), and the reversible caspase-4 and caspase-5 inhibitor Ac-LEVD-CHO (100 μM, Peptanova) diluted in egg water supplemented with 1% DMSO or with Metronidazole (Mtz, 5 mM, Sigma-Aldrich).

Live imaging, Sudan black staining of neutrophils, neutrophil ablation and erythrocyte determination in zebrafish larvae

At 48 and 72 hpf, larvae were anesthetized in tricaine and mounted in 1% (wt/vol) low-melting-point agarose (Sigma-Aldrich) dissolved in egg water (de Oliveira et al., 2013). Images were captured with an epifluorescence Lumar V12 stereomicroscope equipped with green and red fluorescent filters while animals were kept in their agar matrixes at 28.5°C. All images were acquired with the integrated camera on the stereomicroscope and were used for subsequently counting the total number of neutrophils, macrophages or HSPC in whole larvae.

In order to decrease pigmentation and improve the signal from Sudan black staining, 24 hpf larvae were incubated in 200 μ M 1-phenyl 2-thiourea (PTU) until 72 hpf, when they were anesthetized in buffered tricaine and fixed overnight at 4 °C in 4% methanol-free formaldehyde. On the next day, all the larvae were rinsed with PBS thrice, incubated for 15 min with Sudan black (#380B-1KT, Sigma-Aldrich) and washed extensively in 70% EtOH in water. After that a progressive rehydration was performed: 50% EtOH in PBS and 0.1% Tween 20 (PBT) (Sigma-Aldrich), 25% EtOH in PBT and PBT alone. Finally, the larvae were visualized immediately using a Scope.A1 stereomicroscope equipped with a digital camera (AxioCam ICc 3, Zeiss) (Le Guyader et al., 2008).

For neutrophil ablation, larvae *Tg(mpx:Gal4.VP16; UAS:nsfb-mCherry)* were treated at 2 dpf with 5 mM Mtz and kept in dark. At 72 hpf the drug was removed and larvae were treated up to 7 dpf with 1% DMSO alone or containing Ac-YVAD-CMK (100 μ M). The inhibitor was refreshed every 24 h and the larvae were imaged once a day up to 7 dpf and the number of neutrophils determined (Davison et al., 2007; Halpern et al., 2008).

Erythrocyte counts were determined by flow cytometry. At 3 dpf, pools of 50 *Tg(lcr:eGFP)* larvae were anesthetized in tricaine, minced with a razor blade and incubated at 28°C for 30 min with 0.077 mg/ml Liberase (Roche). Afterwards, 10% FBS was added to inactivate liberase and the resulting cell suspension passed through a 40 μ m cell strainer. Flow cytometric acquisitions were performed on a FACSCALIBUR (BD) and analysis was based on forward scatter and side scatter, duplicate exclusion, exclusion of dead cells by addition of SYTOX Blue to a final concentration of 1 μ M, and GFP fluorescence. Before analyzing *Tg(lcr:eGFP)* zebrafish cell suspensions, the flow cytometry gates were set with suspensions from the same number of 3-dpf GFP-negative wild type larvae of the same background. Analyses were performed using FlowJo software (Treestar).

Infection assays of zebrafish larvae

For infection experiments, *Salmonella enterica* serovar Typhimurium strain 12023 (wild type) provided by Prof. Holden was used. Overnight cultures in Luria-Bertani medium (LB) were diluted 1/5 in LB with 0.3 M NaCl, incubated at 37 °C until 1.5 optical density at 600 nm was reached, and finally diluted in sterile PBS. Larvae of 2 dpf were anesthetized in embryo medium with 0.16 mg/ml tricaine and 10 bacteria

were injected into the yolk sac or otic vesicle. Larvae were allowed to recover in egg water at 28-29 °C, and monitored for clinical signs of disease or mortality over 5 days and neutrophil recruitment up to 24 hpi (Tyrkalska et al., 2016).

Whole-mount RNA in situ hybridization (WISH) in zebrafish larvae

Transparent Casper embryos were used for WISH (Thisse et al., 1993). *gata1a*, *spilb*, *gcsfr*, *cmyb*, *runx1* and *rag1* sense and antisense RNA probes were generated using the DIG RNA Labelling Kit (Roche Applied Science) from linearized plasmids. Embryos were imaged using a Scope.A1 stereomicroscope equipped with a digital camera (AxioCam ICc 3, Zeiss).

K562 cell culture and erythroid differentiation assays

K562 cells (CRL-243; American Type Culture Collection) were maintained in RPMI supplemented with 10% FCS, 2 mM Glutamin, and 1% penicillin-streptomycin (Life Technologies). Cells were maintained and split before confluence every 72h. For the differentiation, cells were treated with 50 µM hemin (#16009-13-5, Sigma-Aldrich), prepared as previously described (Smith et al., 2000), in the presence of 0.1% DMSO alone or containing 100 µM Ac-YVAD-CMK or Ac-LEVD-CHO. Cells were collected at different time points (0, 6, 12, 24, 48 hours post-hemin addition), centrifuged, washed with PBS and stored at -80 °C.

Caspase-1 activity assay

The caspase-1 activity was determined with the fluorometric substrate Z-YVAD-AFC (caspase-1 substrate VI, Calbiochem) as described previously (Angosto et al., 2012; Lopez-Castejon et al., 2008; Tyrkalska et al., 2016). In brief, 30 pooled zebrafish larvae and 8x10⁵ K562 cells were lysed in hypotonic cell lysis buffer [25 mM 4-(2-hydroxyethyl)piperazine-1-ethanesulfonic acid (HEPES), 5 mM ethylene glycol-bis(2-aminoethylether)-N,N,N',N'-tetraacetic acid (EGTA), 5 mM dithiothreitol (DTT), 1:20 protease inhibitor cocktail (Sigma-Aldrich), pH 7.5] on ice for 10 min. For each reaction, 80 µg protein were incubated for 90 min at 23° C with 50 µM Z-YVAD-AFC and 50 µl of reaction buffer [0.2% 3-[(3-cholamidopropyl)dimethylammonio]-1-propanesulfonate (CHAPS), 0.2 M HEPES, 20% sucrose, 29 mM DTT, pH 7.5]. After the incubation, the fluorescence of the AFC released from the Z-YVAD-AFC substrate was measured with a FLUOstart spectrofluorometer (BGM, LabTechnologies) at an

excitation wavelength of 405 nm and an emission wavelength of 492 nm. One representative caspase-1 activity assay out of the three carried out is shown accompanying each cell count.

Laser confocal microscopy

Cells were seeded in Poly-L-Lys Cellware 12mm cover (Corning), 50,000 cells in 100 μ l were allowed to attach to the cover during 10 min at room temperature, then medium and treatment were added. After hemin treatment cells were washed with PBS, fixed with 4% paraformaldehyde in PBS 10 min, incubated 20 min at room temperature with 20 mM glycine, permeabilized with 0.5% NP40 and blocked for 1 h with 2% BSA. Cells were then labeled with corresponding primary antibody, followed by Alexa 568-conjugated secondary antibody (Thermo Fisher Scientific). Samples were mounted using a mounting medium from Dako and examined with a Leica laser scanning confocal microscope AOBS and software (Leica Microsystems). The images were acquired in a $1,024 \times 1,024$ pixel format in sequential scan mode between frames to avoid cross-talk. The objective used was HCX PL APO CS $\times 63$ and the pinhole value was 1, corresponding to 114.73 μ m.

Immunoblotting

Lysis buffer for mammalian cell lysis contained 50 mM Tris-HCl (pH 7.5), 150 mM NaCl, 1 mM EDTA, 1 mM EGTA, 1% (w/v) NP-40 and fresh protease inhibitor (1/20, P8340, Sigma-Aldrich), while for zebrafish larvae lysis contained 1% SDS. Protein quantification was done with BCA kit using BSA as a standard. Cell lysates (40 μ g) in SDS sample buffer were subjected to electrophoresis on a polyacrylamide gel and transferred to PVDF membranes. The membranes were incubated for 1 h with TTBS containing 5% (w/v) skimmed dried milk powder or 2% (w/v) BSA. The membranes were immunoblotted in the same buffer 16 h at 4°C with the indicated primary antibodies. The blots were then washed with TTBS and incubated for 1 h at room temperature with secondary HRP-conjugated antibodies diluted 2,500-fold in 5% (w/v) skimmed milk in TTBS. After repeated washes, the signal was detected with the enhanced chemiluminescence reagent and ChemiDoc XRS Biorad. The primary antibodies used are: rabbit polyclonal to human GATA1 (1/200, #sc1234, Santa Cruz Biotechnology) for confocal assay, rabbit mAb to human GATA1 (1/200, #3535, Cell Signaling) for immunoblotting, rabbit polyclonal to CASP1 (1/200, #sc56036 Santa

Cruz Biotechnology) for confocal assay, rabbit polyclonal to zebrafish Gata1a and Spi1b (1/2000, #GTX128333 and GTX128266, GeneTex), rabbit polyclonal to histone H3 (1/200, #ab1791, Abcam) and Monoclonal ANTI-FLAG® M2-Peroxidase (HRP) antibody produced in mouse (A8592 Sigma-Aldrich). Densitometry analysis has been performed using Fiji Image J software (Schindelin et al., 2012).

Immunoprecipitation and recombinant caspase-1 assay

Pull down assays were also performed as described previously (Tyrkalska et al., 2017), with small modifications. Cells were washed twice with PBS, solubilized in lysis buffer (50 mM Tris-HCl, , pH 7.7, 150 mM NaCl, 1% NP-40 and protease inhibitor cocktail) during 30 min in agitation and centrifuged ($13,000 \times g$, 10 min). Cell lysate (1 mg) was incubated for 2 h at 4°C under gentle agitation with 40 µl of slurry of ANTIFLAG® M2 (#A2220 Sigma-Aldrich). The immunoprecipitates were washed four times with lysis buffer containing 0.15 M NaCl, washed twice with PBS and incubated with 10 IU recombinant caspase-1 (#GTX65025, GeneTex) in reaction buffer (50 mM Hepes, pH 7.2, 50mM NaCl, 0.1% Chaps, 10 mM EDTA, 5% Glycerol, and 10 mM DTT) during 2 h at 37 °C. The resin was boiled in SDS sample buffer 5 min at 95 °C and the bound proteins were resolved on 4-15% SDS-PAGE (BioRad TGX #456-1084) and transferred to PVDF membranes for 1h at 300 mA. Blots were probed with antibodies to FLAG and GATA1 (see above).

Analysis of gene expression

Total RNA was extracted from 10^6 K562 cells, whole embryos or larvae (60) or larval tails (100) with TRIzol reagent (Thermo Fisher Scientific) following the manufacturer's instructions and treated with DNase I, amplification grade (1 U/µg RNA; Invitrogen). SuperScript III RNase H⁻ Reverse Transcriptase (Invitrogen) was used to synthesize first-strand cDNA with oligo(dT)18 primer from 1 µg of total RNA at 50°C for 50 min. Real-time PCR was performed with an ABI PRISM 7500 instrument (Applied Biosystems) using Power SYBR Green Master Mix (ThermoFisher Scientific). Reaction mixtures were incubated for 10 min at 95°C, followed by 40 cycles of 15 s at 95°C, 1 min at 60°C, and finally 15 s at 95°C, 1 min 60°C and 15 s at 95°C. For each mRNA, gene expression was normalized to the ribosomal protein S11 (*rps11*) for zebrafish or β-actin (*ACTB*) for human cells content in each sample following the

Pfaffl method (Pfaffl, 2001). The primers used are shown in (Table S2). In all cases, each PCR was performed with triplicate samples and repeated with at least two independent samples.

Isolation of mouse HSCs

Male Spi1-eYFP and Gata1-mCherry mice were euthanized and isolation of HSCs was performed according to previously described protocols (Cabezas-Wallscheid et al., 2014; Hoppe et al., 2016; Kiel et al., 2005). Briefly, femurs, tibiae and vertebrae of adult mice were isolated and crushed in FACS buffer (2% FCS (PAA) + 1mM EDTA in PBS). Bone marrow suspension was subjected to ACK (Lonza) lysis buffer for 2 minutes followed by lineage depletion steps including incubation with biotinylated antibodies cocktail of CD3e, CD19, B220, CD11b, Gr-1 and Ter-119 for 7 minutes, streptavidin-conjugated beads (Roche) for 7 minutes and immune-magnetic (Stem Cell Technologies) separation for 7 minutes. Lineage depleted cells were stained with color-conjugated primary antibodies for 90 minutes. FACS sorting of HSCs was performed on FACS ARIA III (BD Biosciences) using the Lineage⁻ Sca1⁺ cKit⁺ CD34⁻ CD48⁻ CD135⁻ CD150⁺. All steps were performed at 4°C.

Mouse single-cell liquid culture colony assay

Single-cell sort of HSCs was performed in plastic-bottom 384 well plates (Greiner Bio-one) using FACS ARIA III under standard permissive culture media as described (IMDM (Gibco) + 5 % BIT (Stem Cell Technologies) + P/S (Gibco) + SCF + Epo + Tpo + IL3 + IL6) with or without 100 µM Ac-YVAD-CMK. Plates were incubated at 37° C and 5% CO₂. At day 8, color-conjugated antibodies against lineage markers (CD41-APC + CD16/32-BV421) were added (1:5000 dilution) in wells, incubated for 3 hours at 37°C and 5% CO₂ and imaging of hematopoietic colonies was performed on Nikon Eclipse Ti-E microscope. Colonies were scored manually. Granulocyte-monocyte colonies were indicated by morphology, CD16/32 and SPI-eYFP expression while megakaryocyte-erythrocyte colonies were indicated by morphology, CD41 and GATA1-mCherry expression as previously described (Hoppe et al., 2016).

Time-lapse imaging of mouse HSCs

HSCs were sorted using FACS ARIA III and seeded in plastic-bottom 384 well plates (Greiner Bio-one) in multi-lineage supporting culture media as described (Hoppe et al., 2016) (IMDM (Gibco) + 5 % BIT (Stem Cell Technologies) + P/S (Gibco) + SCF + Epo + Tpo + IL3 + IL6) with or without 100 μ M Ac-YVAD-CMK. Time-lapse imaging and quantification of SPI1-eYFP and GATA1-mCherry in HSCs was performed using previously established protocols (Etzrodt et al., 2018; Hilsenbeck et al., 2017; Hilsenbeck et al., 2016; Hoppe et al., 2016).

Quantification and Statistical Analysis

Data are shown as mean \pm SEM and were analyzed by analysis of variance (ANOVA) and a Tukey or Bonferroni multiple range test to determine differences among groups. The differences between two samples were analyzed by the Student *t*-test. Fisher's exact and Chi-square tests were used for the analysis of contingency tables. A log rank test with the Bonferroni correction for multiple comparisons was used to calculate the statistical differences in the survival of the different experimental groups.

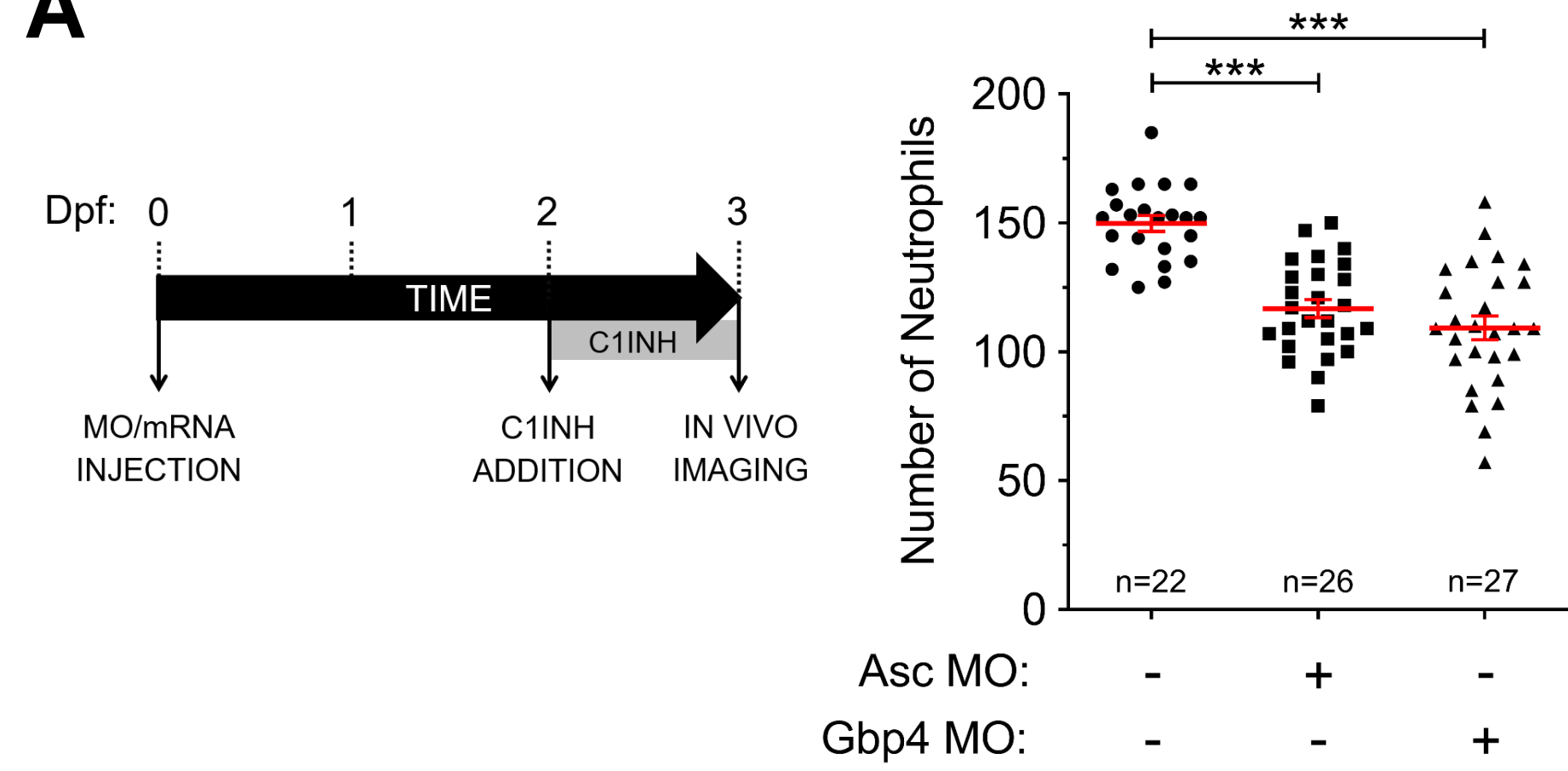
KEY RESOURCES TABLE

REAGENT or RESOURCE	SOURCE	IDENTIFIER
Antibodies		
Rabbit polyclonal to human GATA1	Santa Cruz Biotechnology	Cat#sc1234
Rabbit mAb to human GATA1	Cell Signaling	Cat#3535
Rabbit polyclonal to CASP1	Santa Cruz Biotechnology	Cat#sc56036
Rabbit polyclonal to zebrafish Gata1a	GeneTex	Cat#GTX128333
Rabbit polyclonal to zebrafish Spi1b	GeneTex	Car#GTX128266
Rabbit polyclonal to histone H3	Abcam	Cat#ab1791
Monoclonal ANTI-FLAG® M2-Peroxidase (HRP) antibody produced in mouse	Sigma-Aldrich	Cat#A8592
Streptavidin-BV711	BD Biosciences	Cat#563262
anti-Sca1 conjugated with BV510	Biolegend	Cat#108129
anti-cKIT conjugated with BV421	Biolegend	Cat#105828
anti-CD135 conjugated with PerCPeFL710	eBioscience	Cat#46-1351-82
anti-CD34 conjugated with eFL660	eBioscience	Cat#50-0341-82
anti-CD48 conjugated with APCeFL780	eBioscience	Cat#47-0481-82
anti-CD150 conjugated with BV650	Biolegend	Cat#115932
anti-B220-Biotin	eBioscience	Cat#13-0452-86
anti-CD19-biotin	eBioscience	Cat#13-0191-86
antiCd3e-biotin	eBioscience	Cat#13-0031-85
anti-CD11b-biotin	eBioscience	Cat#13-0112-85
anti-Gr1-biotin	eBioscience	Cat#13-5931-85
anti-Ter119-biotin	eBioscience	Cat#13-5921-85
anti-CD41-APC	eBioscience	Cat#17-0411-82
anti-CD16/32-BV421	Biolegend	Cat#101332
Bacterial and Virus Strains		
<i>Salmonella enterica</i> serovar Typhimurium, strain 12023 (wild type)	Prof. David Holden	
Chemicals, Peptides, and Recombinant Proteins		
EnGen® Cas9 NLS from <i>Streptococcus pyogenes</i>	New England Biolabs	Cat#M0646

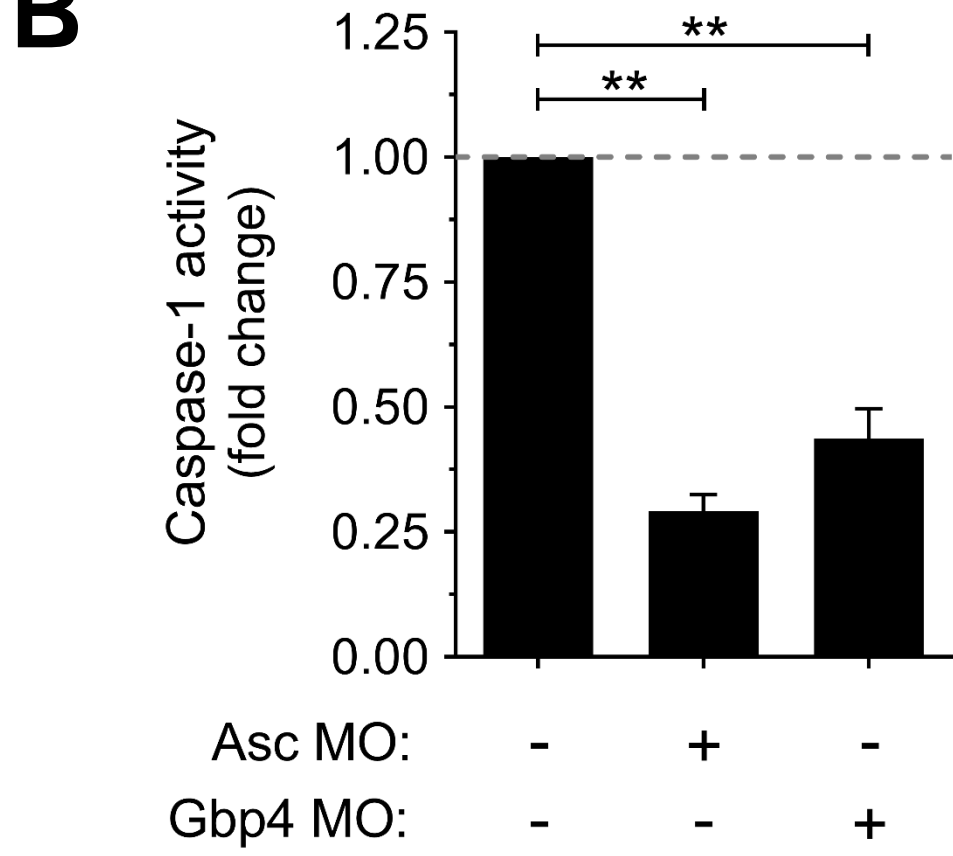
Ac-YVAD-CMK	Peptanova	Cat#3180-v
Ac-YVAD-CHO	Peptanova	Cat#3165-v
Ac-LEVD-CHO	Peptanova	Cat#864-42-v
Metronidazole	Sigma Aldrich	Cat#M1547
Sudan black	Sigma-Aldrich	Cat#380B-1KT
Z-YVAD-AFC	Merck	Cat#688225
ANTIFLAG® M2	Sigma-Aldrich	Cat#A2220
Recombinant caspase-1	GeneTex	Cat#GTX65025
4-15% SDS-PAGE	BioRad	Cat#456-1084
DNase I, amplification grade	ThermoFisher Scientific	Cat#18068015
SuperScript III RNase H ⁻ Reverse Transcriptase	ThermoFisher Scientific	Cat#18080085
Power SYBR Green Master Mix	ThermoFisher Scientific	Cat#4368708
Liberase TM research Grade	Sigma-Aldrich	Cat#05401119001
Experimental Models: Cell Lines		
K562	ATCC	Cat#CCL243
Experimental Models: Organisms/Strains		
Zebrafish casper line (<i>roy^{a9/a9}; nacre^{w2/w2}</i>)	Prof. LI Zon	
<i>Tg(mpx:eGFP)ⁱ¹¹⁴</i>	Prof. SA Renshaw	
<i>Tg(mpeg1:eGFP)^{g122}</i>	Prof. G Lieschke	
<i>Tg(mpeg1:GAL4)^{g125}</i>	Prof. G Lieschke	
<i>Tg(lyz:dsRED)^{nz50}</i>	Prof. P Crosier	
<i>Tg(mpx:Gal4.VP16)ⁱ²²²</i>	Prof. SA Renshaw	
<i>Tg(lcr:eGFP)^{cz3325}</i>	Prof. LI Zon	
<i>Tg(runx1:GAL4)^{utn6}</i>	Prof. LI Zon	
<i>Tg(UAS:nfsB-mCherry)^{c264}</i>	Prof. M. Halpern	
<i>Tg(spint1a)^{hi2217}</i>	Prof. M. Hammerschmidt	
SPI1-eYFP/GATA1-mCherry1 reporter mice (C57BL/6J background)	Prof. Timm Schroeder	
Recombinant DNA		
Tol2kit	Dr. K. Kwan	http://tol2kit.genetics.utah.edu/index.php/Main_Page

Figure 1

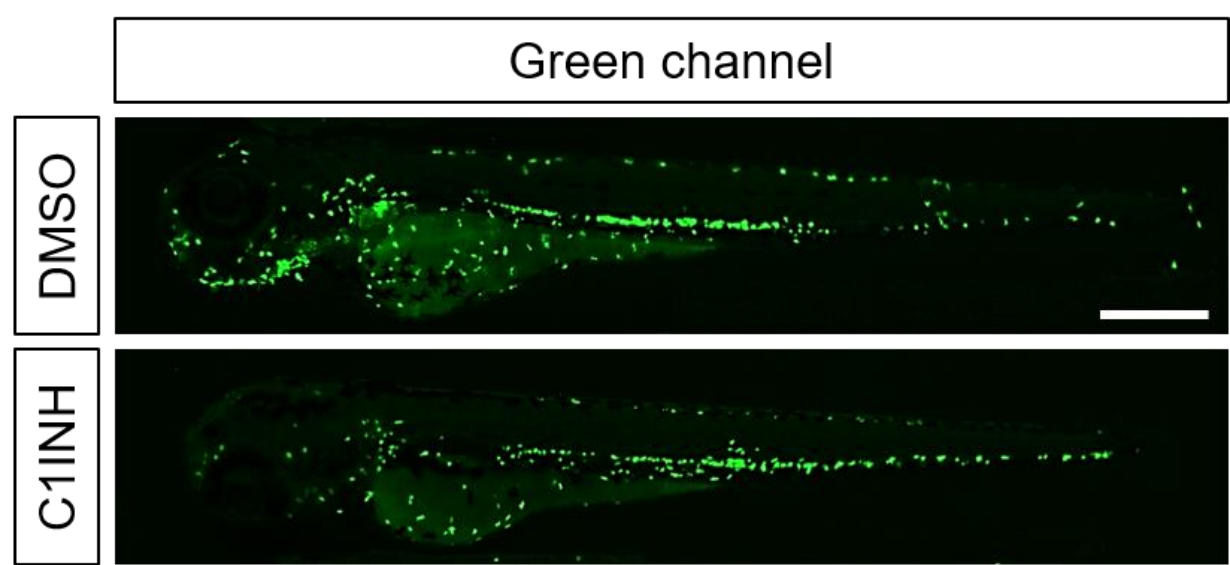
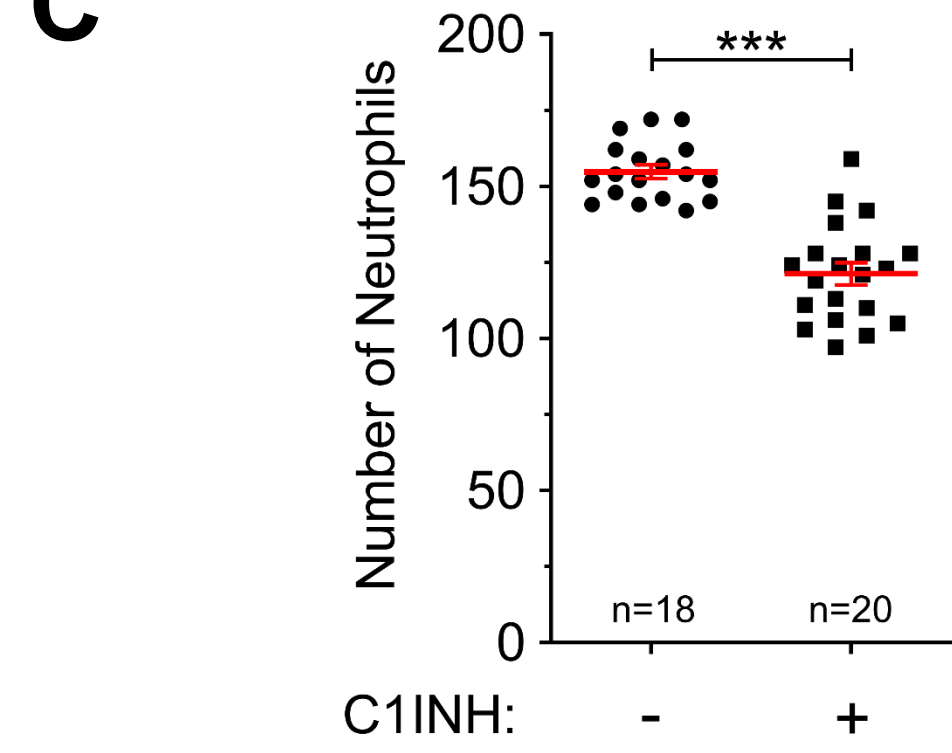
A



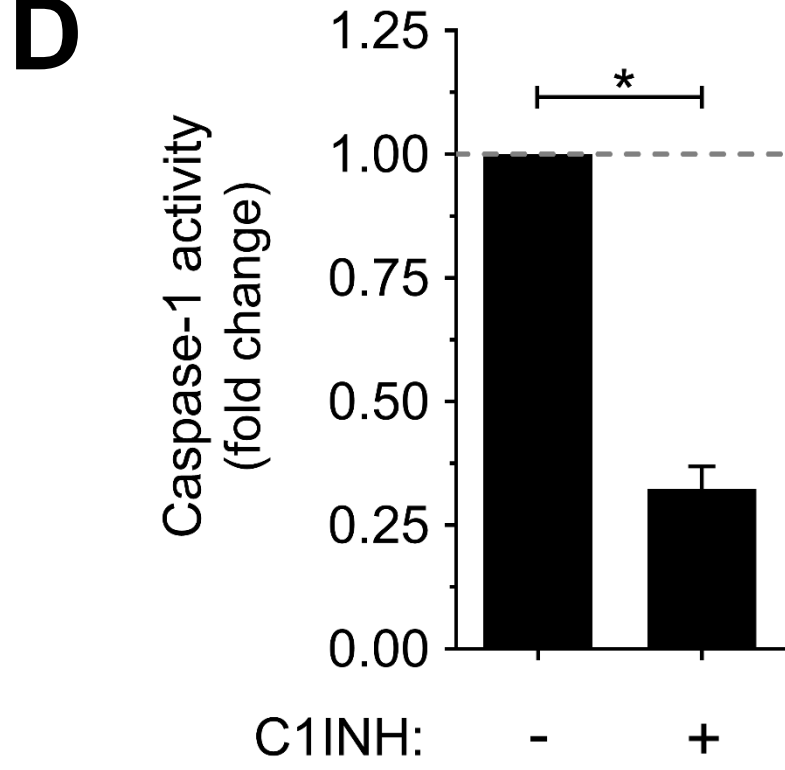
B



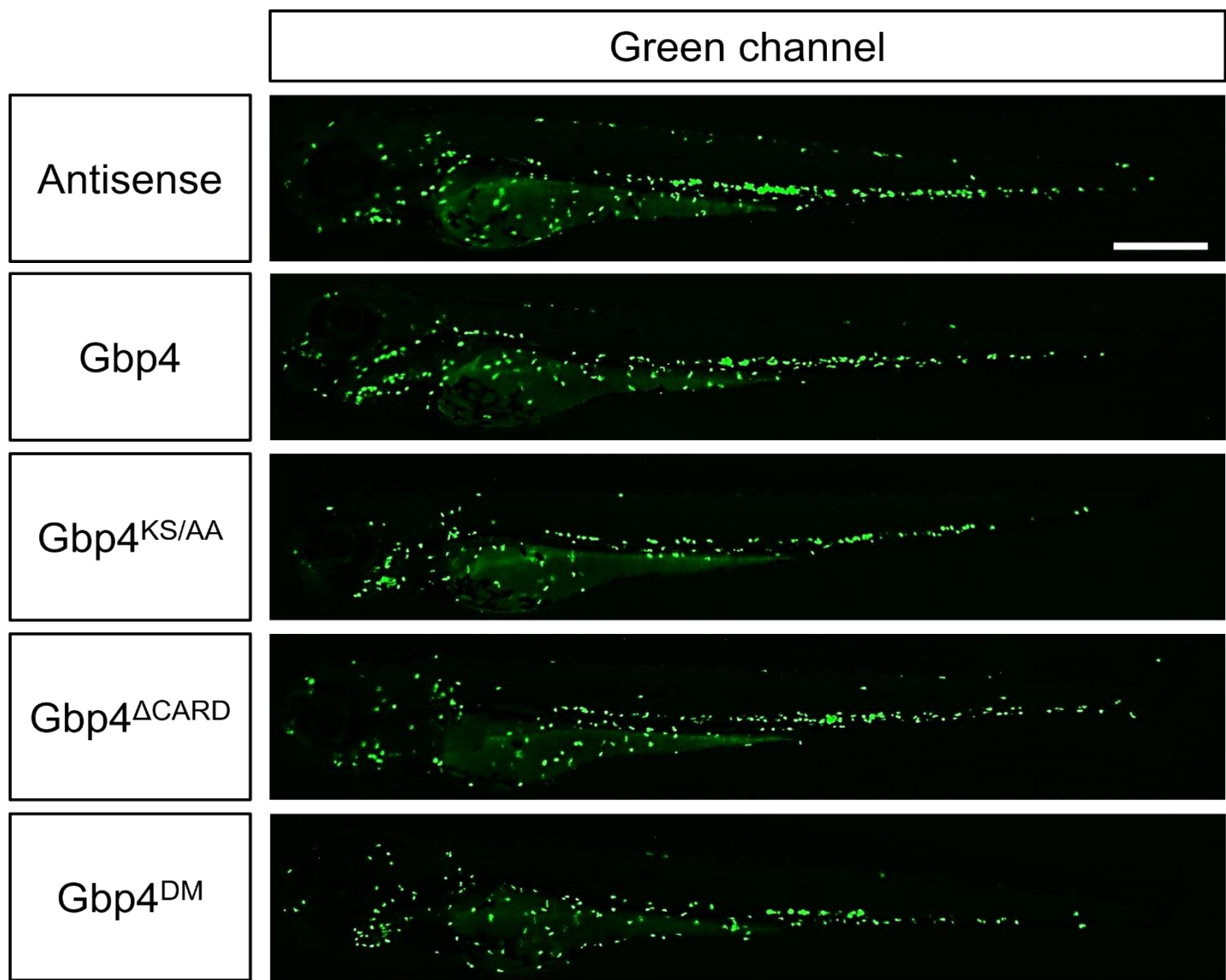
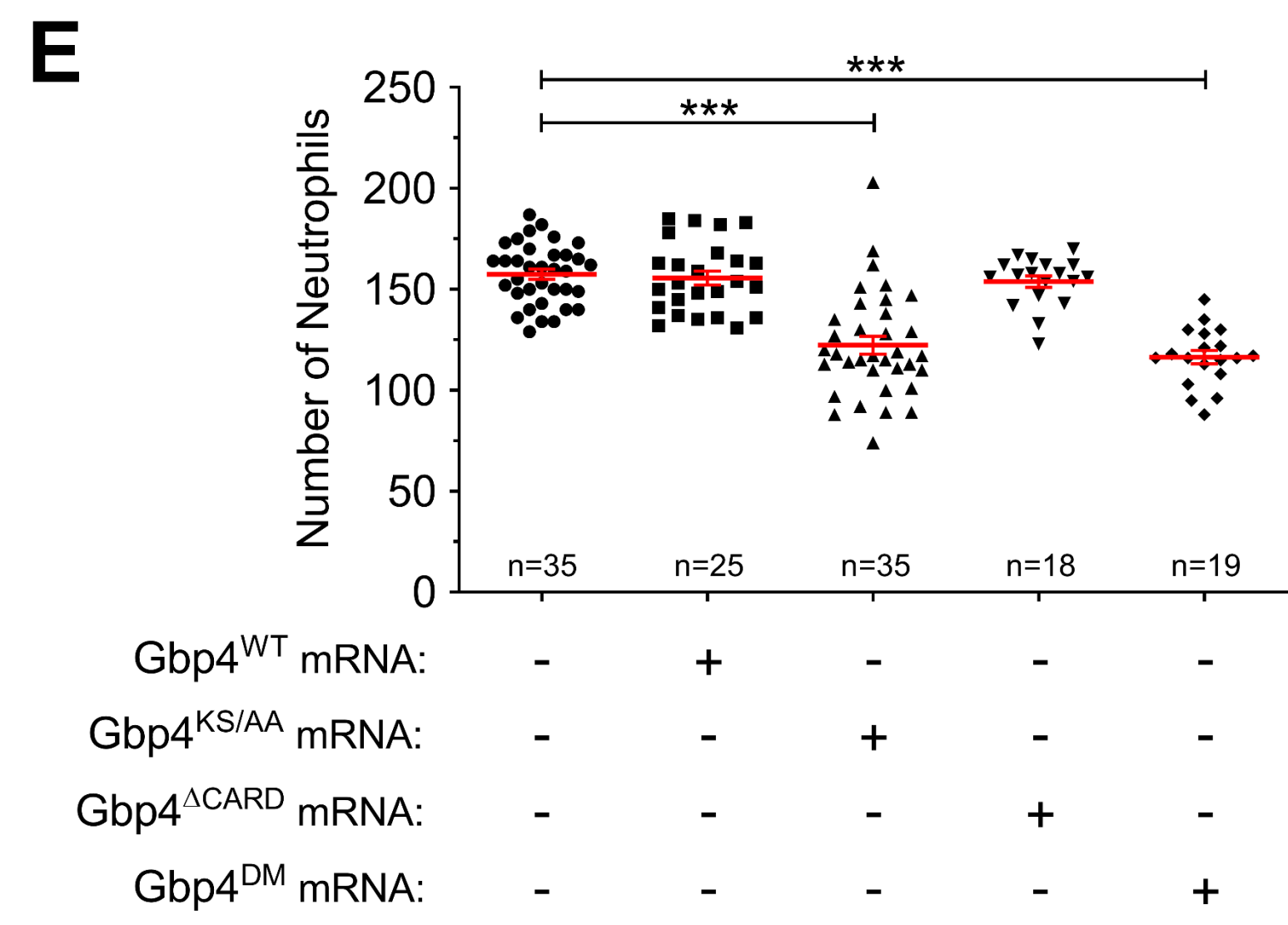
C



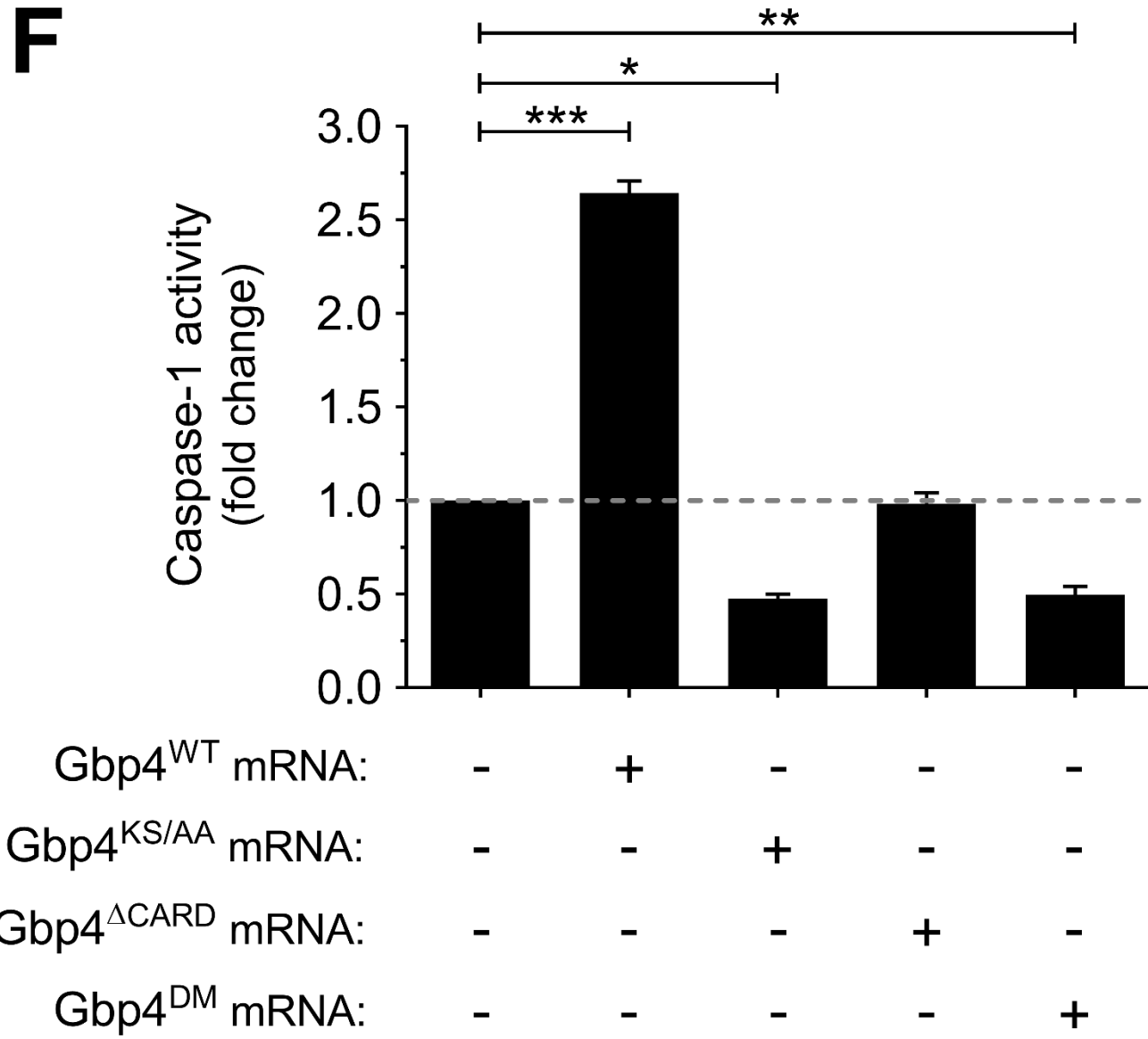
D



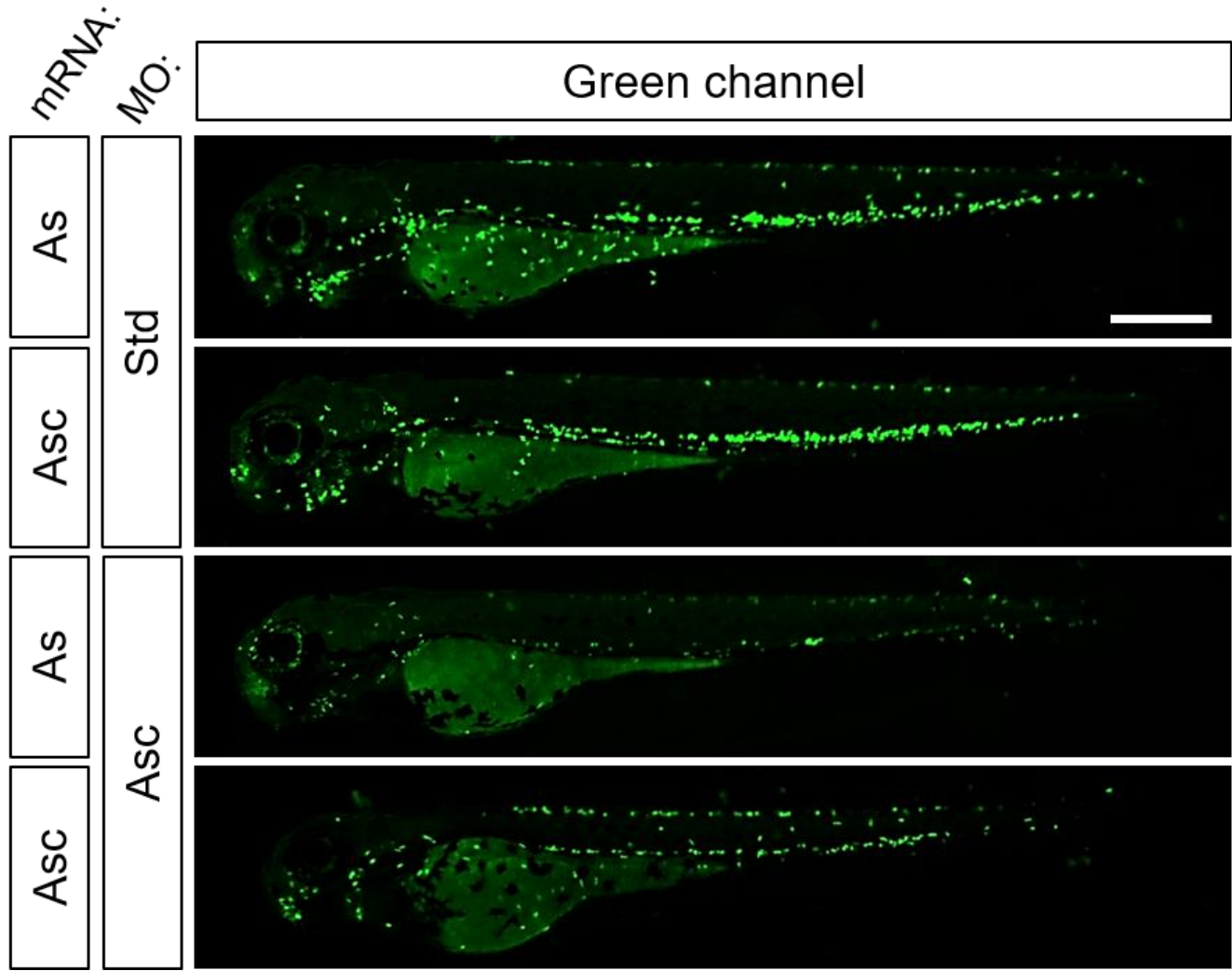
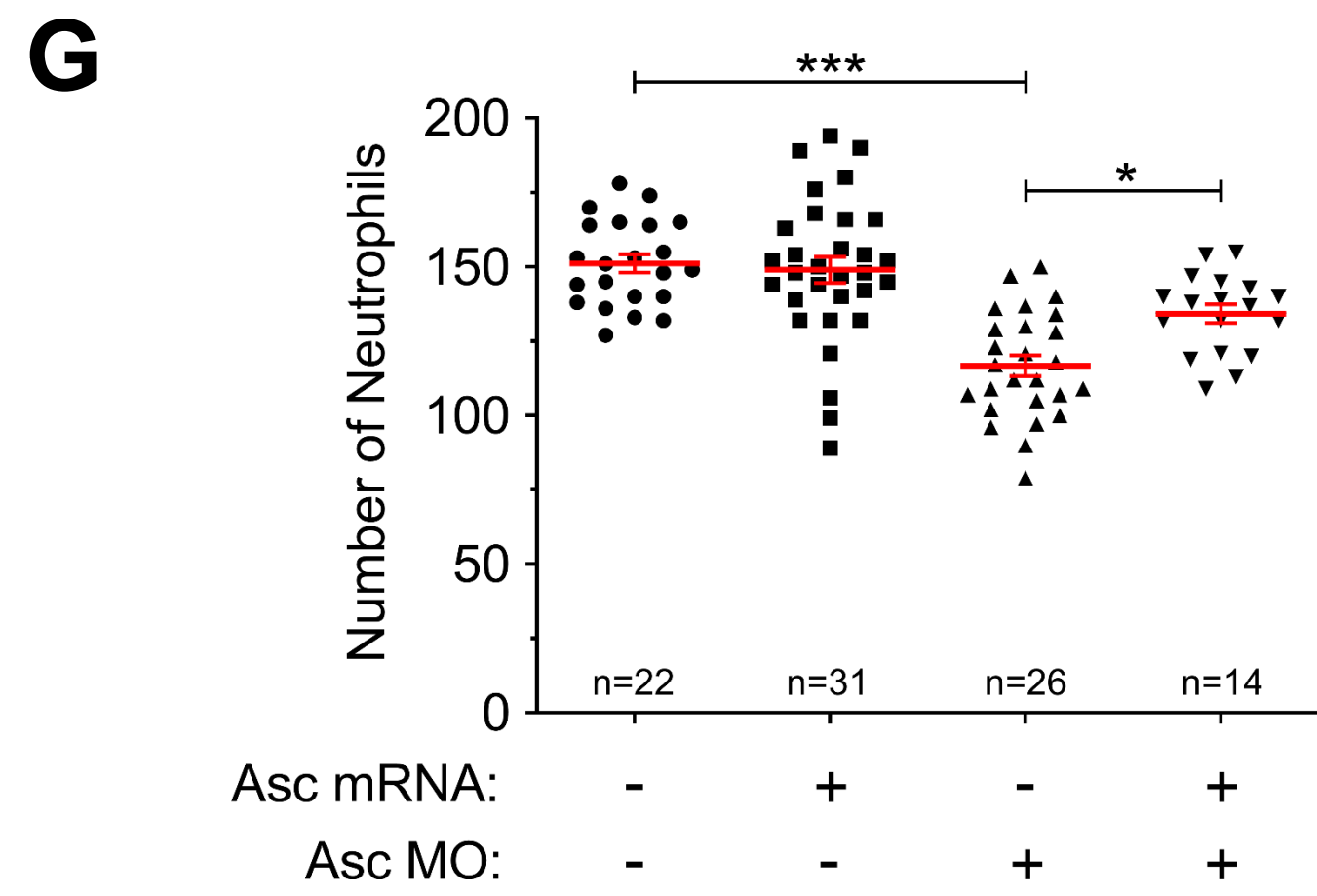
E



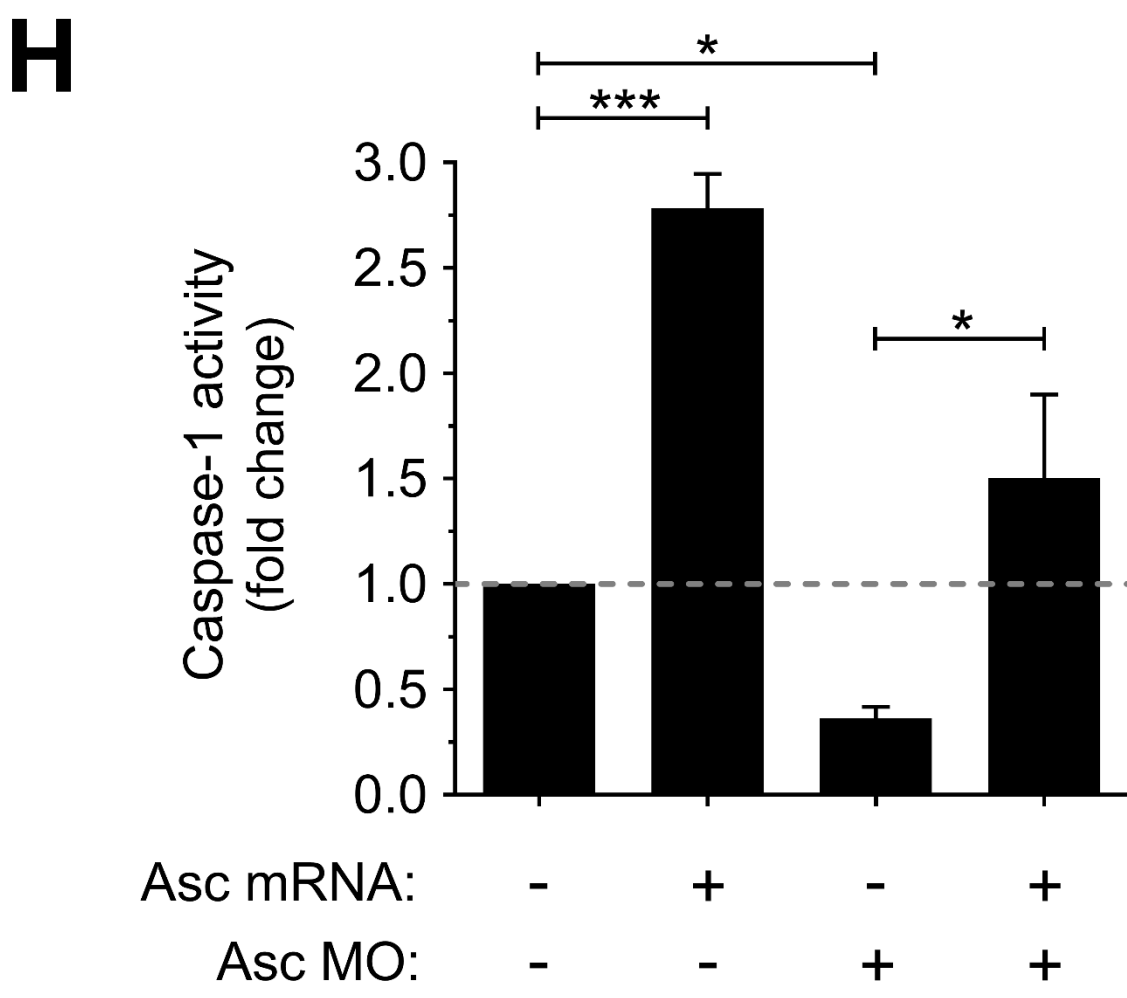
F



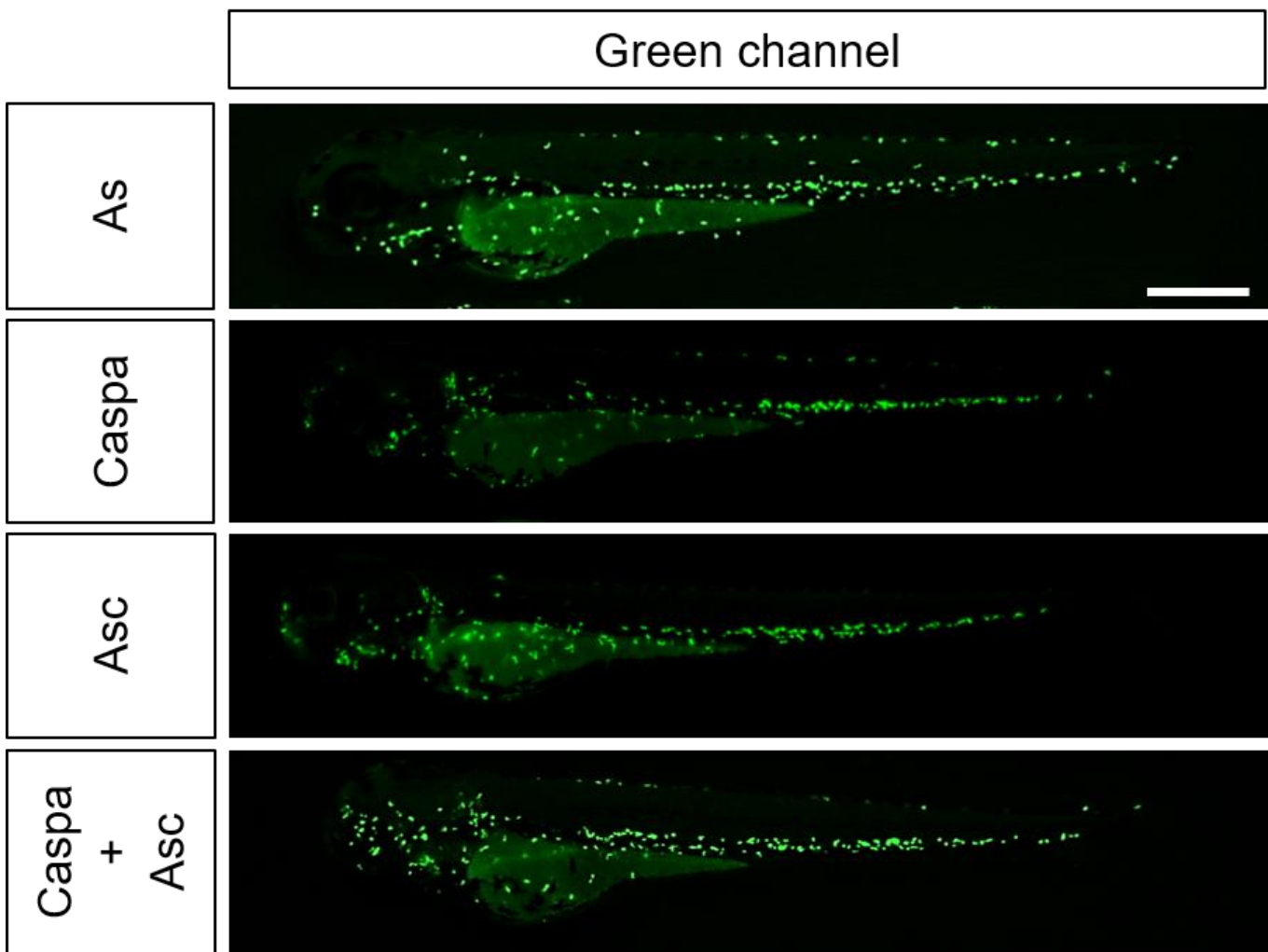
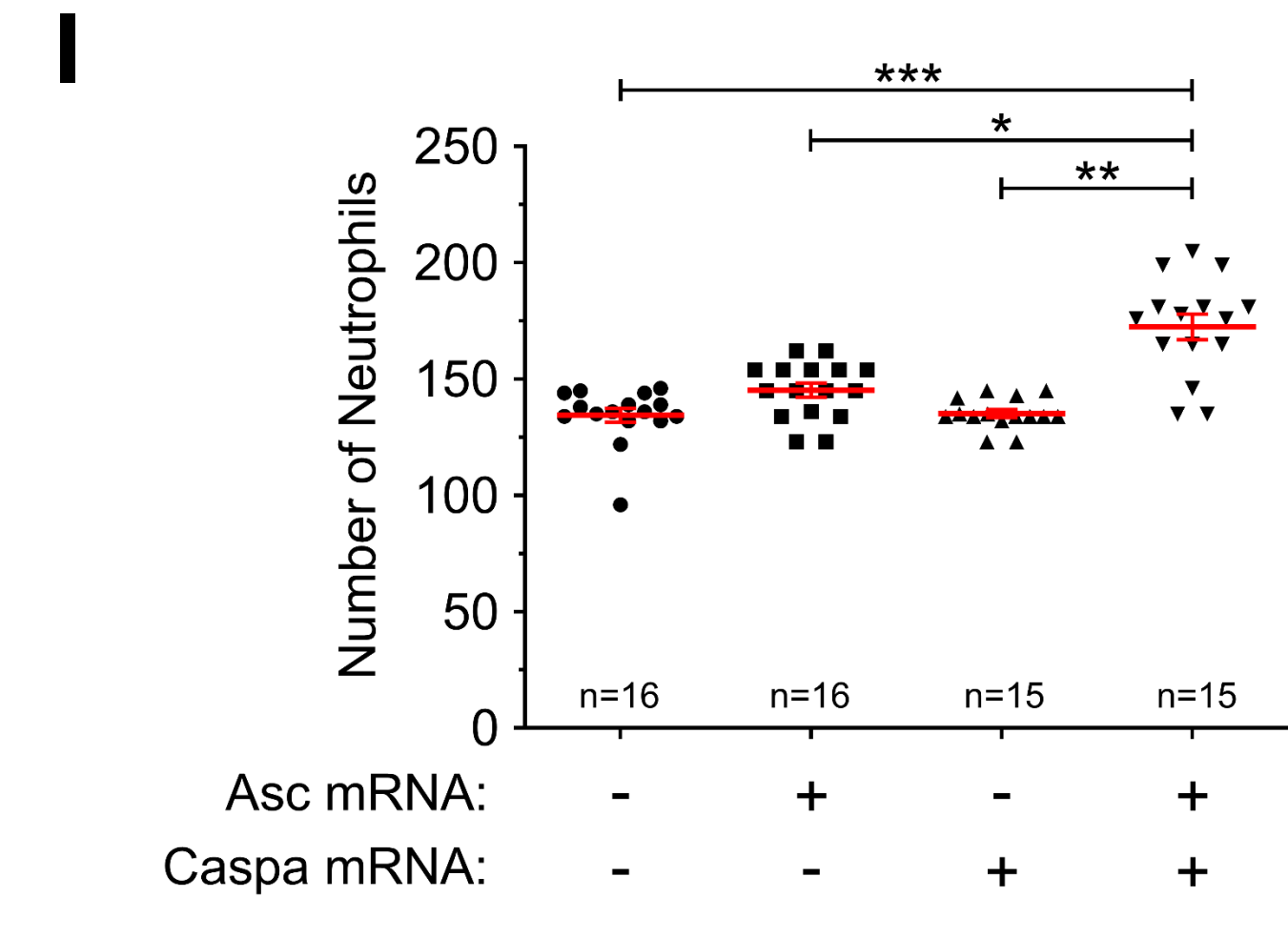
G



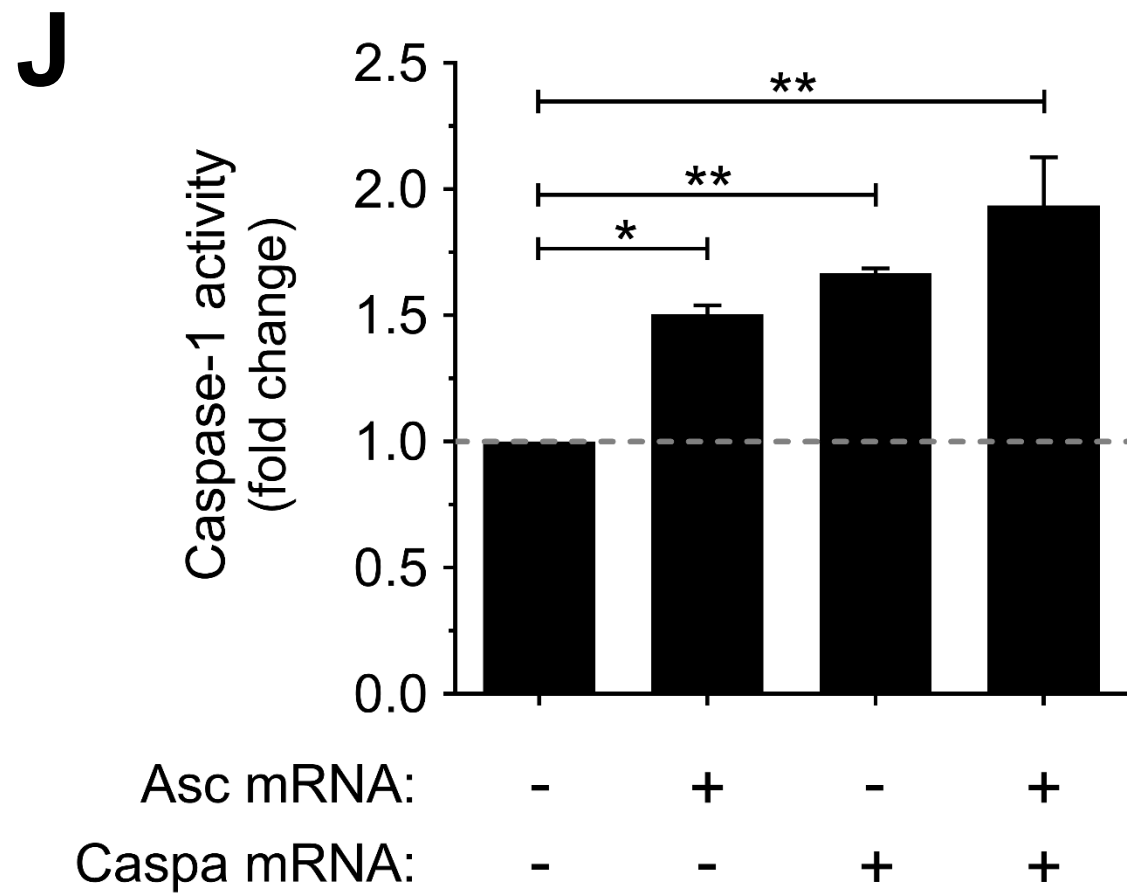
H



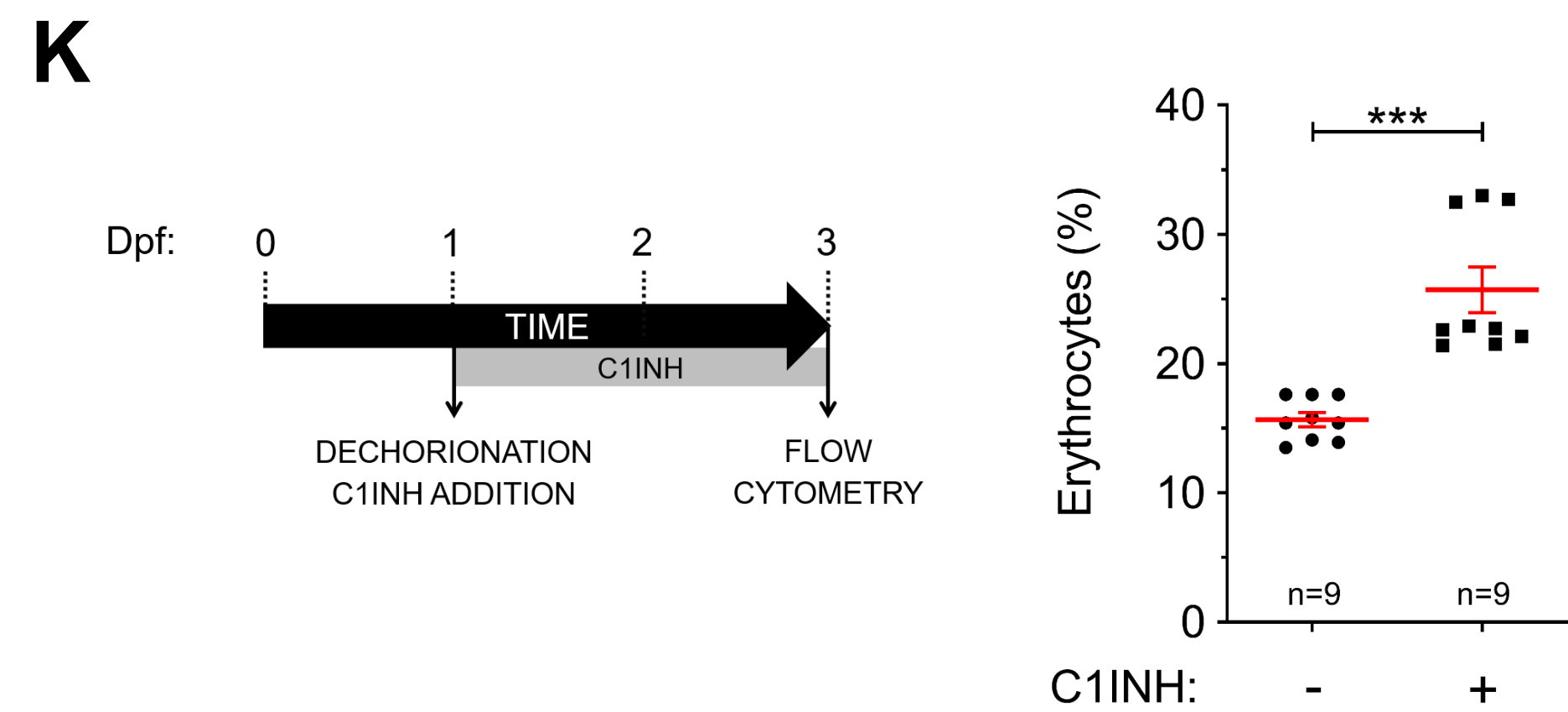
I



J



K



L

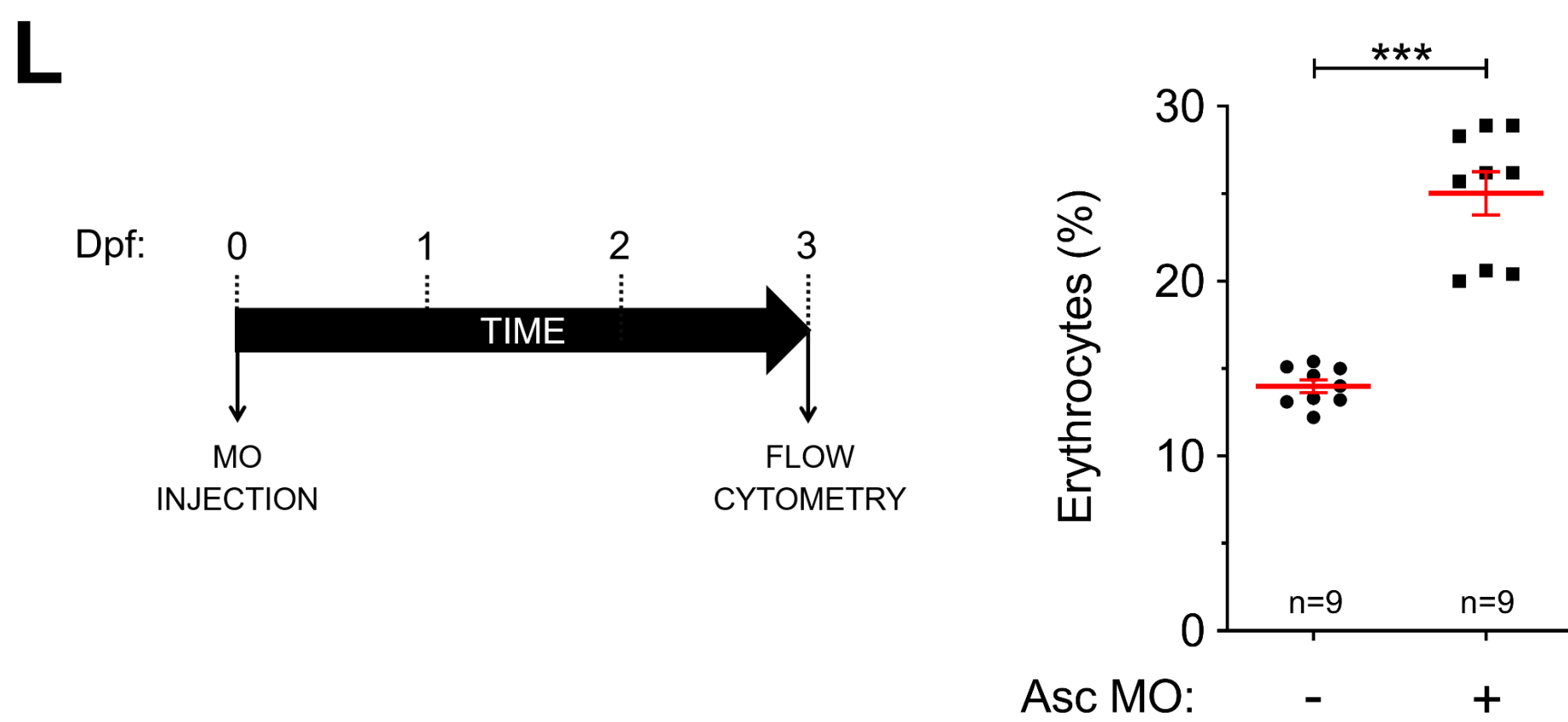


Figure 2

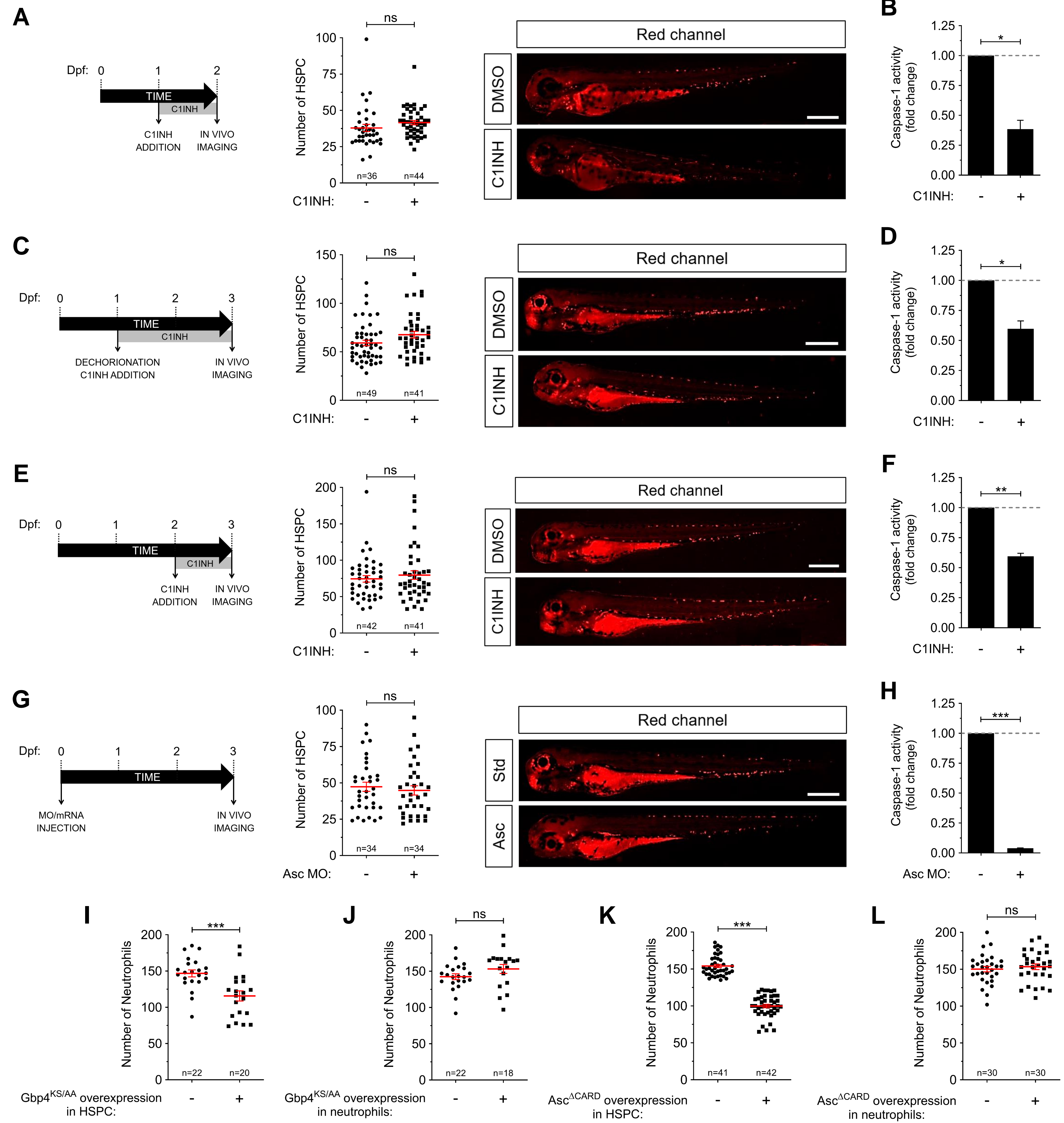
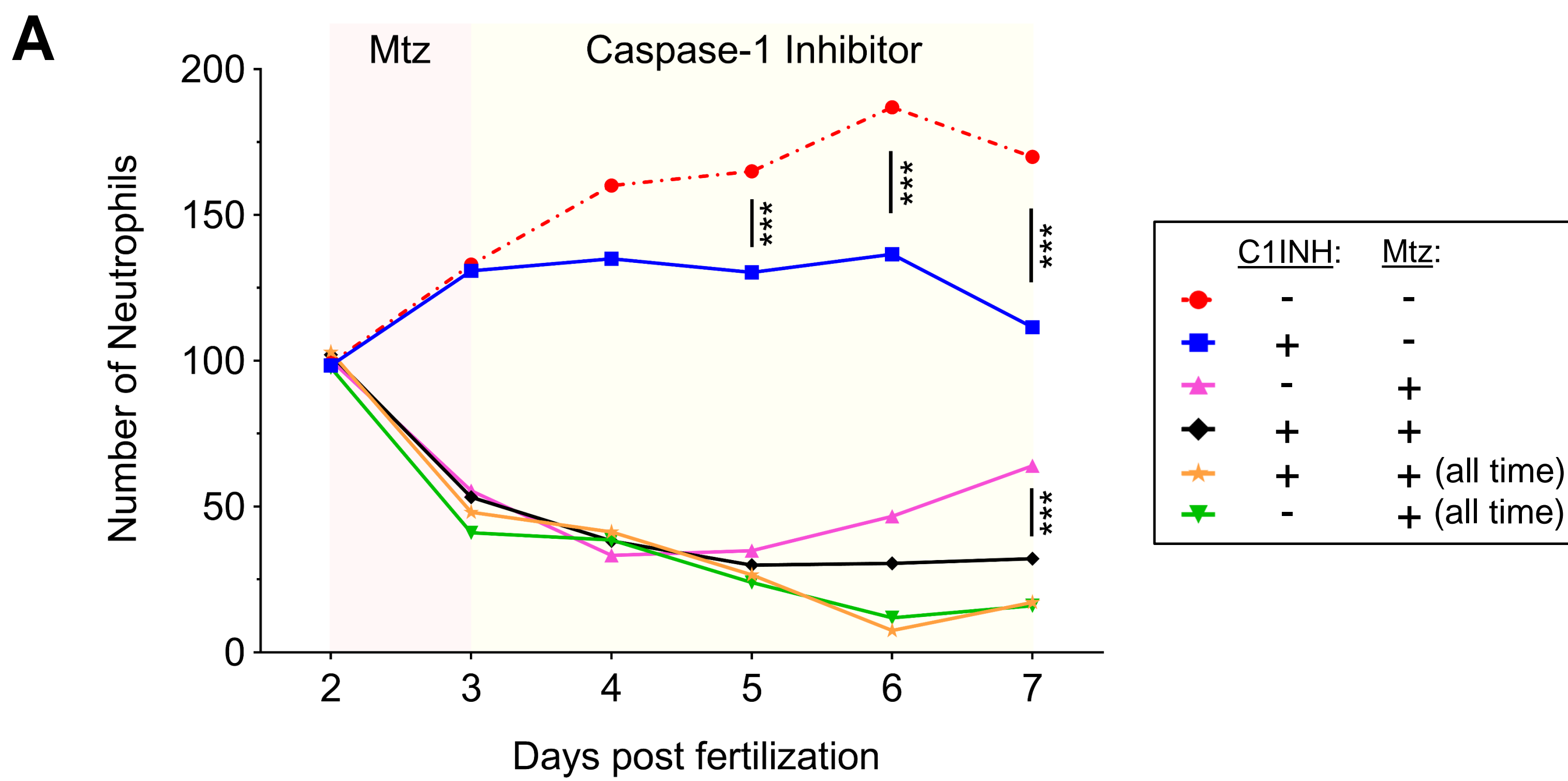


Figure 3



B

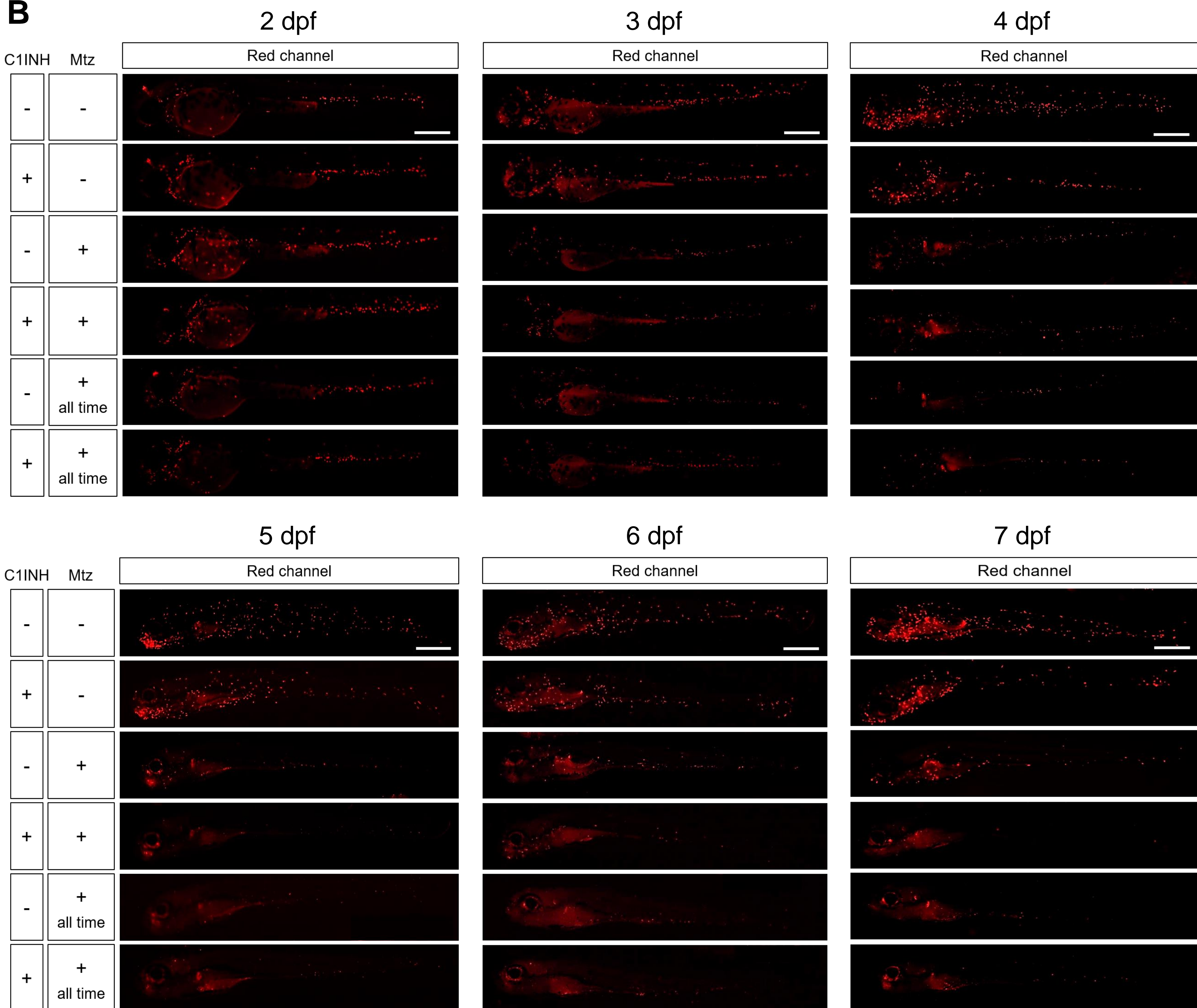


Figure 4

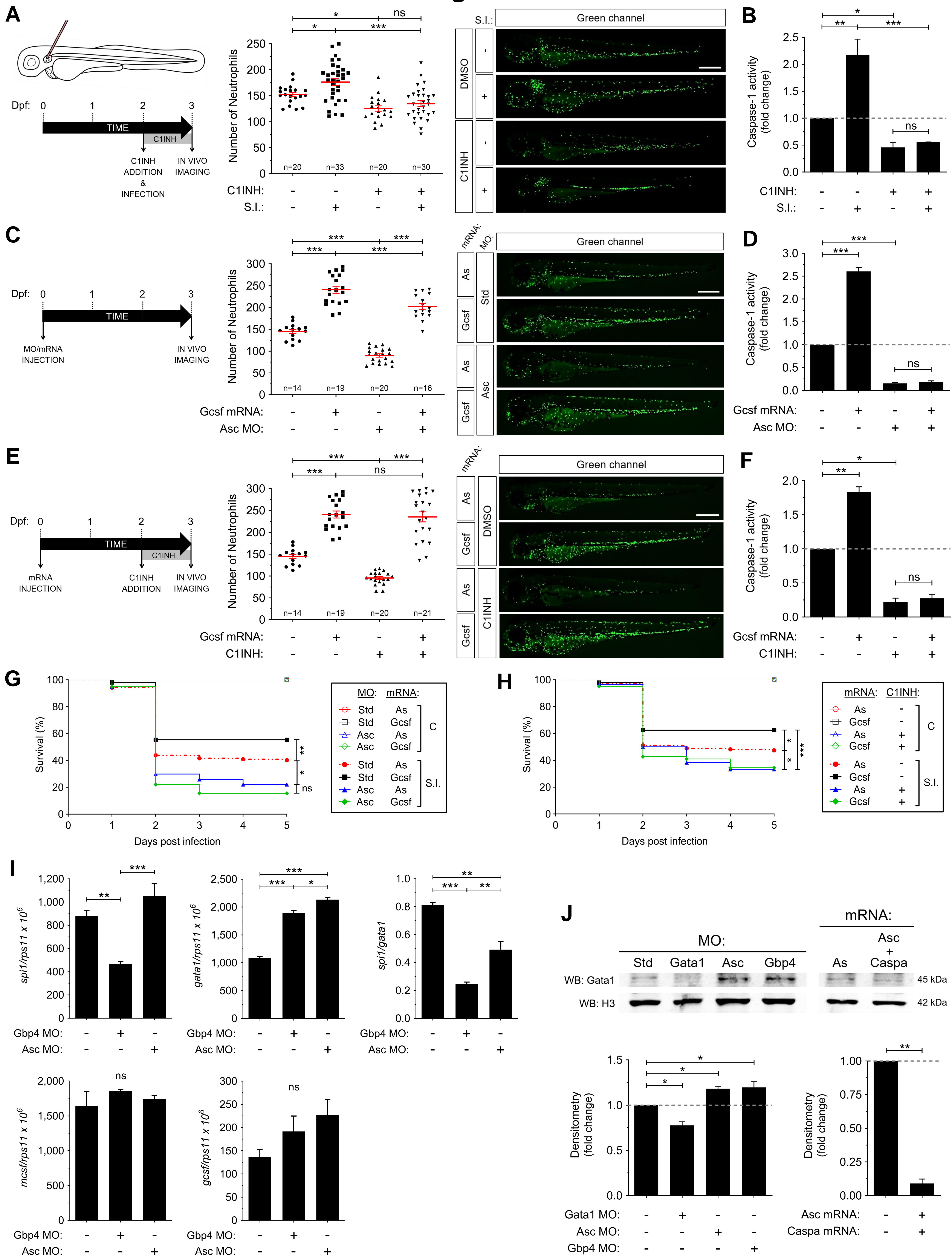


Figure 5

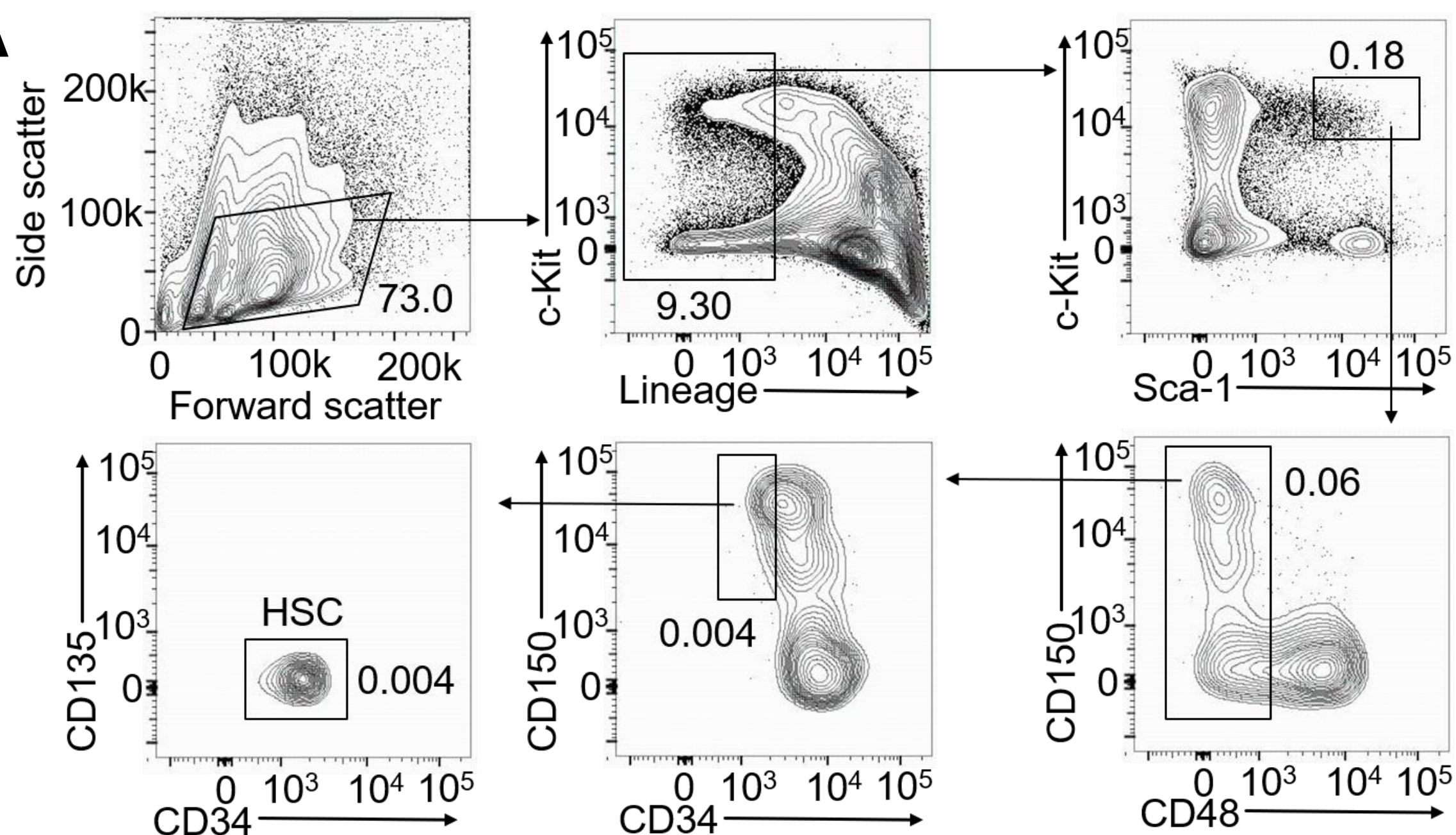
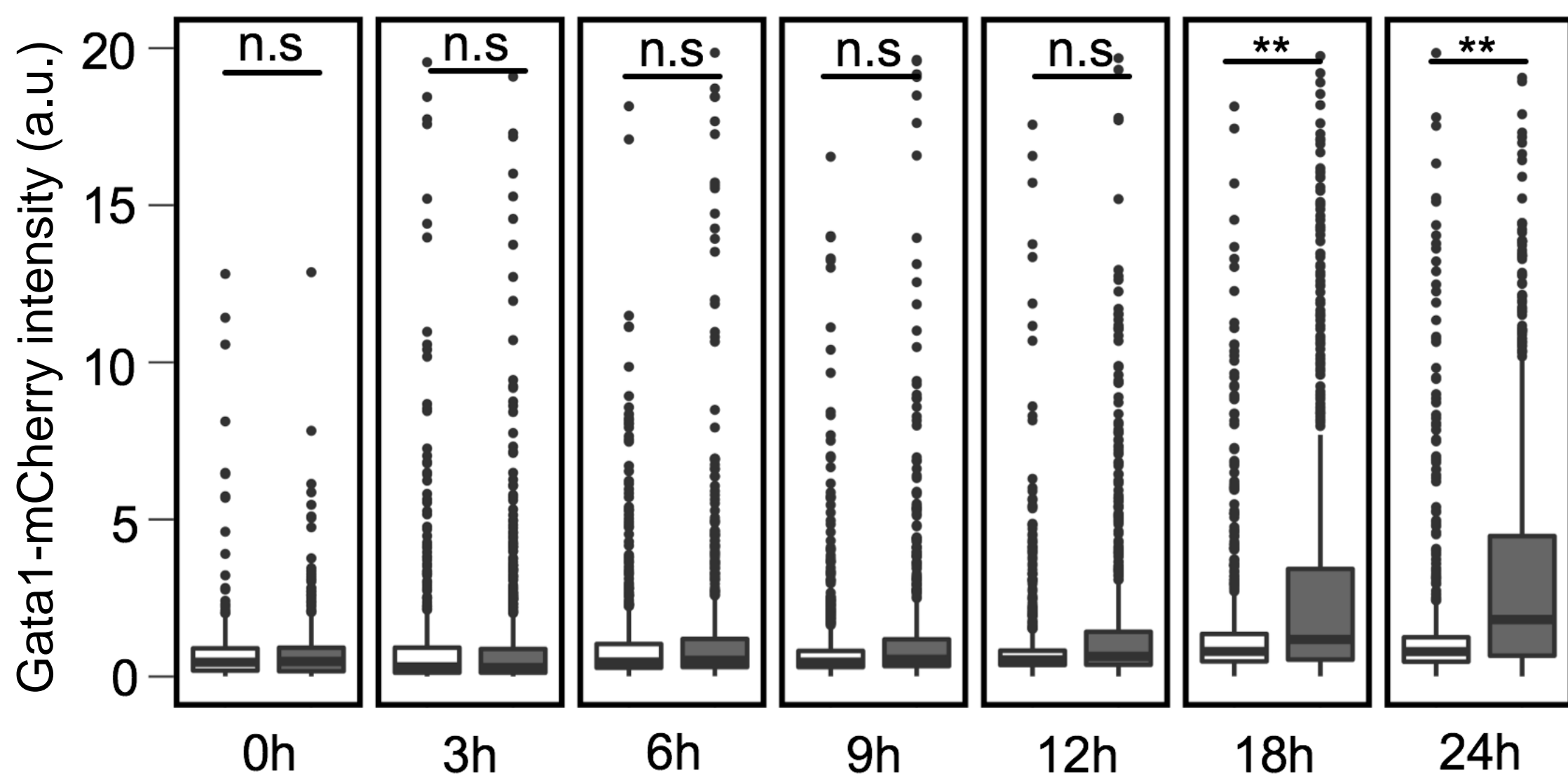
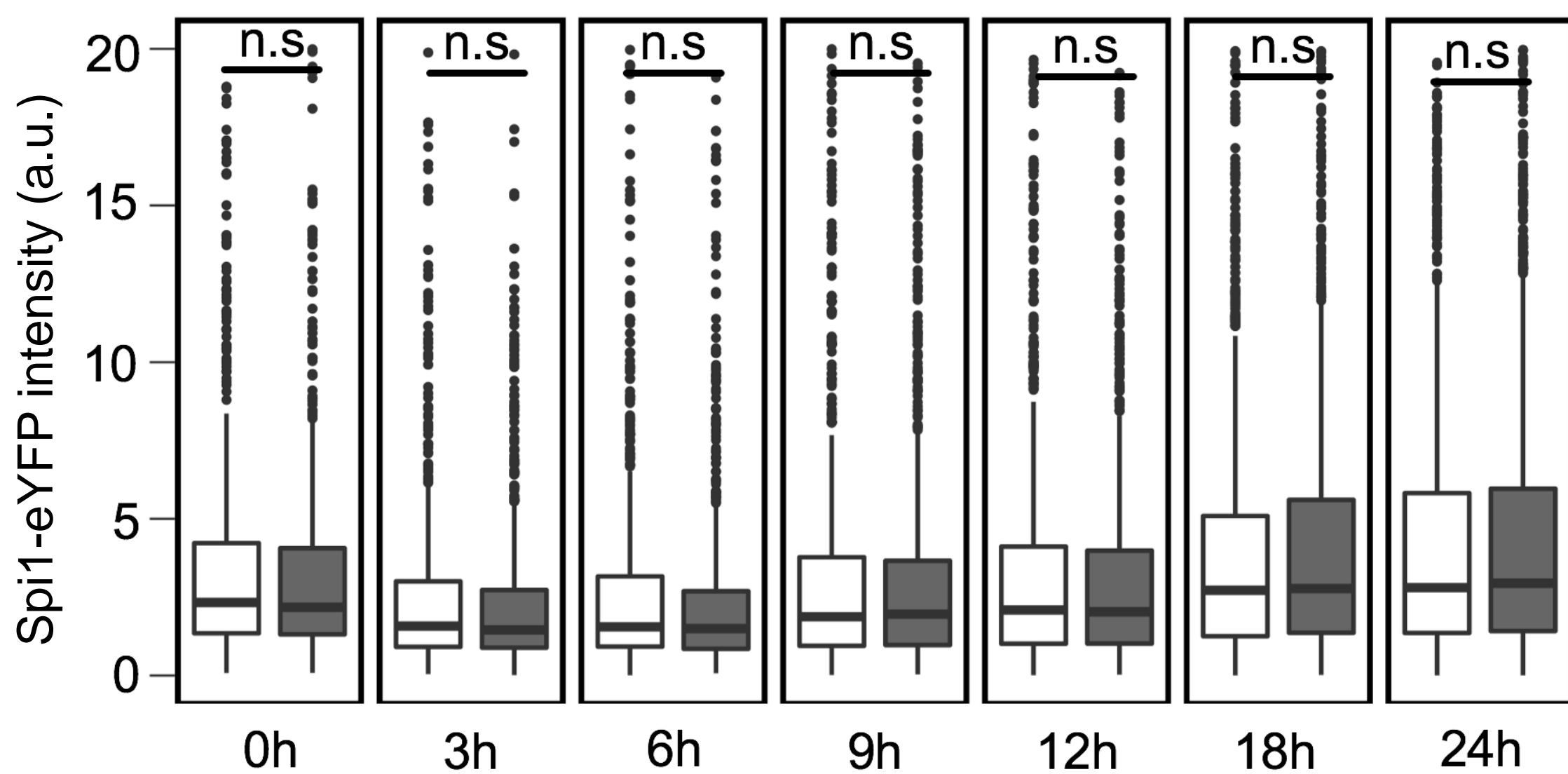
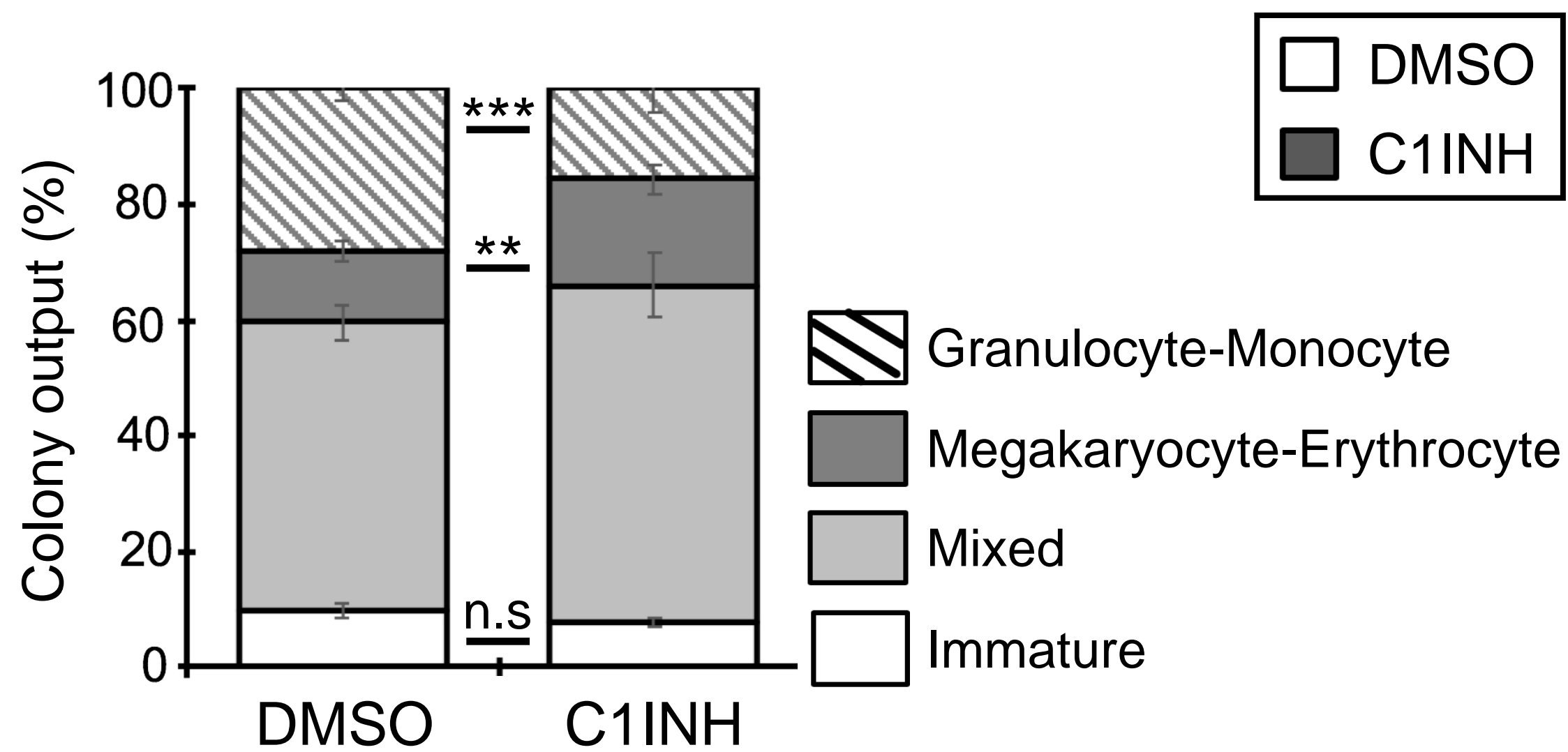
A

B

C

D


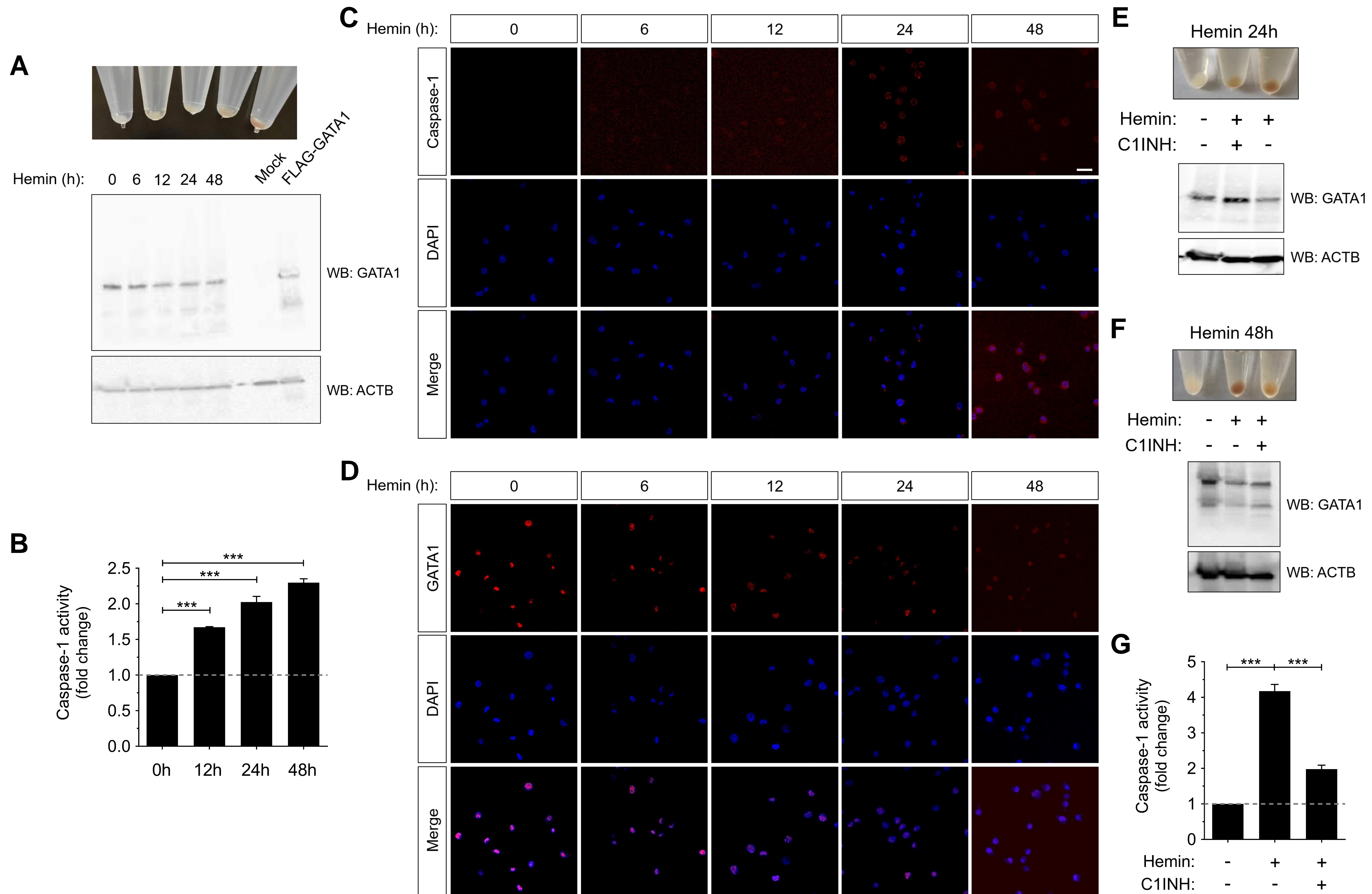
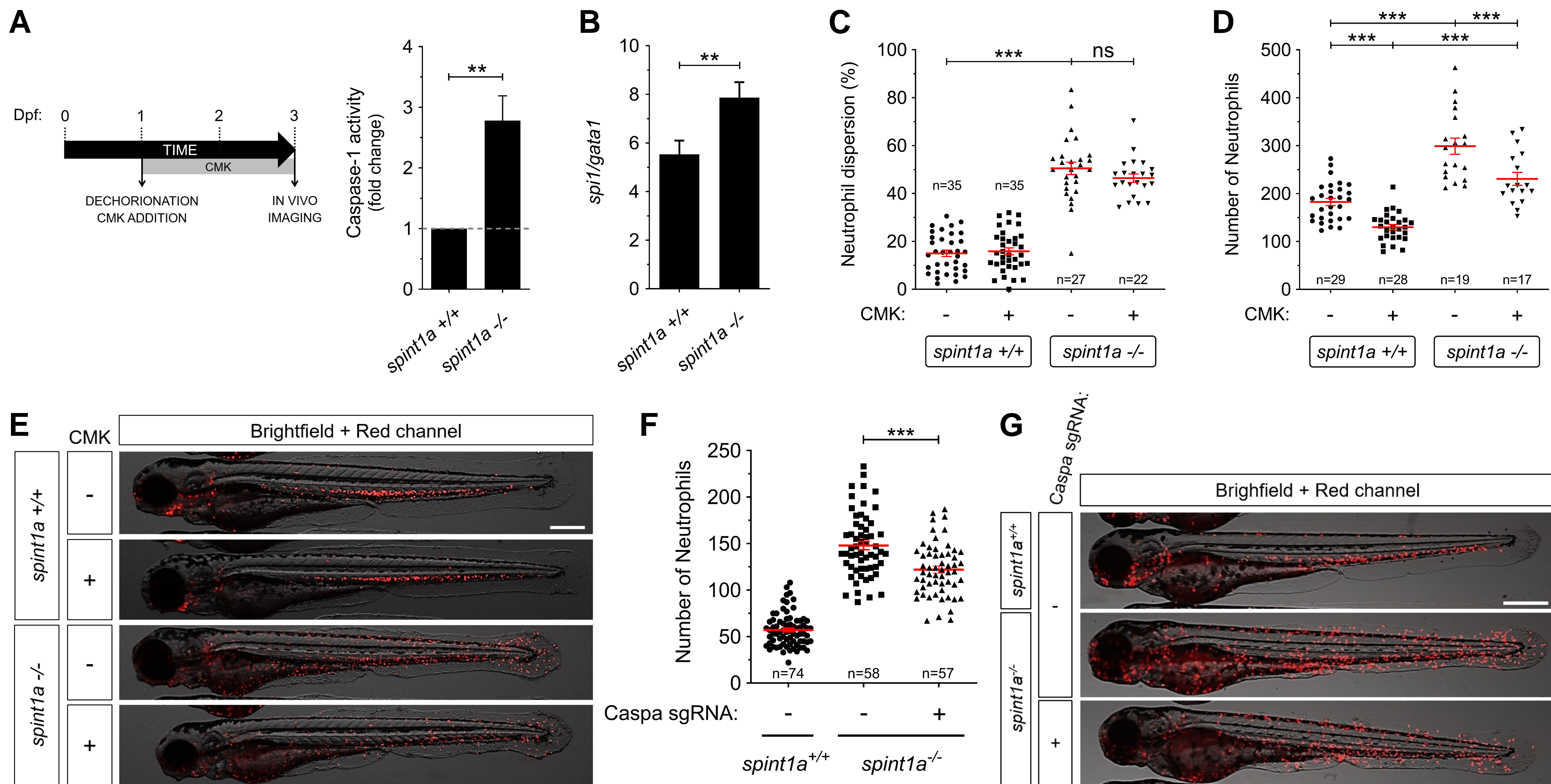
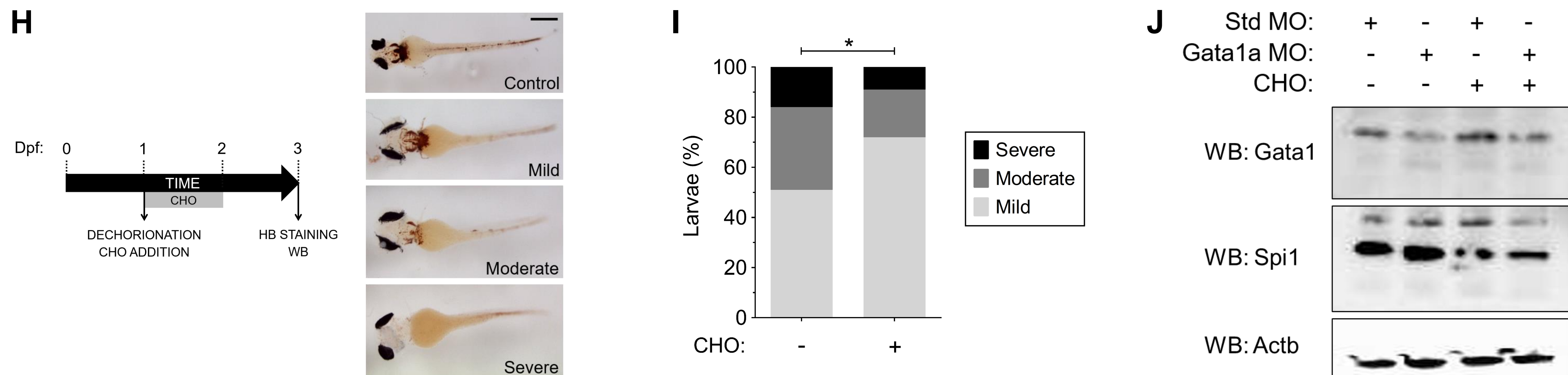
Figure 6

Figure 7

Neutrophilic inflammation



Diamond-Blackfan anemia



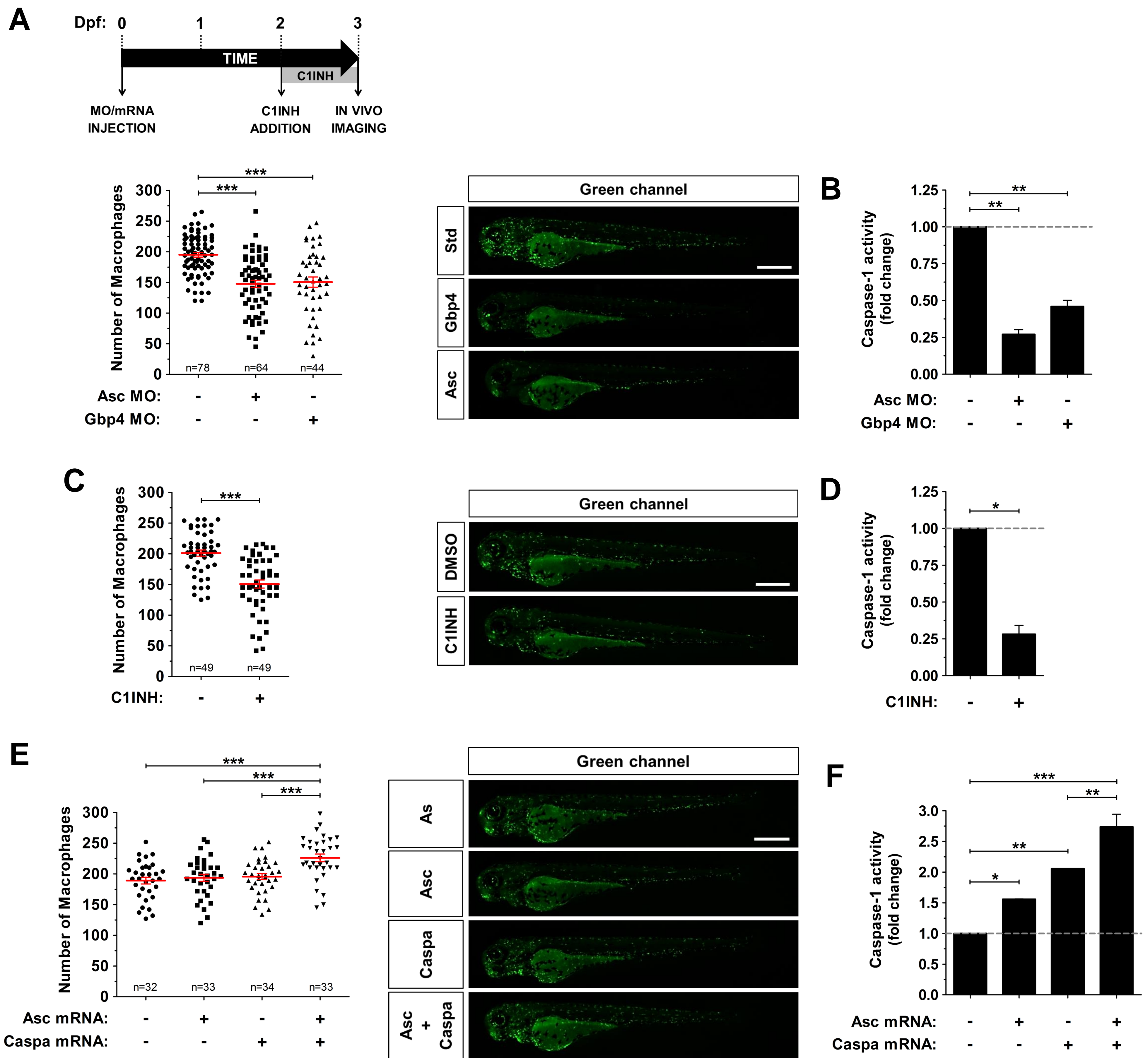


Figure S1. Inflammasome inhibition decreases the number of macrophages in zebrafish larvae. Related to Figure 1. *Tg(mpeg1:eGFP)* zebrafish one-cell embryos were injected with standard control (Std), Asc or Gbp4 MOs (A, B), or with antisense (As), Asc or/and Caspa mRNAs (E-F). Alternatively, *Tg(mpeg1:eGFP)* embryos were dechorionated manually at 48 hpf and treated by immersion with DMSO or the irreversible caspase-1 inhibitor Ac-YVAD-CMK (C1INH) (C, D). Each dot represents the number of macrophages from a single larva, while the mean \pm SEM for each group is also shown (A, C, E). The sample size (n) is indicated for each treatment. Representative images of green channels of whole larvae for the different treatments are also shown. Scale bars, 500 μ m. Caspase-1 activity in whole larvae was determined for each treatment at 72 hpf (one representative caspase-1 activity assay out of the three carried out is shown) (B, D, F). * $p < 0.05$; ** $p < 0.01$; *** $p < 0.001$ according to ANOVA followed by Tukey multiple range test.

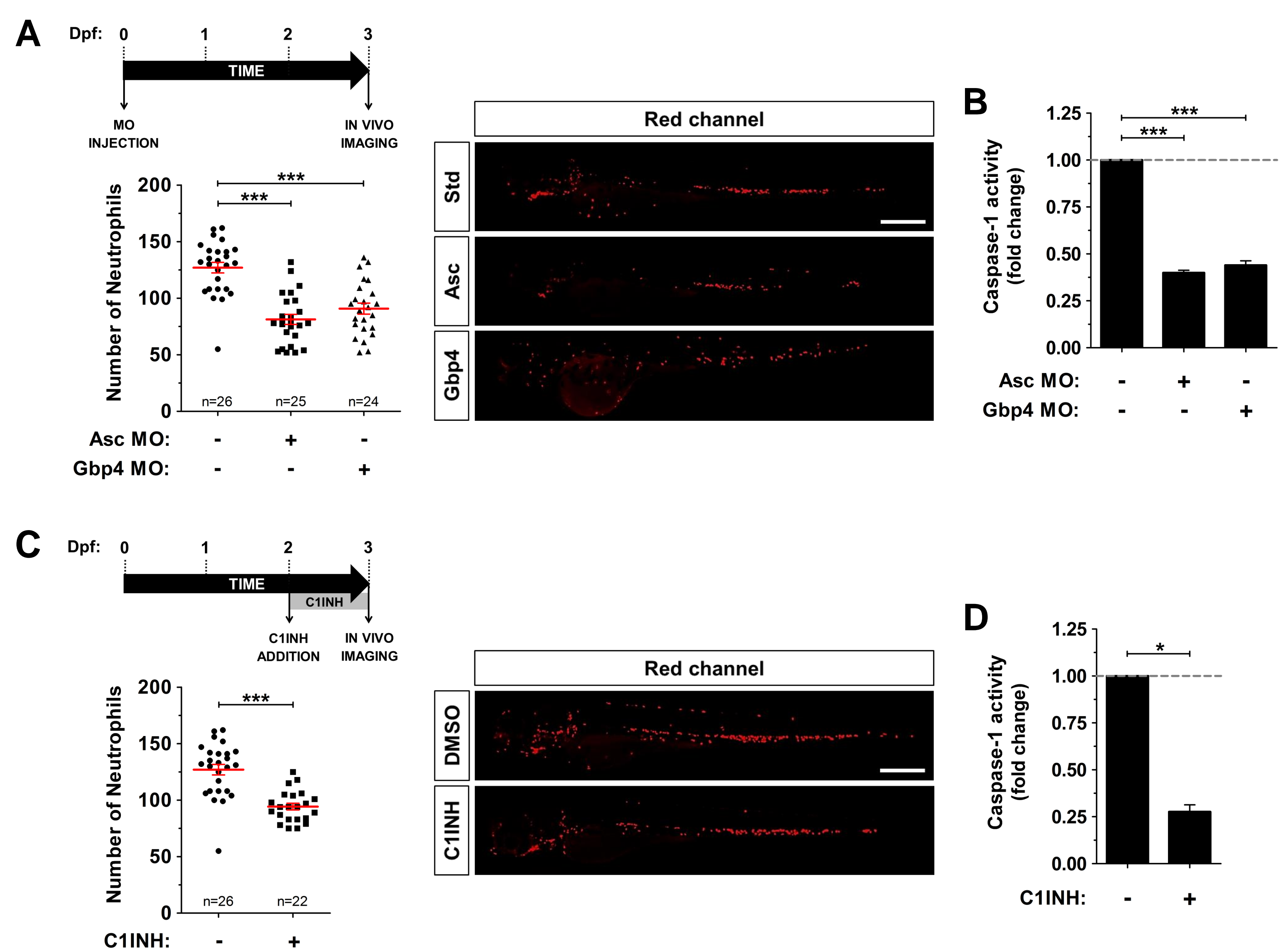


Figure S2. Inflammasome inhibition decreases the number of neutrophils in zebrafish larvae. Related to Figure 1. *Tg(lyz:dsRED)* zebrafish one-cell embryos were injected with standard control (Std), Asc or Gbp4 MOs (A, B). Alternatively, *Tg(lyz:dsRED)* larvae were manually dechorionated at 48 hpf and treated by immersion with DMSO or the irreversible caspase-1 inhibitor Ac-YVAD-CMK (C1INH) (C, D). Each dot represents the number of neutrophils from a single larva, while the mean \pm SEM for each group is also shown. The sample size (n) is indicated for each treatment. Representative images of red channels of whole larvae for the different treatments are also shown (A, B). Scale bars, 500 μ m. Caspase-1 activity was determined in whole larvae for each treatment at 72 hpf (one representative caspase-1 activity assay out of the three carried out is shown). (B, D). * $p < 0.05$; *** $p < 0.001$ according to ANOVA followed by Tukey multiple range test.

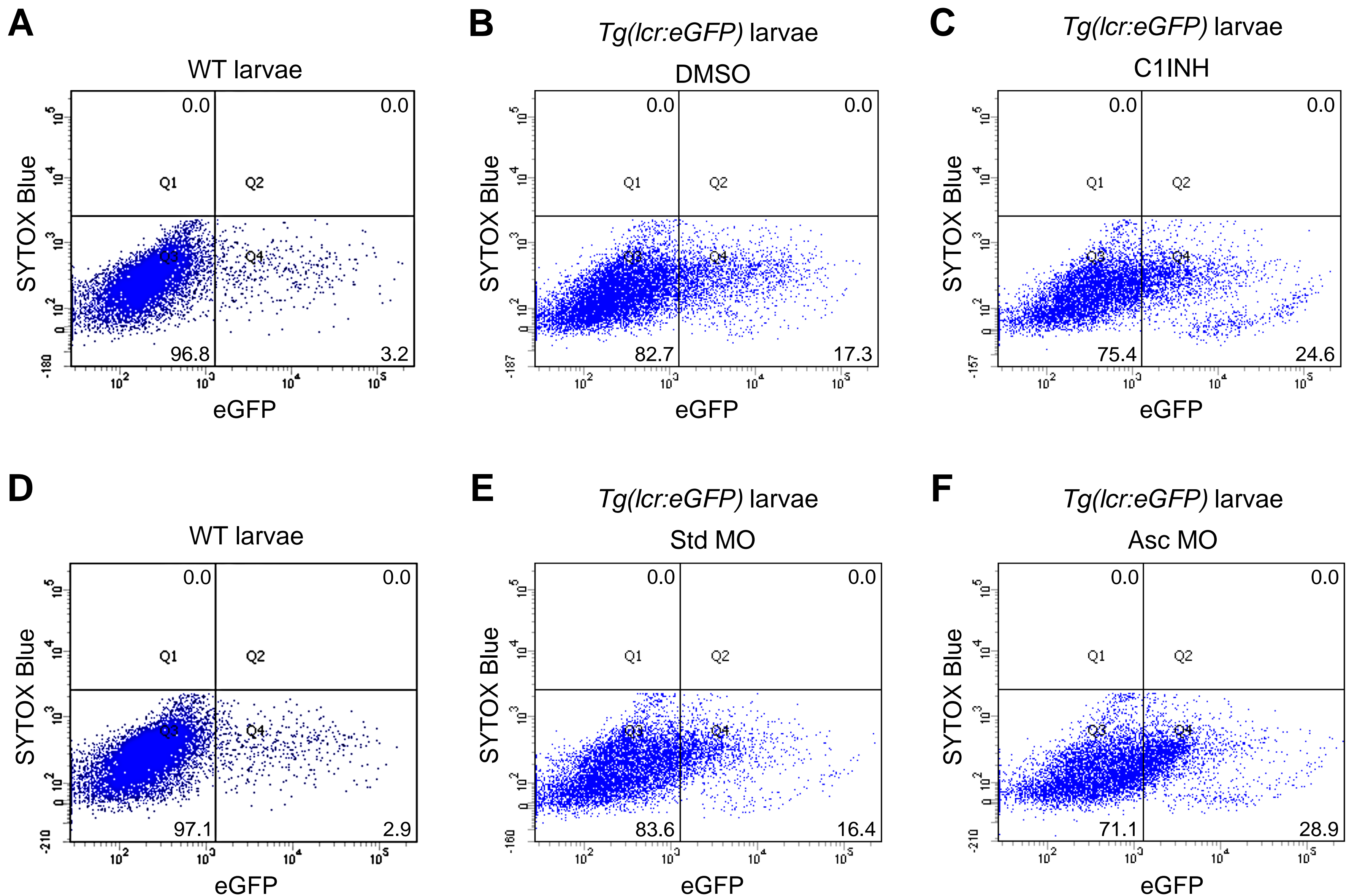


Figure S3. Representative dot plots of green and blue channels of cells from wild type and *Tg(lcr:eGFP)* zebrafish larvae. Related to Figure 1. Wild type (A, D) and *Tg(lcr:eGFP)* (B, C, E, F). zebrafish embryos were manually dechorionated at 24 hpf and treated by immersion with DMSO or the irreversible caspase-1 inhibitor Ac-YVAD-CMK (C1INH) during 48 h (B, C). Alternatively, *Tg(lcr:eGFP)* one-cell embryos were injected with standard control (Std) or Asc MOs (E, F). The percentage of cells in each quadrant is shown.









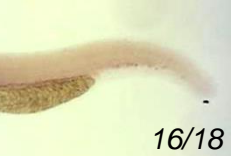









	Std MO	Asc MO	Gbp4 MO	
<i>gata1a</i>	 12/19	 12/13	 12/16	24 hpf
	 17/20	 8/13	 9/15	
<i>spi1b</i>	 12/18	 11/18	 16/18	
<i>cmyb</i>	 15/18	 6/20	 2/16	48 hpf
<i>runx1</i>	 20/20	 18/18	 17/17	
<i>rag1</i>	 18/18	 19/19	 18/18	5 dpf

Figure S4. Inflammasome activity regulates *gata1* expression levels in zebrafish larvae. Related to Figures 1 and 2. Casper zebrafish one-cell embryos were injected with standard control (Std), Asc or Gbp4 MOs. At the indicated times, whole-mount *in situ* hybridization (WISH) was performed using antisense probes to the *gata1a*, *spi1b*, *gcsfr*, *cmyb*, *runx1* and *rag1* genes. Numbers in pictures represent the animals with the shown phenotype per total analyzed animals.

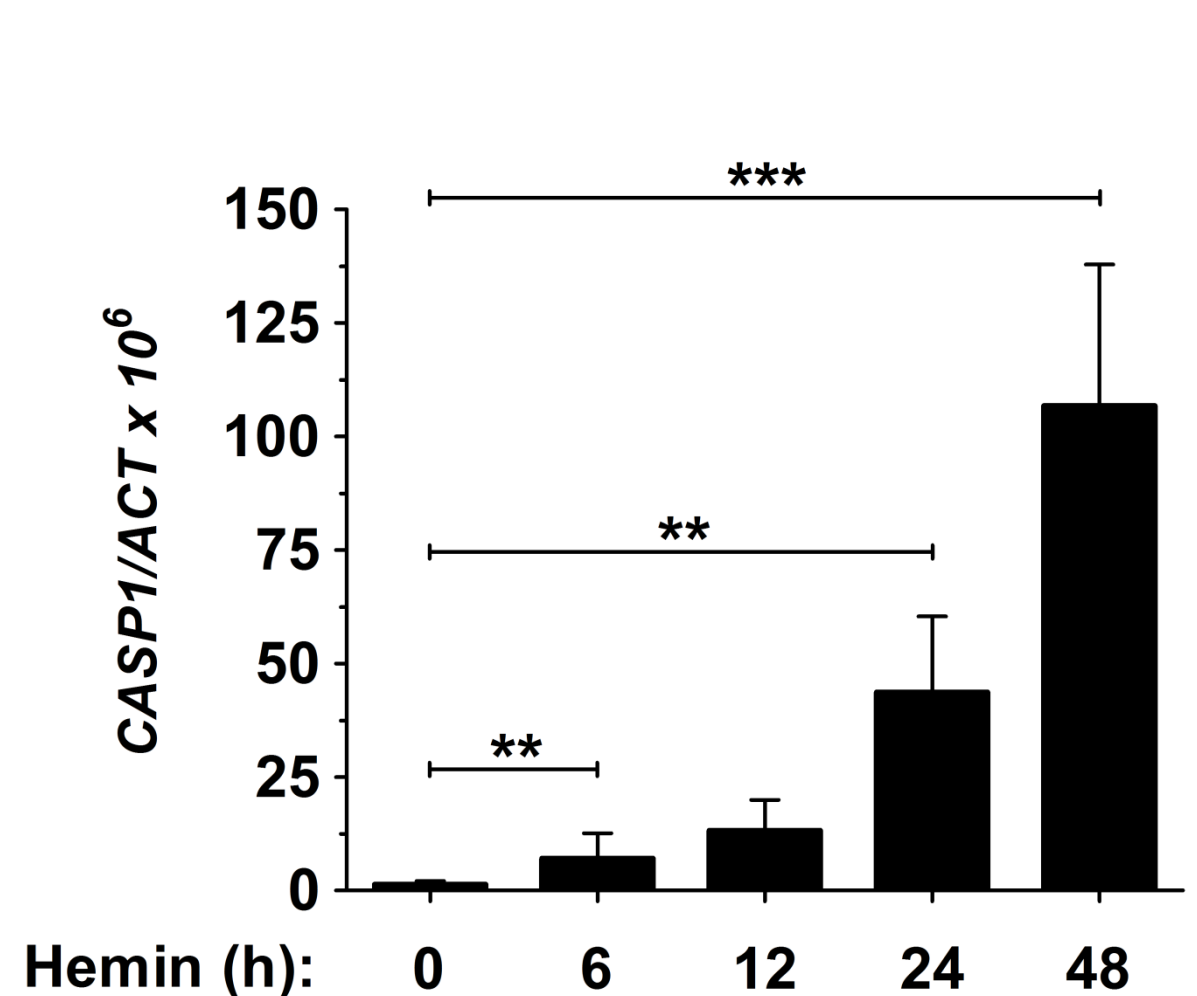
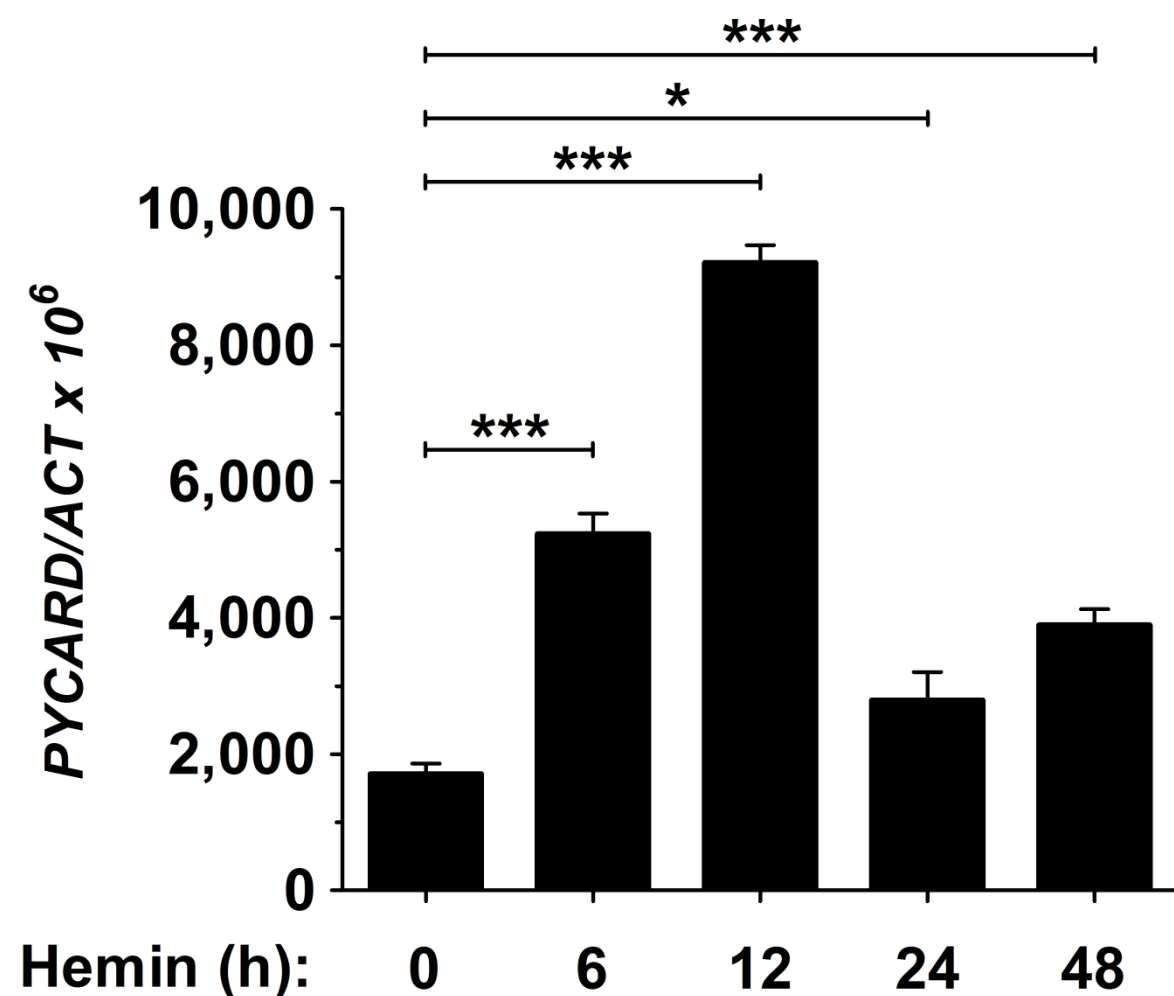
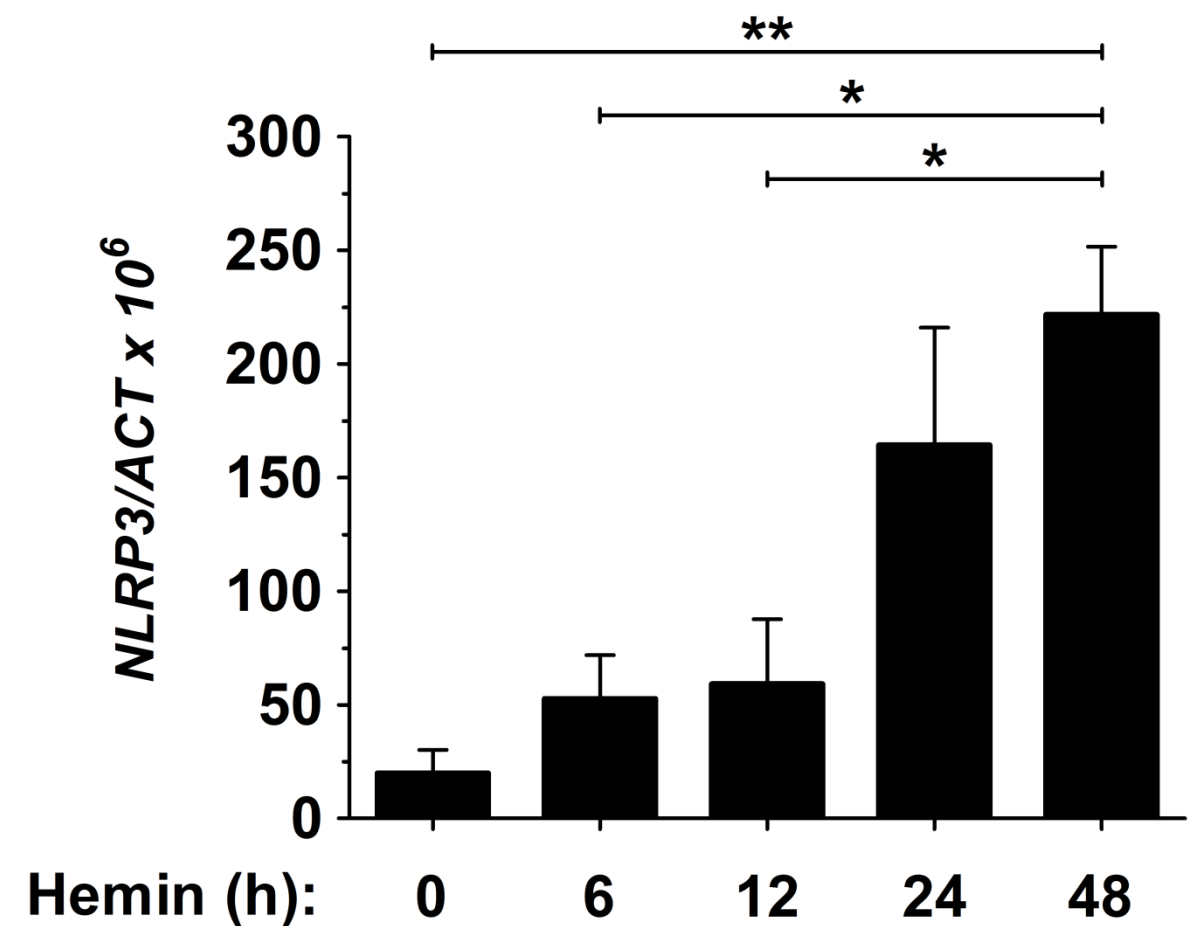
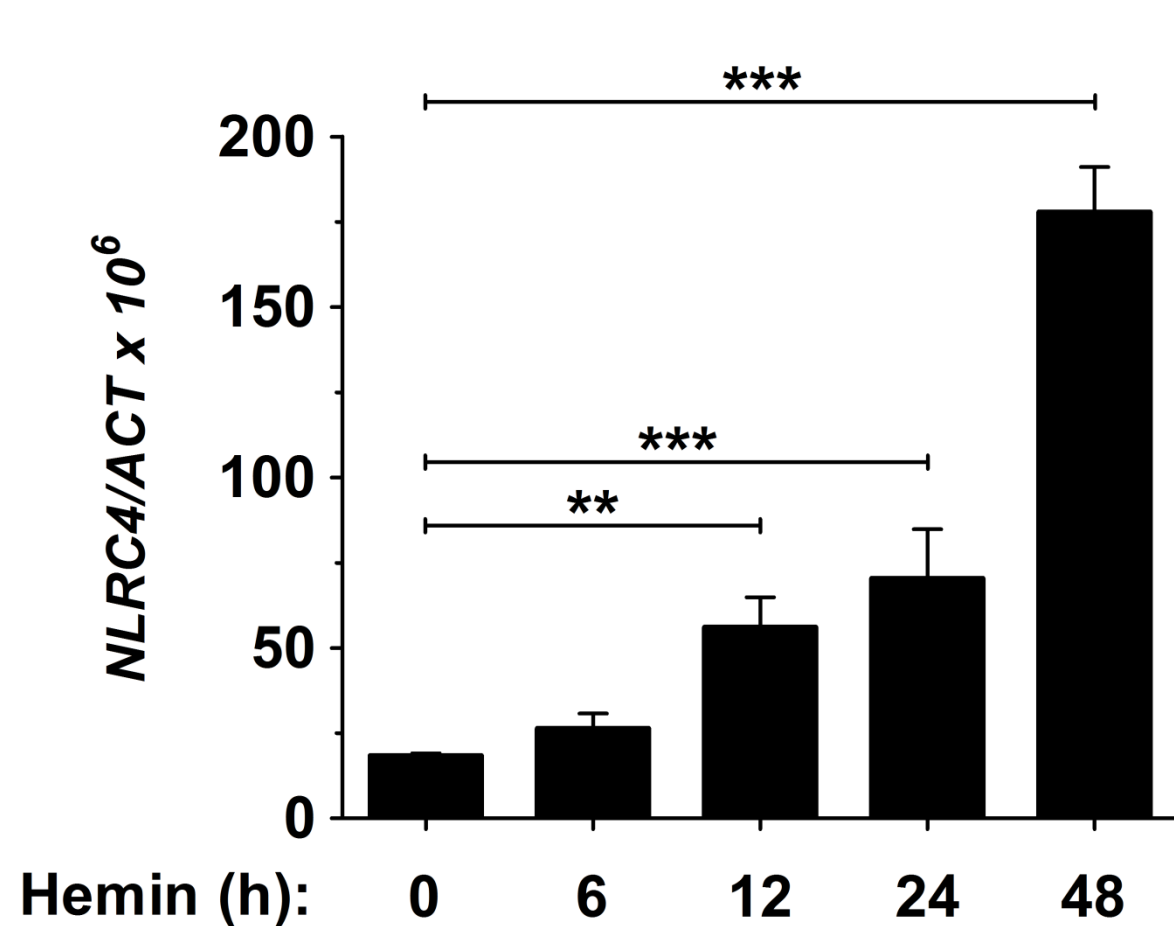


Figure S5. The expression of genes encoding inflammasome components are regulated during the erythroid differentiation of K562 cells. Related to Figure 6. K562 cells were incubated with hemin for 48 h and then the mRNA levels of the genes *NLRC4*, *NLRP3*, *PYCARD* and *CASP1* were determined by RT-qPCR (n=3). The results are shown as the mean \pm SEM. *p<0.05; **p<0.01; ***p<0.001 according to ANOVA followed by Tukey multiple range test.

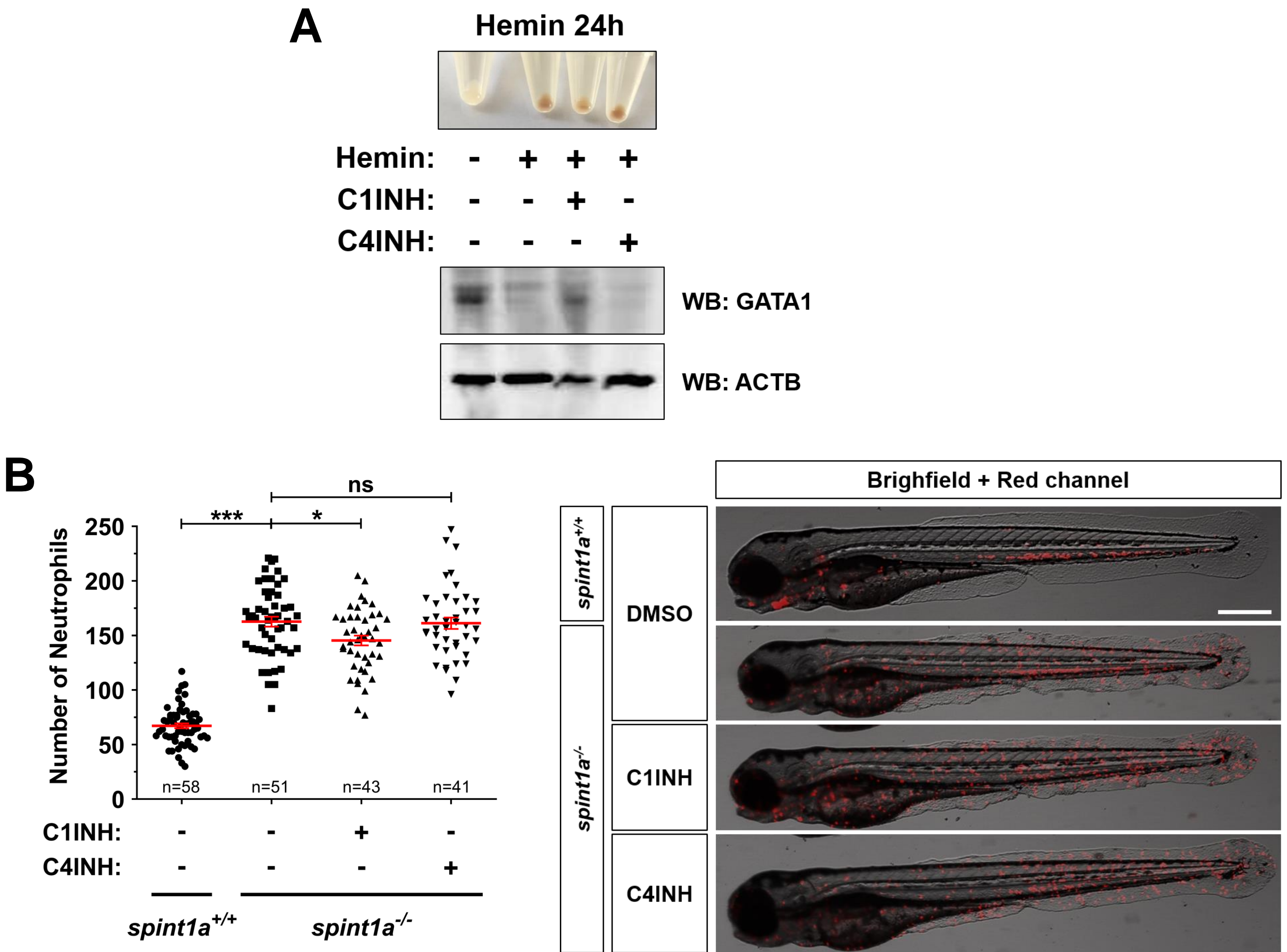


Figure S6. Pharmacological inhibition of caspase-4/caspase-5 failed to regulate erythroid differentiation of K562 cells and neutrophil numbers in zebrafish. Related to Figures 6 and 7. (A) K562 cells were incubated with 50 μ M hemin for 24 h in the presence or absence of the caspase-1 inhibitor Ac-YVAD-CMK (C1INH, 100 μ M) or the caspase-4/caspase-5 inhibitor Ac-LEVD-CHO (C4INH, 100 μ M) and the cell pellets imaged, lysated and resolved by SDS-PAGE and immunoblotted with anti-GATA1 and anti-ACTB antibodies. (B) *spint1a* mutant larvae were manually dechorionated and treated from 1-3 dpf with Ac-YVAD-CMK (C1INH, 100 μ M) or Ac-LEVD-CHO (C4INH, 100 μ M). The number of neutrophils was then determined. Each dot represents the number of neutrophils from a single larva, while the mean \pm SEM for each group is also shown. The sample size (n) is indicated for each treatment. Representative overlay images of green and bright field channels of whole larvae for the different treatments are shown. One representative hemoglobin accumulation (A) and western blot (A) assay out of the three carried out is shown. Scale bar, 500 μ m. ns, not significant; * p <0.05; *** p <0.001 according to ANOVA followed by Tukey multiple range test.

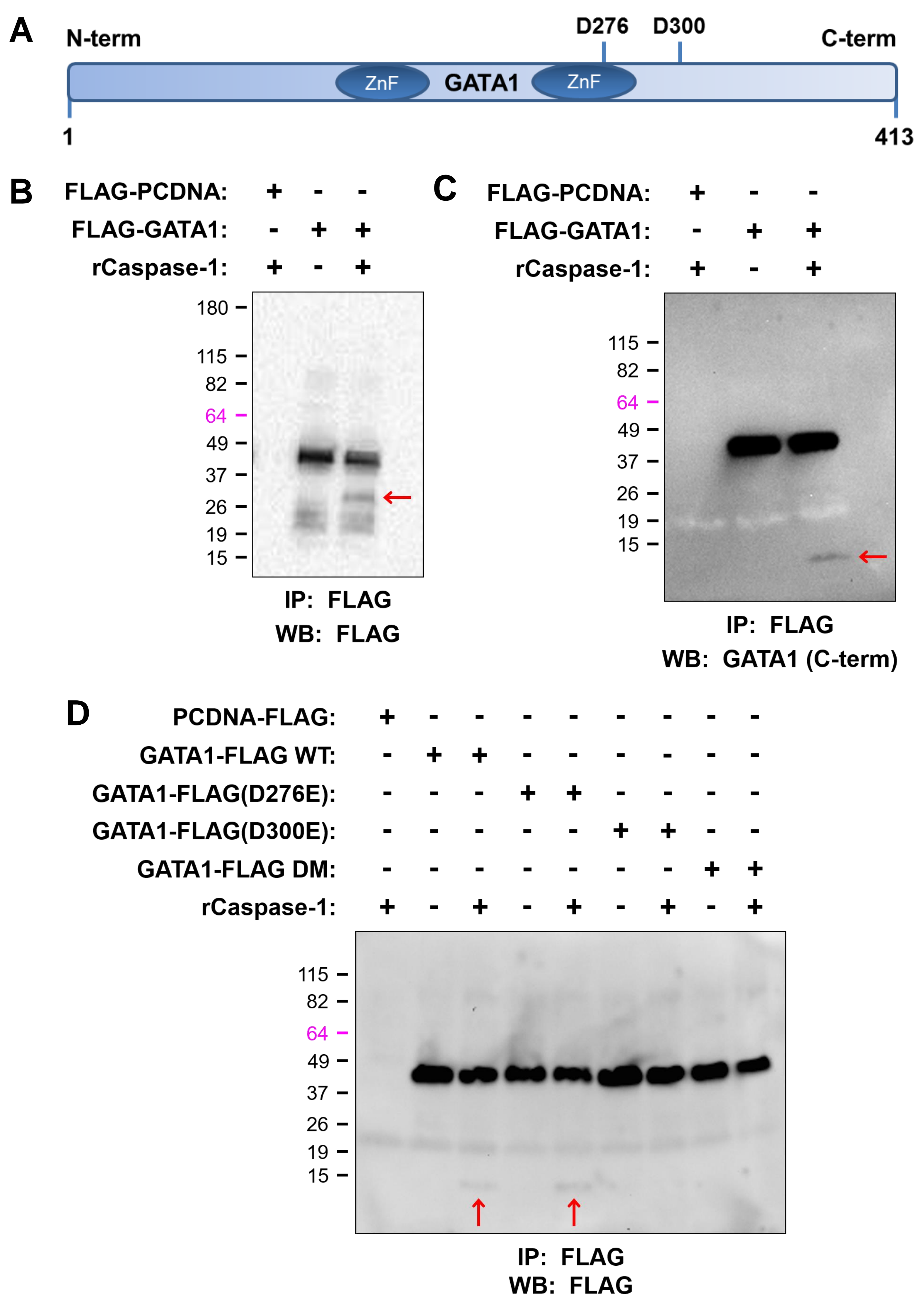


Figure S7. Caspase-1 cleaves *in vitro* human GATA1 in residue D300. Related to Figure 6. (A) Scheme of human GATA1 showing the zinc finger domains and residues D276 and D300. (B-D) HEK293T cells were transfected with FLAG-empty or FLAG-GATA1 (B, C) and empty-FLAG, GATA1-FLAG wild type, GATA1-FLAG(D276A), GATA1-FLAG(D300E) or GATA1-FLAG(D276E/D300E) (DM) (D) expression plasmids. Twenty four hours after transfection, GATA1 was pulled down from cell extracts with anti-FLAG M2 affinity gel and treated or not for 2 h at 37°C with 10 IU human recombinant caspase-1. Full length GATA1 and the generated proteolytic fragments were resolved in SDS-PAGE and immunoblotted with anti-FLAG to visualize N-term (B) and C-term (D) GATA1, or anti-GATA1 to visualize C-term GATA1 (C). One representative western blot assay out of the two carried out is shown.

Table S1. Morpholinos used in this study. Related to Figures 1, 2 , 4, 7, S1 and S2.
The gene symbols followed the Zebrafish Nomenclature Guidelines (http://zfin.org/zf_info/nomen.html).

Gene	Ensembl ID	Target	Sequence (5'→3')	Concentration (mM)	Reference
<i>pycard</i>	ENSDARG00000040076	atg/5'UTR	GCTGCTCCTTGAAAGATTCCGCCAT	0.6	Tyrkaska et al., 2016
<i>gfp4</i>	ENSDARG00000068857	e1/i1	GCTGTTTGTGTGTCTCTAACCTGTT	0.1	
<i>gata1a</i>	ENSDARG00000013477	e1/i1	GTTTGGACTIONCACCTGGACTGTGTCT	0.2	Galloway et al., 2005

Table S2. Primers used in this study for RT-qPCR. Related to Figure 4 and S5. The gene symbols followed the Zebrafish Nomenclature Guidelines (http://zfin.org/zf_info/nomen.html). ENA, European Nucleotide Archive (<http://www.ebi.ac.uk/ena/>).

Gene	ENA ID	Name	Sequence (5'→3')/Vendor
<i>rps11</i>	NM_213377	F1	GGCGTCAACGTGTCAGAGTA
		R1	GCCTCTTCTCAAAACGGTTG
<i>gata1a</i>	NM_131234	F1	CGTTGGGTGTCCCCCGGTCT
		R1	ACGAGGCTCGGCTCTGGACG
<i>spi1b</i>	NM_198062	F1	TGTTACCCTCACAACGTCCA
		R1	GCAGAAGGTCAAGCAGGAAC
<i>gcsfa</i>	FM174388	F1	TGAAGCAACGACCCTGTCGCA
		R1	CCGCGGCCTCAGTCTGGAAA
<i>mcsfa</i>	NM_001114480	F1	AGCCCACAAAGCCAAGGTAA
		R1	CTGACGCTCTGTGAAGGTGT
<i>ACTB</i>	NM_001101	H_ACTB_1	Sigma-Aldrich
<i>PYCARD</i>	NM_013258	H_PYCARD_1	
<i>CASP1</i>	NM_001257118	H_CASP1_1	
<i>NLRC4</i>	NM_001199138	H_NLRC4_1	
<i>NLRP3</i>	NM_001243133	H_NLRP3_1	